

Development of a Transendothelial Shuttle

by Macrophage Modification

by

Johan Georg Visser

*Thesis presented in fulfilment of the requirements for the degree of
Master of Science in the Faculty of Science at Stellenbosch University*



Supervisor: Prof. Carine Smith

December 2016

Declaration

By submitting this thesis electronically, I declare that the entirety of the work contained therein is my own, original work, that I am the sole author thereof (save to the extent explicitly otherwise stated), that reproduction and publication thereof by Stellenbosch University will not infringe any third party rights and that I have not previously in its entirety or in part submitted it for obtaining any qualification.

Copyright © 2016 Stellenbosch University

All rights reserved

Abstract

Background: Targeted stem cell delivery via macrophage modification is a novel and relatively non-invasive therapeutic intervention. Monocytes circulate through the vasculature and infiltrate damaged tissue in response to chemotactic signalling. Here they differentiate into functionally different macrophage phenotypes - the classically activated pro-inflammatory (M1) or alternatively activated anti-inflammatory (M2) phenotypes. The M1 macrophages are able to cross endothelial barriers, while the M2 anti-inflammatory macrophages are unable to transverse endothelium and instead remain tissue associated. The focus of our research was to produce M1 macrophages *in vitro* that could transverse endothelium while carrying engulfed stem cells, in order to deliver more stem cells in a relatively short time, to any injured tissue to facilitate recovery.

Methods: Primary isolated monocytes were cultured with Granulocyte Monocyte Colony-Stimulating Factor, Lipopolysaccharide and Interferon gamma for 6 days to pre-differentiate them into M1 macrophages. Cells were treated with a Wortmannin-Concanamycin A-Chloroquine cocktail to achieve phagosome maturation arrest and thus preserve ingested cells in a viable state. Preservation of engulfed stem cells (simulated with fluorescent latex beads covalently labelled with IgG antibody) was qualitatively and quantitatively determined by flow cytometry and live cell imaging, respectively. Bead-containing macrophages were co-cultured with HUVEC cells in a Transwell system, and exposed to Monocyte Chemoattractant Protein 1 (added to bottom well) to determine migration capacity.

Results: Monocytes were differentiated into M1 classically activated macrophages. The majority of these cells ($68.67 \pm 3.51\%$) were able to engulf opsonised beads after

successful induction of phagosome maturation arrest – a capacity similar to that of untreated cells ($61.19 \pm 4.68\%$). Ingested beads were preserved within macrophages for the duration of our protocol (2 hours), determined by retained red antibody signal on beads and perturbed phagosome acidification. 72.86 ± 16.0 phagosome maturation arrested macrophages were able to transverse a HUVEC coated membrane with $8 \mu\text{m}$ diameter pores (simulated endothelial layer), while only 70.14 ± 12.6 cells per well migrated when carrying a bead cargo.

Conclusion: A delivery system capable of engulfing, preserving and delivering cargo was successfully induced. Further optimisation of this technique could lead to translation into a novel method for delivery of stem cells with regard to regenerative medicine and may even be used as a drug delivery system for the treatment of various malignancies.

Uittreksel

Agtergrond: Geteikende stamsel aflewering via makrofaag manipulerings is 'n nuwe en relatief nie-indringende terapeutiese intervensie. Monosiete sirkuleer deur die bloedvate en infiltrer beskadigde weefsel in reaksie op chemiese seise. Hier kan hulle funksioneel verskillende makrofaag fenotipes vorm - die klassiek-geaktiveerde pro-inflammatoriese (M1) of alternatiewelik geaktiveerde anti-inflammatoriese (M2) fenotipes. Slegs die tipe M1 makrofage is in staat om deur endoteelweefsel te beweeg, terwyl die M2 makrofage in weefsel geleë bly. Die fokus van ons navorsing was om M1 makrofage *in vitro* te produseer, wat endoteel kan deurdring selfs nadat dit 'n stamsel ingeneem het, ten einde meer stamselle af te lewer in 'n relatief korter tydperk en so doende beskadigde weefselherstel aan te help.

Metodes: Primêre geïsoleerde monosiete is vir 6 dae gedifferensieer deur hul kwekingsmedia aan te vul met granulosisiet-monosiet kolonie-stimulerende faktor, lipopolisakkaried en interferon-gamma, om sodoende M1 makrofage te lewer. M1 selle is daarna behandel met 'n kombinasie van Wortmannin, Concanamycin A en Chloroquine om die proses van fagosoomverryping te verhoed en sodoende ingeneemde selle in 'n lewensvatbare toestand te bewaar. Bewaring van gefagositeerde stamselle (nageboots deur gebruik te maak van fluoreserende polistireen krale, gemerk met kovalent-gebonde IgG teenliggame) is kwalitatief en kwantitatief bepaal deur vloeisitometrie en lewende sel mikroskopie onderskeidelik. Makrofage met ingeneemde krale is daarna bo-op HUVEC selle in 'n dubbelpuut (Transwell) sisteem gekweek. Die kultuur is daarna aan monosiet chemo-aantrekkingsproteïen 1 (bygevoeg in onderste puut) blootgestel om migrasie kapasiteit te bepaal.

Resultate: Monosiete is suksesvol gedifferensieer na die klassiek geaktiveerde M1 makrofaag fenotipe. Die meerderheid van hierdie selle ($68,67 \pm 3,51\%$) was in staat om geöpsoniseerde krale te verswelg ná suksesvolle verkoming van phagosoom verryping - 'n resultaat soortgelyk aan dié van onbehandelde selle ($61,19 \pm 4,68\%$). Opgeneemde krale het binne makrofage behoue gebly vir die tydsduur van ons protokol (2 ure), soos bepaal deur die behoud van die rooi teenliggaamsein op krale. In terme van migrasie, was $72,86 \pm 16,0$ behandelde makrofage (per reaksie) in staat om deur 'n HUVEC-bedekte (endoteel) membraan met porieë, $8 \mu\text{m}$ in deursnee (te beweeg, in vergelyking met 'n soortgelyke $70,14 \pm 12,6$ selle per reaksie vir die behandelde selle wat krale bevat het.

Gevolgtrekking: Data bewys dat 'n afleweringstelsel, wat in staat is om 'n vrag in te neem en behoue te laat bly vir aflewering, suksesvol ontwikkel is. Die verdere optimalisering van hierdie tegniek kan lei tot die toepassing daarvan as 'n nuwe terapeutiese modaliteit in regeneratiewe medisyne, vir die aflewering van stamselle en/of farmaseutiese preparate, vir die behandeling van verskeie maligniteite.

Research Outputs

1. Conference contributions:

➤ International seminar

- **Visser JG**, Smith C. Using a macrophage shuttle for transendothelial stem cell delivery. Indian Ocean Rim Muscle Colloquium, Stellenbosch, South Africa, February 2016

➤ National seminar

- **Visser JG**, Smith C. Developing a macrophage shuttle for transendothelial stem cell delivery. Physiology Society of Southern Africa, Observatory, Cape Town, August 2016

➤ International poster presentation

- Smith C, **Visser JG**. A macrophage shuttle for transendothelial stem cell delivery. Physiology 2016, Joint meeting of The Physiological Society and the American Physiological Society, Dublin, Ireland, July 2016

2. Research awards:

- **Visser JG**. Wyndham award third prize for oral presentation at Physiology Society of Southern Africa, River Club, Observatory, Cape Town, August 2016
- **Visser JG**. Award for the most innovative method at Physiology Society of Southern Africa, River Club, Observatory, Cape Town, August 2016

3. Submitted manuscript:

- **Visser JG**, Smith C. Harnessing Phagocytosis for Regenerative Medicine: Lessons from Microbes. Immunology and Cell Biology – Nature. (Outcome pending)

Acknowledgements

I would like to thank the following for their contribution to the success of this project:

- Our God Jesus Christ for perpetual guidance
- My parents and family for financial and emotional support
- Prof Carine Smith for guidance and building up my experience
- National Research Foundation (NRF) of South Africa for financial support
- Stellenbosch University Central Analytical Facility (CAF), Live cell microscopy unit, for technical assistance

Table of Contents

List of Figures	xi
List of Abbreviations	xii
Units of Measure	xvi
1. Chapter 1: Introduction	1
2. Chapter 2: Literature review	3
2.1. Introduction.....	3
2.2. Molecular basis of phagocytosis.....	3
2.2.1. Recognition.....	4
2.2.2. Pseudopodia and Encapsulation	6
2.2.3. Nascent Phagosomal Stage	12
2.2.4. Late Phagosomal Stage	14
2.2.5. Phagolysosome Biogenesis Stage	16
2.3. Pathogenic Phagosome Maturation Arrest.....	17
2.3.1. Inhibition of Phagosome Maturation	18
2.3.2. Interference with Phagosome Acidification	19
2.3.3. Prevention of Lysosome Fusion	20
2.4. Harnessing the Phagocytic Process for Medicine	21
2.4.1. Macrophage IL-10 Enrichment	22
2.4.2. Brefeldin A Treatment.....	23
2.4.3. Microtubule or Dynein Inhibition	24
2.4.4. Wortmannin	26
2.4.5. Concanamycin A	26
2.4.6. Chloroquine	27
2.4.7. Additional Factors to Consider.....	27
2.5. Summary	29
2.6. Hypothesis.....	30
2.7. Objectives.....	30
3. Chapter 3: Materials and Methods	32
3.1. Cell Type Selection	32

3.2. Ethical Considerations.....	33
3.3. Monocyte Isolation	33
3.4. Culture Conditions.....	34
3.5. Pre-differentiation and Polarisation	35
3.6. Culture Detachment	36
3.6.1. Nunc UpCell™ Plates.....	37
3.6.2. 35mm Culture Dish with Accutase® Method	38
3.7. Macrophage Phenotype Analysis.....	38
3.8. Modulating Macrophage Phagosome Maturation	39
3.9. Visualisation of Ingested “Cargo” Using Fluorescent Beads	40
3.10. Phagocytosis	42
3.10.1. Live Cell Imaging of Phagocytosis.....	43
3.10.2. Flow Cytometric Quantification of Phagocytosis.....	44
3.11. Transmigration System.....	45
3.11.1. Fibronectin Coating	46
3.11.2. HUVEC Cell Culture	47
3.11.3. Transmigration Assay.....	48
3.12. Statistical Analysis	51
4. Chapter 4: Results	52
4.1. Monocyte Differentiation and Polarisation	52
4.2. Phagocytosis Model Validation.....	54
4.3. Intervention: Phagosome Maturation Arrest	56
4.3.1. Digestive Capacity	58
4.3.2. Engulfment Capacity	60
4.3.3. Acidification	61
4.4. Macrophage Migration	63
5. Chapter 5: Discussion	66
5.1. Macrophage Polarisation.....	66
5.2. Manipulating Phagosome Maturation	69
5.3. Maintenance of Engulfment Capacity and Migration	72
5.4. Bioactivity and <i>in vivo</i> Translation	73
6. Chapter 6: Conclusions and Recommendations for Future Studies.....	75

References	78
Appendix A: Literature Review	88
Appendix B: S.O.P. s	116
Appendix C: Supplementary Results	132

List of Figures

Figure 4.1: Monocyte differentiation into macrophages.....	52
Figure 4.2: Flow cytometry analysis of macrophage differentiation.....	53
Figure 4.3: Antibody dispersion off of AbsBeads.....	54
Figure 4.4: Acidification of cellular compartments.....	55
Figure 4.5: Time lapse images of live macrophages.....	57
Figure 4.6: Representative flow cytometry scatter plot of macrophage digestion with intensity clusters.....	59
Figure 4.7: Statistical analysis of macrophage digestive capacity.....	60
Figure 4.8: Statistical analysis of macrophage engulfment capacity.....	61
Figure 4.9: Representative flow cytometry scatter plots of macrophage acidification with intensity clusters.....	62
Figure 4.10: Statistical analysis of macrophage acidification.....	63
Figure 4.11: Statistical analysis of migratory capacity of phagosome maturation arrested macrophages.....	64

List of Abbreviations

AbsBeads	Antibody (IgG) Opsonised Polystyrene Beads
ANOVA	Analysis of Variants
ARF	ADP Ribosylation Factor
ATP	Adenosine Triphosphate
ATPase	ATP Phosphatase
BBE	Bovine Brain Extract
BFA	Brefeldin A
C6	Carbon at position 6 of a molecule
C20	Carbon at position 20 of a molecule
CD14	Cluster of Differentiation 14
CD45	Cluster of Differentiation 45
CD64	Cluster of Differentiation 64
CD86	Cluster of Differentiation 86
CD163	Cluster of Differentiation 163
CD206	Cluster of Differentiation 206
CD274	Cluster of Differentiation 274
CHM	Complete HUVEC Media
CO ₂	Carbon Dioxide
COP	Coat Protein Complex
CMM	Complete Monocyte Media
DAMP	Damage-associated Molecular Pattern
ddH ₂ O	Double-Distilled Hydrogen Dioxide (water)
DMSO	Dimethyl Sulfoxide ((CH ₃) ₂ SO)
EDAC	1-ethyl-3-(3-dimethylaminopropyl)- carbodiimide
EDTA	Ethylenediaminetetraacetic acid
EEA1	Endosomal Early Antigen 1
ER	Endoplasmic Reticulum
ER SNARE	ER Soluble N-ethylmaleimide-sensitive Factor-attachment Protein Receptor

FACS	Fluorescence-Activated Cell-Sorting
FBS	Fetal Bovine Serum
Fc	Fragment crystallisable
Fcy	Fragment crystallisable gamma
FcyR	Fragment crystallisable gamma Receptor
FcRn	Neonatal Fragment crystallisable Receptor
FPR	Formyl Peptide Receptor
GA	Gentamicin and Amphotericin
GAP	GTPase-activating Protein
GEF	Guanine Nucleotide-exchange Factor
GM-CSF	Granulocyte Macrophage Colony-Stimulating Factor
GTP	Guanosine Triphosphate
GTPase	GTP Phosphatase
hEGF	Human Epidermal Growth Factor
HLA-DR	Human Leukocyte Antigen – Antigen D Related
HREC	Health Research Ethics Committee
HUVEC	Human Umbilical Vein Endothelial Cell
ICAM-1	Intercellular Adhesion Molecule 1
INF- γ	Interferon gamma
IgG	Immunoglobulin G
IL-4	Interleukin 4
IL-10	Interleukin 10
iNOS	Inducible Nitric-oxide Synthase
IVIS	<i>in vivo</i> Imaging System
JAM-A	Junctional Adhesion Molecule A
LAMP	Lysosome-associated Membrane Proteins
LN ₂	Liquid Nitrogen
LPS	Lipopolysaccharide
M1	Classically Activated M1 Phenotype Macrophage
M2	Alternatively Activated M2 Phenotype Macrophage

MACS	Magnetic-Activated Cell Sorting
MAP1S	Mitogen-associated Protein 1S
MCP-1	Monocyte Chemoattractant Protein 1
M-CSF	Macrophage Colony-Stimulating Factor
MES	2-(<i>N</i> -morpholino)ethanesulfonic acid
MHCII	Major Histocompatibility Complex Class II
MIF	Macrophage Migration Inhibitory Factor
MPR	Mannose-6-phosphate Receptor
MyD88	Myeloid differentiation primary response gene 88
NADPH	Nicotinamide Adenine Dinucleotide Phosphate
NaOH	Sodium Hydroxide
Nef	Viral Negative Factor
NLR	NOD-like Receptor
NLRP3	NLR Pyrin Domain Containing 3
NSF	N-ethylmaleimide-sensitive Factor
ORP1L	Oxysterol-binding Protein Related-protein 1
P	Passage
PAMP	Pathogen-associated Molecular Pattern
PBMCs	Peripheral Blood Mononuclear Cells
PBS	Phosphate Buffered Saline
PD-L1	Programmed Death-Ligand 1
PenStrep	Penicillin-Streptomycin
PET	Polyethylene Terephthalate
PI	Phosphatidylinositol
PI3k	Phosphatidylinositol 3-kinase
PI3P	Phosphatidylinositol 3-phosphate
PI(3,4)P2	Phosphatidylinositol 3,4-bisphosphate
PI(3,4,5)P3	Phosphatidylinositol 3,4,5-triphosphate
PI(3,5)P2	Phosphatidylinositol 3,5-bisphosphate
PI4P	Phosphatidylinositol 4-phosphate

PI4P-5 α	Phosphatidylinositol 4-phosphate 5-kinase α
PI(4,5)P ₂	Phosphatidylinositol 4,5-bisphosphate
PIP ₃	Phosphatidylinositol 3,4,5-triphosphate
PIPAAm	poly(N- isopropylacrylamide)
PMA	Phorbol 12-myristate 13-acetate
PRR	Pattern Recognition Receptor
PTEN	PI 3'-phosphatase
RANTES	Regulated on Activation, Normal T Cell Expressed and Secreted
RILP	Rab7-interacting-lysosomal-protein
RLR	RIG-like Receptor
RNS	Reactive Nitrogen Species
ROS	Reactive Oxygen Species
RPMI	Roswell Park Memorial Institute medium
SapM	Secreted Acid Phosphatase
SEM	Standard Error of the Mean
SNARE	Soluble N-ethylmaleimide-sensitive Factor-attachment Protein Receptor
SNX	Sorting Nexins
TACO	Tryptophan-aspartate Containing Coat
TGF- β	Transforming Growth Factor beta
TLR	Toll-like Receptor
TM+C	Transmigration Media with Chemokine
TM-C	Transmigration Media devoid of Chemokine
TNF- α	Tumour Necrosis Factor α
UPR	Unfolded Protein Response
VAMP	Vesicle-associated Membrane Protein
V-ATPase	Vacuolar-type H ⁺ -ATPase
VCAM-1	Vascular Cell Adhesion Molecule 1
Vpr	Regulatory viral protein
WPBTS	Western Province Blood Transfusion Service

Units of Measure

%	percentage
°C	degrees Celsius
$\mu\text{g}/\text{cm}^2$	microgram per square centimetre
$\mu\text{g}/\text{ml}$	microgram per millilitre
μl	microliter
μm	micrometre
μM	micromolar
g	gravitational acceleration
g/mol	gram per mole
h	hour
M	molar
mg	milligram
mg/ml	milligram per millilitre
min	minutes
ml	millilitre
mm	millimetre
mM	millimolar
ng/ml	nanogram per millilitre
nm	nanometre
nM	nanomolar
kDa	kilo Dalton
RPM	revolutions per minute

Chapter 1: Introduction

Broadly, stem cells are cells capable of differentiation into any cell type following appropriate stimulation. In the context of skeletal muscle, the population of stem cells facilitating muscle regeneration are satellite cells (Parise et al. 2008). Unfortunately, in some cases, regeneration is inhibited under pathological conditions (such as myodystrophy) or due to individual genetic profiles or abnormalities (Snijders et al. 2016). Perturbed regeneration may result from more than one cause, but most relevant to the current thesis, one of these contributing factors is a relative lack of sufficient satellite cell numbers at the site of regeneration (Dayanidhi et al. 2015). Therefore, therapeutic delivery of additional satellite cells to the required site should increase the rate and extent of regeneration. Stem cell delivery could thus beneficially attenuate regeneration in chronic pathological states, or recovery acutely after physical injuries. This technique would also utilise the donor's own stem cells and monocytes. Following *in vitro* proliferation of these cells, this autologous stem cell therapy could treat chronic diseases. Although this thesis focused on application in skeletal muscle, if successful, this technique could be extrapolated and developed for broader application in a multitude of tissue areas or organs.

Turning attention now to how such stem cell delivery could be achieved, we have identified leukocytes, and in particular phagocytes, as potential vehicles for delivery. Phagocytes – such as macrophages and neutrophils – are responsible for the initial recognition and destruction of invading pathogens. So effective are these phagocytes that nearly 95% of the animal kingdom can elicit self-protection without the need of B or T cells, relying only on evolutionarily conserved innate immune defence (Mills et al. 2015). At least two characteristics of these cells make them ideally suited for this task.

Firstly, they are highly mobile cells, with the ability to readily cross membranes, such as endothelium. This affords them the uncommon cellular trait of migration across different body or tissue compartments to reach the site where they are required. Secondly, these cells have the capacity for phagocytosis. This primary anti-microbial weapon is an intricate process, starting with pseudopodia extension to engulf particle matter and ending in particle neutralization within a destructive phagolysosome. The fact that these two mechanisms in the “defence” response are highly conserved across species (Mills et al. 2015), testifies to its potency and overall importance for host health. However, from both the microbiology and immunology literature, it is also known that the process of phagocytosis is not infallible. Several papers have described the ability of evolved microbes, such as *Mycobacterium tuberculosis* (Seto et al. 2011), *Leishmania donovani* (Gogulamudi et al. 2015) and *Candida glabrata* (Rai et al. 2015), to hide from the immune system by remaining inside phagocytes without being digested in the phagolysosome. We believe that a lesson can be learned from these microbes, and harnessed to the benefit of regenerative medicine practises.

The next chapter will provide an overview of the literature related to molecular events of phagosome maturation, as well as microbe-associated phagosome maturation arrest and experimental manipulation of these strategies. This is followed by a detailed report of method development regarding the manipulation of phagosome maturation arrest, as well as assessment of potential effects of this intervention on macrophage phagocytic and migratory capacities (Chapter 3). Results are presented and discussed in chapters 4 and 5, before the thesis is rounded off with a discussion of the practical applicability of this technique, additional work required and some recommendations for improvements or further development of the technique.

Chapter 2: Literature Review

A truncated version of this literature review (please refer to **Appendix A**) has been submitted for publication to *Immunology and Cellular Biology* (outcome pending).

2.1. Introduction

In this review, we will present our hypothesis on how macrophages may be altered for regenerative medicine, and specifically for homologous stem cell delivery. However, we first present an overview of what is currently known about the molecular processes involved in the phagocytic process, aiming to elucidate the molecular mechanisms of phagosome maturation in a temporal and concise manner as to better understand this phenomenon. This will be followed by a discussion of phagosome maturation arrest and the mechanisms used by microbial agents to evade phagosomal neutralization, as well as similar mechanisms at play during normal cell death processes.

2.2. Molecular Basis of Phagocytosis

Phagocytosis involves considerable membrane and cytoskeletal rearrangements in order to encircle and capture (engulf) potential pathogens or matter foreign to the immune system – forming phagosomes – and to mature these nascent phagosomes into phagolysosomes (Huynh et al. 2007). Microbial material is captured inside a nascent phagosome that matures through events relating to the endocytic and autophagic pathway, where fission and fusion events allow for its destructive ability. In the next few sections, these intricate processes will be explained in detail, using macrophages as representative phagocytic immune cell.

2.2.1. Recognition

Matter is recognised as foreign – and thus as potential threat – via binding to specific pattern recognition receptors (PRRs) located both in the cytosol and cell surface of immune cells of both the innate and adaptive branch of the immune system, as well as on epithelial cells such as the vascular endothelium (Anderson & Wadee 2012). PRRs differentiate between molecules that are released by dying self-cells and foreign material through respectively binding to damage-associated molecular patterns (DAMPs) and pathogen-associated molecular patterns (PAMPs) (Abbas et al. 2014). Necrotic self-cells release formylated peptides like N-formylmethionine from damaged mitochondria (Zhang et al. 2010). These self-originating proteins (classified under DAMPs) can bind to formyl peptide receptors (FPRs) on monocytic cells, initiating chemotaxis and eventually ending in phagocytosis (Bardoel & Van Strijp 2011). Interestingly, these formylated peptides are also characteristic of bacterial proteins. In our opinion, this supports the endosymbiotic theory of mitochondrial evolution, which proposes that mitochondria are foreign organelles that were incorporated into eukaryotic cells for energy production. In this manner cells containing damaged mitochondria, i.e. metabolically compromised cells, are removed via recognition of these DAMPs, irrespective of self or non-self. Recognition of PAMPs is oriented toward many PRR subtypes, such as NOD-like receptors (NLRs) (recognise DAMPs as well), RIG-like receptors (RLRs) and Toll-like receptors (TLRs). NLRs are mainly associated with sterile inflammation like gout via NLRP3 associated inflammasome formation (Misawa et al. 2013). The membrane bound TLRs bind bacterial hallmark molecules both intra- and extracellularly and exhibit some target specificity. The TLR5 subtype typically binds to flagella, while TLR2 and TLR4 bind components of the bacterial cell wall like peptidoglycan and lipopolysaccharide (LPS), respectively

(Abbas et al. 2014). TLR2 forms a heterodimer with TLR1 or TLR6 to bind the N-terminal cysteine modification on lipoproteins of bacteria, as illustrated in mycobacterium (Bardoel & Van Strijp 2011). Furthermore, this lipoprotein modification is uniquely conserved in over 2000 different bacterial proteins (Babu et al. 2006), which can all be recognised by binding of this heterodimer. Other TLRs like TLR3, TLR7, TLR8 and TLR9 are intracellular receptors and recognize bacterial dsRNA and DNA.

TLR activation induces recruitment of adaptor proteins and activation of transcription factors for production and release of cytokines, adhesion molecules and costimulators (Abbas et al. 2014). Active TLRs indirectly regulate phagocytosis through Myeloid differentiation primary response gene 88 (MyD88) signalling and activation of the p38 residue to accelerate phagocytosis (Shi et al. 2016). The newly identified mitogen-associated protein 1S (MAP1S) autophagy-related protein (Xie et al. 2011) was also very recently reported to be necessary for TLR activation and effective bacterial phagocytosis (Shi et al. 2016), but more research is required to fully elucidate its role in this context. Many other receptors such as lectin, mannose, complement and RIG-like receptors also assist with pathogen recognition, but the IgG receptors are more closely associated with phagocytosis. IgG antibodies directed against specific pathogenic microbes can attach to bacteria to opsonise them. Opsonisation facilitates phagocytosis of material otherwise 'invisible' to macrophages. Macrophages recognise the constant γ heavy chain in Fc regions of IgG antibodies with Fc γ receptors (CD64) on their cell surface. Recognition of IgG opsonised material induces Fc γ R clustering at the site of material contact that leads to actin polymerization and engulfment through pseudopod extension (Swanson & Hoppe 2004). Formation of pseudopodia and actin polymerization is highly dependent on phosphatidylinositol 3-

kinase (PI3k) recruitment for production of various phosphatidylinositides. The ADP ribosylation factor (ARF) proteins play a pivotal role in activating phosphatidylinositol kinase enzymes to regulate membrane modification (Nie et al. 2003). Specifically, ARF6 has many functions – one of which is being recruited to the tip of forming pseudopodia where it activates type I PI3k substrate production via activation of other phosphatidylinositol kinases (Honda et al. 1999). ARF6 is also essential for actin polymerization during pseudopod extension (Zhang et al. 1998). This collectively ensures particle capture and membrane fusion behind the opsonised particle to form a phagosome. FcγR mediated phagocytosis is the main form of phagocytosis simulated in experimental phagocytosis models, because engulfment does not require stimulation by other cells types like T cells or NK cells, explained further by Liu et al. (2013).

2.2.2. Pseudopodia and Encapsulation

Following recognition, phagocytosis is initiated with the extension of pseudopodia. Particle internalisation and phagosome formation is achieved within 5 min after introduction of the foreign agent under culture conditions (Visser & Smith, unpublished data). Macrophages specifically are extremely ambitious in their phagocytic ability and are able to engulf particles into phagosomes which are closely comparable with their own size (Huynh et al. 2007). Interestingly, a form of cell suicide termed “frustrated phagocytosis” has been reported, where macrophages even tried to engulf the opsonised culture plate surfaces they were grown on (Cox et al. 1999). This phenomenon presented a useful model with which to investigate the mechanics of pseudopod formation. These “frustrated” macrophages were able to increase their surface area by over 20% (Cox et al. 1999). The way in which this phenomenal change in cell shape can be achieved, has been debated to some extent. One theory

postulated that the macrophage membrane is corrugated, possibly allowing a flattening out of the membrane during extra-large particle engulfment (Hallett & Dewitt 2007). However, quantitative spectroscopy has shown that during healthy phagocytosis, membrane surface area indeed enlarges to such a degree that surface flattening alone cannot fully account for it (Hackam et al. 1998). In addition, portions of the plasma membrane are also lost from the cell surface when it forms the membrane of newly formed phagosomes, so that even more membrane replenishment is required.

These findings raise the questions of where the extra membrane comes from and what controls it, since these are vital considerations in understanding the processes determining the efficacy and speed of phagocytosis. Specific membrane reservoirs have not been identified within cells, but general cellular sources are known. For example, in the case of osteoclasts, exocytosis of late endosomes has been shown to function distinctively to deliver membrane components and increase cell surface area during bone reabsorption (Rousselle & Heymann 2002). In the context of macrophages and pseudopod formation specifically, a few candidates have been investigated. Initially, Gagnon et al. (2002) proposed that the Endoplasmic Reticulum (ER) may fuse with the plasma membrane at the base of extending pseudopodia, forming a continuity through which the particle can slide into the ER lumen. This idea was supported by Becker et al. (2005) who neutralized the ER soluble N-ethylmaleimide-sensitive factor-attachment protein (SNARE) receptor (ER SNARE), ERS24, with intracellular antibodies and showed that phagocytosis efficiency of large particles ($>3\mu\text{m}$) was reduced. Subsequently, Hatsuzawa et al. (2006) also blocked ERS24 (together with syntaxin 18 and D12) and postulated a pivotal role of syntaxin 18 during ER fusion with phagosomes after finding syntaxin 18 expression on isolated

phagosomes, although they acknowledged that this does not prove actual ER-membrane fusion. Furthermore, although, many ER proteins are recruited to phagosomes during events such as pseudopod extension (vesicle-associated membrane protein 3, VAMP3) (Coppolino et al. 2001) and phagosome maturation (syntaxin 7 and 13) (Collins et al. 2002), this does not substantiate a direct fusion of the ER with phagosomes. As evidenced by several reviews on this topic, the theory of Gagnon and colleagues seemed to have been accepted by some groups (Garin et al. 2001; Desjardins 2003), but not all. Several other authors have argued that the role of the ER during phagocytosis still needs some elucidation (Touret et al. 2005; Groothuis & Neefjes 2005). More recently, using a variety of techniques including immunological, biochemical, electron microscopy and fluorescence microscopy, Huynh et al. (2007) indeed could not find any evidence of the ER fusing to the plasma membrane during phagocytosis. Also, since phagosomes acidify during maturation via a proton gradient created by the vacuolar-type H⁺-ATPase (V-ATPase) proton pump, and the ER membrane is permeable to protons and devoid of V-ATPase (Paroutis et al. 2004), the theory of simple ER fusion is probably unlikely to fully explain the phenomenon. Considering all points of view and data available to us, we speculate that the ER likely fuses with phagosomal membranes – however, it could be in a ‘kiss and run’ or ‘kiss of death’ fashion, as seen during autophagosome fusion with lysosomes (Jahreiss et al. 2008) and cytotoxic CD8⁺ T cell mediated cell death (Trambas & Griffiths 2003). This could result in an exchange or delivery of ER localised proteins to phagosomes, without complete membrane exchange through fusion. Furthermore, ER engagement was observed during large particle uptake (>3µm) and mostly during FcγR mediated phagocytosis (Becker et al. 2005), meaning that ER engagement is likely size and receptor specific.

A more likely candidate is the enzyme group of PI3ks that phosphorylate the 3' inositol phospholipid of inositol rings. These kinases are classified into three families based on their substrate used for lipid phosphorylation: types I, II and III.

The type I PI3ks consists of four isoforms: PI3k α , β , γ and δ . All these isoforms use phosphatidylinositol 4,5-bisphosphate (PI(4,5)P₂) as a substrate to generate phosphatidylinositol 3,4,5-triphosphate (PI(3,4,5)P₃, or PIP₃) (Hawkins & Stephens 2015). This PI3k substrate concentration is kept at optimal level by phosphatidylinositol 4-phosphate 5-kinase α (PI4P-5k α) through its phosphorylation of phosphatidylinositol 4-phosphate (PI4P) to PI(4,5)P₂ (Beemiller et al. 2006). The PI3k δ isoform is unique to immune cells as it is normally only expressed on lymphoid and myeloid cell lineages (Okkenhaug 2013).

Botelho et al. (2000) found transiently high PI(4,5)P₂ expression on extending pseudopodia with its disappearance shortly after phagocytic cup closure and nascent phagosome formation. Furthermore, type I PI3ks recruitment and subsequent PIP₃ expression has been shown to occur on extending pseudopodia during engulfment of antibody-opsonised particles (Marshall et al. 2001). Throughout the literature, PIP₃ is seen as the main propagating agent during pseudopod extension. However, apart from the apparent steric association of PI(4,5)P₂ to PI3ks – necessary for its phosphorylation to PIP₃ – PI(4,5)P₂ itself seems to have an equally important role in pseudopod formation. Active ARF6 induces PI(4,5)P₂ production through activation of PI4P-5k α during phagocytosis (Honda et al. 1999). The produced PI(4,5)P₂ can then recruit WASP/N-WASP proteins to facilitate actin polymerization during phagocytosis (Miki et al. 1996). More recently, Scott et al. (2002) presented supporting findings that inhibition of PI(4,5)P₂ hydrolysis or overexpression thereof, prevented actin disassembly (required for successful material engulfment). The 3' phosphorylated

inositols, PIP₃ and phosphatidylinositol 3,4-bisphosphate (PI(3,4)P₂), are known to regulate actin polymerization in a G-protein coupled manner, resulting in changes in cell shape, cell movement and phagocytosis itself (Mazaki et al. 2012). However, previously mentioned findings support a role of PI(4,5)P₂ together with its alternatively 3-position phosphorylated homologues during actin regulation, even if only in disassembling actin by its disappearance. This highlights the independent role of PI(4,5)P₂ (by extension also ARF6 and PI4P-5κ) as an engulfment regulator and not only a type I PI3k substrate for PIP₃ production. The role of type I PI3ks was further elucidated by Vieira et al. (2001) who postulated, via antibody mediated type I PI3ks inhibition, that this type of PI3ks together with its substrate (PI(4,5)P₂) and product (PIP₃) were essential for pseudopod formation around relatively large particles (>3μm in diameter) and their subsequent ingestion, but not for the further maturation of phagosomes.

The Type II PI3ks are not well described but current evidence points to the notion that this enzyme family produces either PI(3,4)P₂ or phosphatidylinositol 3-phosphate (PI3P) on endosomal or plasma membranes (Falasca & Maffucci 2012; Posor et al. 2013) by either of their three isoforms: PI3kC2α, C2β, C2γ. Thus, type II PI3ks, could contribute to production of PI(3,4)P₂ on extending pseudopodia for actin regulation and additional membrane, or it could facilitate phagosome maturation through production of PI3P on phagosomes.

The last PI3k family is the type III PI3ks that consist of only one catalytic subunit, VPS34, in humans: hVPS34. Type III PI3ks phosphorylate phosphatidylinositol (PI) to PI3P on endosomes and autophagosomal structures (Backer 2008). Formation of PI3P is accompanied by the closure of the phagocytic cup and subsequent disappearance of PI(4,5)P₂ (Botelho et al. 2000) that lead to and are essential for

maturation of newly formed phagosomes (Vieira et al. 2001). Thus the function of PI3P is centred more around phagosomal/endosomal maturation than as a source of extra membrane during engulfment. Additionally, PI3P expression could be negatively regulated during maturation by the (FYVE domain containing protein) PI 5'-kinase, PIKfyve, via phosphorylation at the 5-position to produce phosphatidylinositol 3,5-bisphosphate (PI(3,5)P₂) (Hazeki et al. 2012).

From the literature consulted, it seems that the origin of these relatively large amounts of “extra” membrane is most likely the phosphoinositides produced by PI3k enzymes. In support of this, non-specific inhibition of the PI3ks enzyme superfamily (which induced drastically decreased PIP₃, PI(3,4)P₂ and PI3P synthesis during phagocytosis), prevented treated cells from producing the 20% surface area increase usually observed during suicidal “frustrated phagocytosis” (Cox et al. 1999). This suggests that PI3ks activity is one of the chief sources of membrane during pseudopodia extension and phagocytosis. Additionally, a significant amount of membrane could also be supplied by recycling endosomes and sorting nexins (SNX), which collect membrane and other phagocytic components from endosomes and newly formed phagosomes called nascent phagosomes. Interestingly, this recycling machinery is also dependent on PI3P expression for docking onto intracellular structures (Fair & Grinstein 2012), further supporting our notion of PI3ks as important role player in this context. Not all engulfed material is destined for degradation and subsequently need to be recycled by the recycling endosomes and SNX mentioned above. Recycling endosomes, partly identified by the Rab11 superfamily, is responsible for pinching off reusable cargo during the nascent phagosomal stage (Lemmon & Traub 2000). One of three Rab11 isoforms, Rab11a, is expressed on the nascent phagosome itself and facilitates phagosome fusion with early endosomes and

Golgi-derived vesicles (Fairn & Grinstein 2012). Rab11a also has a crucial role in proinflammatory signalling as it delivers TLR4, responsible for detection of lipopolysaccharide such as *E. coli* LPS, to maturing phagosomes (Husebye et al. 2010). The Rab11 superfamily seems necessary for engulfment itself as well, since Cox et al. (2000) reported that prevention of Rab11 GDP/GTP cycling by mutant alleles, inhibited particle internalization. Furthermore, the GTPase, ARF6, also controls trafficking of recycling endosomes to the membrane (van Ijzendoorn 2006) and inhibition thereof resulted in a block in pseudopod extension (Niedergang, F. et al. 2003), suggesting that recycling endosomes serve as an additional reservoir for plasma membrane during pseudopod extension. The greater part of cargo retrieval and sorting is done in the early phagosomal stage because most of the machinery is dependent on PI3P for docking (Fairn & Grinstein 2012), supporting the findings of Cox et al. (1999) previously mentioned. However, some of the SNX can form higher order structures with Vps26, Vps29 and Vps35 – these are called retromers (Cullen & Korswagen 2011). These retromers function in the presence of PI3P, but also active Rab7, giving them a limited time gap to recycle cargo between early stage and late stage phagosome maturation (between Rab5 to Rab7 transitioning), discussed below. This is in no doubt a finely tuned, complex process that merits further research in order to be fully elucidated.

2.2.3. Nascent Phagosomal Stage

This stage can be structurally distinguished from the pseudopod extension/engulfment stage by phagocytic cup closure behind the engulfed material of interest. Pseudopod closure is highly dependent on type I PI3k together with expression of PIP₃ and PI(4,5)P₂. Inhibition of PI3k with the nonspecific protein inhibitor, LY294002,

prevented successful antibody opsonized particle engulfment due to unsuccessful pseudopod closure (Beemiller et al. 2006).

In contrast to pseudopod formation, the process of phagosome formation and maturation is relatively well described, although some controversies remain. Successfully engulfed material is encapsulated into nascent phagosomes characterized by Rab5 GTPase expression (Fairn & Grinstein 2012). Rabex-5, a guanine nucleotide-exchange factor (GEF), is initially recruited to newly formed endosomes by the already present Rab22a (Zhu et al. 2009) and functions to activate Rab5 (Horiuchi et al. 1997). Active Rab5 then recruits endosomal early antigen 1 (EEA1) (Scott et al. 2002) and the type III PI3k, hVPS34, (Kinchen et al. 2008) to the nascent phagosome. hVPS34 generates PI3P on the cytosolic face of nascent phagosomes that serve as docking station for a variety of maturation effectors. The FYVE domain of EEA1 can then dock onto PI3P to ensure later EEA1-mediated tethering and fusion of phagosomes with late endosomes for further maturation (Vieira et al. 2002). EEA1 thus seems to play a central role in phagosome maturation, as postulated by Fratti et al. (2001), after they illustrated that intracellular antibodies against EEA1 arrested phagosome maturation. However, around the same time as this study, Vieira et al. (2001) reported a dominant negative mutant of EEA1 which did not induce maturation arrest. They suggested that other FYVE domain containing proteins could be involved in PI3P binding that lead to subsequent maturation. Zinc finger FYVE domains, present in proteins like EEA1 and PIKfyve, recognize the hydrophilic head of PI3P on the cytosolic leaflet and allow binding of these proteins with substantial specificity to PI3P, resulting in this docking (Patki et al. 1998). These contradicting findings on the necessity of EEA1 could be explained by its tendency for complex formation with other proteins. EEA1 has been reported to form a

macromolecular complex with Rabaptin-5, Rabex-5 and N-ethylmaleimide-sensitive factor (NSF) that interacts with syntaxin 13 (another SNARE) to facilitate membrane fusion (McBride et al. 1999). NSF disassembles these SNARE complexes via ATP hydrolysis after membrane fusion, blocking further action (Jahn & Scheller 2006). This could mean the maturation inhibition reported by Fratti et al. (2001) was achieved through the inability of antibody-bound EEA1 to form a macromolecular complex (likely due to steric hindrance), but the dominant negative form of EEA1 could, thus resulting in unperturbed phagosome maturation.

2.2.4. Late Phagosomal Stage

Transition to the late phagosomal stage is marked by GTPase-activating protein (GAP)-mediated Rab5 inactivation/dissociation (Fairn & Grinstein 2012) and Rab7 recruitment, together with late endosome fusion and expression of other markers such as mannose-6-phosphate receptor (MPR), lysobisphosphatidic acid (Fratti et al. 2001) and lysosome-associated membrane proteins (LAMP) (Desjardins 1995). It is also during this stage that PI3P is incorporated and degraded inside the phagosomal lumen via inward budding of the limiting membrane (Gillooly et al. 2000). Briefly, the PI 3'-phosphatase (PTEN) and PIKfyve eliminate PI3P via hydrolysis to PI and phosphorylation to PI(3,5)P₂, respectively (Hazeki et al. 2012). Elimination of PI3P is likely necessary for the removal of nascent phagosomal effector proteins dependent on PI3P expression, such as EEA1 and other FYVE domain containing proteins. The late phagosomal stage initiates about 10-30 min after nascent phagosome formation, at least under *in vitro* conditions (Fratti et al. 2001). This is in accordance with the disappearance of PI3P about 10 min after its formation (Vieira et al. 2001).

Rab7 is expressed on both late endosomes/late phagosomes and lysosomes (Meresse et al. 1995). This expression profile allows Rab7 to regulate membrane trafficking between early endosome/nascent phagosomes and late endosomes as well between late endosome/late phagosomes and lysosomes (Press et al. 1998). The fusion between nascent phagosomes and late endosomes may allow the close proximity of Rab7 and PI3P that facilitates SNX retromer functioning reported by Cullen & Korswagen (2011), as mentioned in section 2.2.2. In this manner, the SNX retromers possibly recycle cargo between nascent phagosomes and late phagosomes, rather than nascent phagosomes and recycling endosomes, as hinted at earlier. This Rab7 GTPase accelerates maturation to the phagolysosome biogenesis stage with the help of Rab7-interacting-lysosomal-protein (RILP) (Harrison et al. 2003). The Rab7 associated proteins RILP and oxysterol-binding protein related-protein 1 (ORP1L) together link phagosomes to dynein (Johansson et al. 2007), which centripetally moves these late phagosomes along microtubules toward lysosomes for fusion (Harrison et al. 2003). Johansson et al. (2005) reported that ORP1L preferentially binds to active, GTP-Rab7 and that this association seems to sustain the GTP-bound state of Rab7. This prolonged activation could be required for successful dynein linkage. Dynein mediated fusion with lysosomes seems to be dependent on the HOPS complex as well as Rab7 (Akbar et al. 2011). HOPS is a tethering protein responsible for keeping phagosomes in close proximity to lysosomes, a function parallel to that of EEA1 (Hickey & Wickner 2010). Furthermore, disassembly of the microtubular network with nocodazole ablated centripetal movement of phagosomes, suggesting a dependency of macrophages to dynein for maturation (more detail provided in section 2.4.3.).

2.2.5. Phagolysosome Biogenesis Stage

Phagosome fusion with lysosomes is the last stage of maturation and is referred to as phagolysosome biogenesis (Seto et al. 2011). This stage was reported to occur about 1h after nascent phagosome formation under *in vitro* conditions (Jahraus et al. 1998). Our unpublished data indicate this stage is initiated closer to 30 min after nascent phagosome formation; however, it is important to keep in mind the nature of the internalised particle as this will influence progression to further stages and subsequent digestion. Fusion is mediated by the SNARE proteins (syntaxin 7, syntaxin 8, VAMP7 and VAMP8) (Becken et al. 2010) and provides the phagolysosome with the needed proteases (e.g. cathepsin D), reactive nitrogen species (RNS) and reactive oxygen species (ROS) with which to neutralize the ingested particle. Lysosome fusion also increases LAMP expression and effectuates an acidic phagosomal environment (Jahraus et al. 1994).

It may seem that Rab5 and Rab7 are the chief GTPases regulating endosomal and phagosomal maturation, as discussed in the previous section, but research has discerned significant roles for some other Rab proteins as well. For example, Rab10 has been shown to regulate sufficient recycling of proteins back to the plasma membrane and is present on nascent phagosomes even before Rab5 (Cardoso et al. 2010). Also, phagolysosomal protein degradation is hugely dependant on proteases like cathepsin D, delivered from the Golgi. Delivery is controlled by the trans-Golgi network-localised Rabs (22b, 32, 34,38 and 43) (Ng et al. 2007) that were shown to have various association and dissociation kinetics with the maturing phagosome (Seto et al. 2011). Blockage of cathepsin D delivery via dominant-negative Golgi-localized Rab alleles resulted in arrested phagosome maturation. Rab34 has also been implicated in phagolysosome biogenesis through its association with RILP (Wang &

Hong 2002). Another ER-localized Rab, Rab20, was shown to co-localize with V-ATPase on the phagosome, suggesting an involvement in phagosome acidification and maintenance thereof (Curtis & Gluck 2005). Seto et al. (2011) more recently reinforced this finding by reporting that dominant negative alleles of Rab20 and Rab39 prevent phagosomal acidification.

Phagocytosis has seemingly evolved from an endocytic nutrient gathering process in almost all eukaryotic cells to a specialized mechanism of self-defence conserved uniquely to professional phagocytes. In this manner a certain degree of redundancy exists in phagocytosis, most likely in order to be “fool proof”. However, as seen in the literature, at least some pathogens are able to adapt in order to escape degradation and neutralisation by phagocytosis to ensure their own survival. The most effective mechanisms employed by these microbes entail phagosome maturation arrest. Interestingly, these pathogens do not evade being transported into the phagocytic cell – rather they use the host cell as nutrient supply, so that they not only survive, but thrive.

2.3. Pathogenic Phagosome Maturation Arrest

Pathogenic phagosome maturation arrest is a hallmark of bacterial and viral host immune evasion. Many intracellular pathogens like *Mycobacterium tuberculosis*, *Candida glabrata*, HIV-1 and *Leishmania donovani* have evolved divergent mechanisms to modulate phagocytic digestion (Thi et al. 2012). Well characterized mechanisms of phagosome maturation arrest include (a) interference with PI3k function and PI3P biogenesis (*M. tuberculosis* & *C. glabrata*; Rai et al. 2015), (b) perpetuation of Rab5 expression (*L. pneumophila*, Clemens et al. 2000), (c) prevention of centripetal movement of nascent phagosomes (*M. tuberculosis* & HIV-1; Dumas et

al. 2015), (d) blocking of fission and fusion with lysosomes and endosomal organelles (*M. tuberculosis* & *L. donovani*; Gogulamudi et al. 2015), (e) raising pH levels by causing phagosomal acid leakage (*C. neoformans*; Tucker & Casadevall 2002), (f) lysis of the phagosomal membrane to escape digestion (*Salmonella spp.*; Fairn & Grinstein 2012) and even (g) active macrophage killing (filamentous *C. albicans*; Gaur et al. 2013). Although the mechanisms by which these pathogens evade phagocytosis have been identified, they are not well understood and only a few have been sufficiently studied in the context of phagocytosis. For the sake of brevity, we limited ourselves here to a very brief overview of the mechanisms most relevant to this review.

2.3.1. Inhibition of Phagosome Maturation

M. tuberculosis survive intracellularly mainly by working against PI3ks, secreting the acid PI 3'-phosphatase (SapM) to dephosphorylate PI3P, thus preventing EEA1 from docking onto the phagosome (Vergne et al. 2005). Mycobacterial phagosomes also retain the tryptophan-aspartate containing coat (TACO) protein, expressed on the cytosolic leaflet of the plasma membrane involved in intracellular membrane trafficking, cytokinesis and cytoskeletal remodelling (Gogulamudi et al. 2015). TACO retention causes prolonged Rab5 expression - although some maturation effectors can still bind the phagosome, this occurs in relative absence of PI3P, so that the FYVE domain mediated binding of EEA1 is greatly perturbed (Simonsen et al. 1998), which largely prevents lysosome fusion (Ferrari et al. 1999) to ensure a more alkaline and hydrolase deficient phagosome (Clemens et al. 2000).

In contrast, the survival mechanisms of *C. glabrata* are largely dependent on active PI3ks. *C. glabrata* encodes the enzyme PI3k and (similar to the type III PI3ks, hVPS34) produces fungal PI3P through phosphorylation of PI (Strahl & Thorner 2007). In this

manner, the PI3P content of phagosomes could increase during the early stages of maturation where PI3P has not yet come into play. This could then lead to a PI3P rich phagosome being identified as already partly matured due to its PI3P phenotype, thus halting further maturation processes. Deletion of the two functional subunits of fungal PI3k (CgVps15 and CgVps34), led to alleviated phagosomal maturation arrest with greatly reduced fungal survival (99% of fungus died) and virulence in phorbol 12-myristate 13-acetate (PMA) differentiated THP-1 macrophages (Rai et al. 2015), providing evidence for its importance.

In addition, HIV-1 invasion is associated with inhibited phagosome formation as well as phagosome maturation arrest through microtubule perturbations. Several viral role players have been implicated here, such as the viral negative factor (Nef) (Mazzolini et al. 2010) and the regulatory viral protein (Vpr) (Dumas et al. 2015). Although we could not find a study to specifically implicate PI3k in these mechanisms, it is highly likely that these mechanisms are also PI3k related, since both Nef and Vpr (as well as Tat) have been shown to achieve several other effects, such as Regulated on Activation, Normal T Cell Expressed and Secreted (RANTES) production and down-regulation of the ARF6 endocytic pathway, via PI3k-dependent routes (Blagoveshchenskaya et al. 2002; Zhu et al. 2009; Gangwani et al. 2013; Nookala et al. 2013).

2.3.2. Interference with Phagosome Acidification

Hydrolase deficiency and retarded acidification are mainly brought about in two ways by *M. tuberculosis*. Firstly, hydrolysis is exacerbated by limited expression of Rab7. This GTPase has been shown to transiently localise to mycobacterial phagosomes, preventing needed RILP recruitment, but also limiting cathepsin D protease delivery

(Seto et al. 2010). Secondly, mycobacteria also stimulate dissociation of the V-ATPase associated Rab20, preventing phagosomal acidification (Seto et al. 2011).

2.3.3. Prevention of Lysosome Fusion

Leishmania promastigotes are phagocytosed into phagosomes that retain TACO, blocking fusion with lysosomes and ensuring a neutral pH environment in which this parasite can multiply and differentiate into its amastigote stage (Mukkada et al. 1985; Ferrari et al. 1999). However, after differentiation, this parasite allows phagosome fusion with lysosomes to achieve an acidic environment in which the amastigotes can thrive. Interestingly, these phagosomes then also exhibit low expression of late phagosomal/endosomal markers such as LAMP, V-ATPase and Rab7 (Vinet et al. 2009)

In addition to preventing lysosome fusion, *Leishmania* further protects itself by inhibited recruitment of nicotinamide adenine dinucleotide phosphate (NADPH) oxidase to the phagosome, resulting in perturbed ROS production (Moradin & Descoteaux 2012). Similarly, *M. tuberculosis* was reported to stimulate release of Tumour Necrosis Factor α (TNF- α) and interleukin 10 (IL-10) by infected macrophages (Sendide et al. 2005), resulting in a deactivation of ROS and NOS release from these macrophages (Redpath et al. 2001) to inhibit their microbicidal effect. IL-10 specifically also down-regulates secretion of pro-inflammatory cytokines like interferon gamma (INF- γ) and TNF- α (Redpath et al. 2001) and results in a shift toward a Th2-type cell expansion in the alveoli (de Almeida et al. 2012) with a shift towards an alternatively activated, anti-inflammatory, M2 macrophage phenotype (Smith et al. 2008).

These studies illustrate quite clearly that pathogens are able to manipulate the phagocytic process in various different ways. In doing so, they ensure not only their

survival, but also their propagation and distribution through the host. However, in our opinion, it is also this manipulability of the phagocytic process that makes it ideal for use in regenerative medicine.

2.4. Harnessing the Phagocytic Process for Medicine

The current detailed understanding of the exact molecular mechanisms governing phagocytosis as well as perturbations achieved by pathogenic mechanisms, allows exploitation of this process for therapeutic purposes. After thorough study of the relevant literature, we have formulated a hypothesis on the use of this knowledge for potential therapeutic application in regenerative medicine and possibly other clinical fields as well.

Macrophages can engulf particles seemingly endless in size if one takes into account the suicidal “frustrated phagocytosis” reported by Cox et al. (1999). This suggests that they are able to engulf the majority of pathogenic microbes and almost all host somatic cells. Other factors influence phagocytosis, such as bacterial receptor ligands and macrophage co-stimulation by T-cells or other innate immune cells (e.g. NK cells) (Liu et al. 2013). Fortunately, the innate immune system has evolved to ensure macrophage target affinity and specificity together with the capacity to reach isolated tissue areas to neutralise hidden pathogens (Mills et al. 2015). Unfortunately, pathogen evolution alongside macrophages has equipped them with mechanisms to elude host defence, many of which are centred on perturbing phagocytosis to sustaining the pathogen inside macrophages. Though unwanted and detrimental to the host in the presence of pathogens, we believe that these modulations that pathogens can elicit on the process of phagocytosis, may be exploited for gain. We hypothesise that by inducing phagosome maturation arrest in a manner similar to that

of pathogens, but without pathogen involvement, the highly motile macrophages may be modified to render them useful as shuttles to carry “cargo” to specific areas within the host. The nature of this cargo could range from drugs to be delivered, to live stem cells, depending on the therapeutic aim. Of all potential options, the idea of a macrophage carrying a live stem cell – for example to increase muscle regenerative capacity in patients suffering from myodystrophy – is most enticing.

Let us consider for a moment what this would practically entail. Fundamentally, these macrophages would have to be isolated from patient blood and modified *in vitro* in order for it to maintain an ingested stem cell in a viable state within its phagosomes after autologous reinfusion. To achieve this, we propose induction of “artificial” phagosome maturation arrest. This will have to be achieved in a manner that will not compromise macrophage capacity for particle ingestion. A variety of methods by which this may be achieved have been unknowingly uncovered by researchers elucidating the details of phagosome maturation. Below, we evaluate the feasibility of these methods in terms of safety for *in vivo* application.

2.4.1. Macrophage IL-10 Enrichment

IL-10 is used by *M. tuberculosis* as a powerful inhibitor of phagosome maturation, discussed earlier. This is also supported by O’Leary et al. (2011) who found that macrophages containing killed *M. tuberculosis* produced less IL-10 than cells infected with live *M. tuberculosis*, showing that *M. tuberculosis* upregulates IL-10 production to protect itself against destruction. As this anti-inflammatory and anti-microbicidal cytokine is produced *in vivo* one can argue that it is a promising agent to use for therapeutic phagosome maturation arrest, although some problems do exist.

As shown previously, the IL-10-mediated maturation inhibiting effect of *M. tuberculosis* is also dependent on MAPKp38 activation in human macrophages (Song et al. 2003). This is supported by data reported by O'Leary et al. (2011), who significantly restored phagosome maturation by inhibiting MAPKp38 in *M. tuberculosis*-containing macrophages. Subsequent addition of rIL-10 to these cells resulted in the reoccurrence of maturation arrest, testifying to the plasticity of this technique. However, O'Leary et al. (2011) reported that the IL-10-induced maturation arrest occurs both in the presence of viable and non-viable *M. tuberculosis*, but not in its absence, suggesting that *M. tuberculosis* infection is necessary for IL-10 to induce maturation arrest. This problem can probably be overcome by identification of the essential bacterial component, which – if not antigenic or pathogenic itself – can be administered as co-treatment. A more problematic fundamental flaw to this approach is the phenotypic change that IL-10 effects in macrophages. IL-10 is known to polarize macrophages towards the alternatively activated (M2) phenotype (Chazaud et al. 2009; Mia et al. 2014). Although the anti-inflammatory phenotype is desired in terms of resolution of inflammation and wound healing, M2 macrophages do not readily cross endothelial barriers (Arnold et al. 2007). This would significantly inhibit the actual delivery of the ingested stem cell to the intended target tissue. This complication however highlights the need for another step in the process – macrophages will have to be polarised towards the M1 phenotype, to ensure sufficient mobility.

2.4.2. Brefeldin A Treatment

The fungal antibiotic, Brefeldin A (BFA), inhibits a subtype of Golgi associated GEFs (ARF-GEFs) that facilitate the GDP/GTP cycling of ARF family proteins (Donaldson et al. 1992). These ARF-GEFs express a Sec7 domain that Brefeldin A recognises and inhibits by direct binding to it (Shin & Nakayama 2004). ARFs play a central role in

regulating plasma membrane traffic (Zhang et al. 1998), actin polymerization and activating phosphatidylinositol kinases for phosphatidylinositol production. Active ARF mediated membrane trafficking is controlled via coat proteins expressed on cellular transport vesicles (Kreis et al. 1995). ER and Golgi bilaterally traveling transport vesicles are coated with proteins such as calnexin and coat protein complex type I (COPI) and type II (COPII) (Letourneur et al. 1994). COPI is recruited to phagosomes and contributes to recycling of phagosomal components (Berón et al. 2001). Active ARF1 is necessary for this COPI recruitment and inhibited COPI expression has been shown by Berón et al. (2001) to partly perturb phagosomal recycling events. Thus, because BFA sensitive ARF-GEFs control ARF1 activity that in turn allows COPI recruitment, BFA treatment could potentially induce phagosome maturation arrest by preventing sufficient recycling of phagosomal components. However, Beemiller et al. (2006) found BFA-mediated inhibition of ARF-GEFs did not lead to subsequent inactive ARF1 expression on phagosomes. This suggests that the cells adapted to ARF-GEF inhibition by recruiting GEFs that are insensitive to BFA treatment. In addition, dual specificity of ARF was reported for BFA: ARF1 and ARF5, but not ARF6 – the main ARF implicated in encapsulation – was reported to be sensitive to BFA (Zeeh et al. 2006). The effect of BFA on phagosome maturation thus remains largely unknown.

2.4.3. Microtubule or Dynein Inhibition

As mentioned earlier, dynein is vital for centripetal and centrifugal delivery of phagosomes to lysosomes for fusion. The dynactin complex has been shown to facilitate cargo binding to dynein for centripetal movement (Blocker et al. 1997), while the Rab5 GTPase regulates motility of endosomes (Nielsen et al. 1999), likely through a phosphoinositide and EEA1 dependent manner. It is widely accepted that

microtubule disruption negatively influences phagosome centripetal movement and coinciding maturation. In regard to this, Blocker et al. (1996) has shown inhibition of phagosome movement via microtubule disassembly after nocodazole treatment. Nocodazole could thus induce phagosome maturation arrest, but the associated microtubule disassembly could perturb pseudopod extension via inhibited PI3k delivery, thereby inhibiting uptake of stem cells into macrophages. Furthermore, it is possible that nocodazole induced microtubule disassociation could block cellular motility and chemotactic reactivity, ablating the very characteristic of macrophages we intend to exploit.

Thus, placing focus on dynein motor inhibition could pose a more viable solution. Ciliobrevin D is a dynein motor blocker that inhibits the GTPase activity of dynein (Chou et al. 2011). Ciliobrevin D is also a dynein specific inhibitor and does not affect kinesin-1 and 5 ATPase activity (Firestone et al. 2012), making this compound a promising unidirectional inhibitor of centripetal movement only. Furthermore, Ciliobrevin D does not disrupt microfilament structure (Misawa et al. 2013). Moreover, Sainath & Gallo (2014) found that Ciliobrevin D inhibited bidirectional mitochondria, lysosome and Golgi-derived vesicle transport. Ciliobrevin D has recently been suggested as modulator of lysosome mechanics (Lin et al. 2015) and has been used in autophagy studies (Li et al. 2016). It has further been utilised to elucidate the formation of NLR pyrin domain containing 3 (NLRP3) mediated inflammasome formation in bone marrow derived macrophages (Misawa et al. 2013), but its effects on phagosome maturation have not been reported. This compound seems to be promising for the purpose of inducing phagosome maturation arrest and should be further investigated in this context.

2.4.4. Wortmannin

This fungal steroid metabolite is a known potent, selective and irreversible inhibitor of all three PI3k subtypes (Vieira et al. 2001) via covalent binding (Yuan et al. 2007). A subsequent study by Vieira et al. (2003) reported virtually complete elimination of phagosome fusion with late endosomes and lysosomes after Wortmannin treatment. These inhibitory roles for Wortmannin suggest it to be an ideal candidate for our purposes. However, not all effects of Wortmannin are equally desired. For example, PI3K-inhibition by Wortmannin was reported to enhance TLR-mediated inducible nitric-oxide synthase (iNOS) expression, to activate NF- κ B and to up-regulate cytokine mRNA production (Hazeki et al. 2006), suggesting a pro-inflammatory role. In addition, Wortmannin treatment was also shown to prevent large particle ($>3\mu\text{m}$) engulfment through inhibiting PI3P formation (Cox et al. 1999). Together these data suggest that the use of Wortmannin for macrophage modification will require a finely optimised protocol, to ensure maximal phagosome maturation arrest, without compromising the encapsulation process or eliciting an inflammatory response.

2.4.5. Concanamycin A

Concanamycin A is a plecomacrolide that specifically inhibits the V-ATPase proton pump. This enzyme is responsible for energizing the membranes of eukaryotic cells, both intracellular and plasma membranes (Huss et al. 2002). V-ATPase is also expressed on the late phagosome and ensures an acidic pH during phagosome maturation. The V-ATPase consists of two complexes, the catalytic V_1 located on the cytosolic side of membranes and the translocating V_0 unit bound to the membrane (Huss & Wieczorek 2012). Concanamycin A covalently binds to the subunit c of the translocating V_0 complex (Huss et al. 2002), thereby preventing proton influx into

phagosomes, resulting in an alkaline pH of about 7.5 (Yates et al. 2005). Concanamycin A is commonly used in experimental models for its inhibition of autophagy (e.g. Yano et al. 2016).

2.4.6. Chloroquine

Chloroquine is a 4-aminoquinoline that indirectly prevents acidification of intracellular vacuoles (Akpovwa 2016). This weak base accumulates within vacuoles or phagosomes via ion trapping and reduces the pH to about 6.5 if used at 10 μ M (Weber et al. 2000). This compound is readily used as an anti-malarial drug and was very recently suggested as a possible Ebola drug, since its alkalinizing action would prevent intracellular viral replication, provided that its concentration can be maintained at effective dose (Akpovwa 2016). The fact that chloroquine is a known medication is a benefit, since its safety for human consumption has been established. Similar to Concanamycin A, chloroquine has proven efficacy in the context of (auto)phagosome maturation arrest.

From this information, we conclude that a number of potential treatments may be considered as candidate treatments with which to achieve macrophage modification for the purpose of hosting one or more live stem cells, increasing the feasibility of our hypothesis.

2.4.7. Additional Factors to Consider

Of course, although the maintenance of the stem cell inside the macrophage is a major consideration and an important problem to solve, it is not the only one. In order for the stem cells to be ingested by the modified macrophage, they will have to be opsonised, especially since autologous cells will ideally be used for this technique, to

minimise side-effects. Furthermore, the opsonisation process should not interfere with stem cell function after delivery at the site earmarked for regeneration. However, we believe that this can be overcome using advanced technology and a multidisciplinary approach. Recently, great advances have been made in the field of abiotic membrane-active polymers that can coat cell membranes whilst maintaining cell viability (Marie et al. 2014). These polymers can be “decorated” with an opsonin to enhance encapsulation, after which the polymer can be deconstructed by e.g. slight temperature change or vibration.

Another question is whether the number of stem cells ingested should be limited. From the frustrated phagocytosis model, it is known that macrophages have an exceptional capacity for membrane “extension”, so that several stem cells can theoretically be ingested by an individual macrophage. Indeed, this was the case in preliminary studies in our lab (Visser & Smith, unpublished data). However, we believe that the number of stem cells ingested per macrophage can be limited by optimising the time allowed for engulfment. Alternatively, flow cytometry sorting could be employed to sort for cells with optimal number of ingested stem cells.

Once reinfused, macrophages should naturally migrate to sites requiring regeneration. Of course, in order to achieve maximal benefit, the chemotactic signal could also be manipulated, and the known vast array of exciting tracking methods may be employed to track the final destination of the modified macrophages. These processes are, however, not within the scope of this review, which is focused on modification of the macrophage itself.

The final consideration to include in this review is the release of the stem cell at the appropriate destination site. A plethora of mechanisms exist to induce cell death or

exocytosis. One example is Brefeldin A. Although it has doubtful application for phagosome maturation arrest, BFA may prove useful in later stages of cell cargo delivery, by inducing apoptosis in the macrophage. BFA can induce ER stress (Tseng et al. 2014) through inhibited anterograde protein trafficking between the ER and Golgi (Alvarez & Sztul 1999). Prolonged BFA treatment can cause chronic ER stress and subsequent mobilization of the compensatory unfolded protein response (UPR). If the UPR is unable to resolve ER stress, this compensatory mechanism shifts from pro-survival to pro-death and mobilizes cell death responses like apoptosis (Hetz 2012). Apoptosis is achieved under chronic treatment conditions (15h – 40h) (Alvarez & Sztul 1999), which allows sufficient time for the processes of engulfment, reinfusion and *in vivo* transportation to be completed. A favourable consideration in this context is that BFA does not affect engulfment capacity of large (3 μ m) or small (0.8 μ m) particles, despite its ER traffic inhibitory effects (Becker et al. 2005), possibly due to the insensitivity of ARF6 to BFA mentioned earlier. Of course, as with all other phases, other candidate methods – such as targeted exocytosis – should also be considered and optimised. *Leishmania donovani* promastigotes multiply and differentiate into amastigotes inside arrested phagosomes (Moradin & Descoteaux 2012). These amastigotes then escape the macrophage to continue their life cycle. This poorly understood phenomenon could be exploited to induce exocytosis in stem cell carrying macrophages.

2.5. Summary

In summation, modern science has substantially increased our understanding of molecular role players not only in the phagocytic process, but also in regenerative medicine. We firmly believe that by pooling resources across multiple disciplines, the

remaining obstacles can be overcome to achieve the therapeutic technique we outlined here. If phagosome maturation could be arrested, these macrophages could be used as an *in vivo* delivery system for phagocytosed “cargo”.

Delivery of laboratory-enhanced or conditioned stem cells, using an autologous physiologically relevant vehicle, will be a significant step forward in terms of individualised medicine, and especially in disease states where no current mainstream therapy has proven effective.

2.6. Hypothesis

The scope of this thesis was to address the first steps in creating such a delivery system. We hypothesised that macrophage phagosome maturation arrest could be experimentally induced by *in vitro* treatment with a Wortmannin, Concanamycin A and Chloroquine cocktail, without limiting phagocytic engulfment capacity or transendothelial migratory capability of macrophages.

2.7. Objectives

In order to test our hypothesis, we formulated the following objectives:

1. Isolation of a pure population of primary monocytes
2. Culturing and polarisation of peripheral human monocytes to induce a classically activated (M1) macrophage phenotype
3. Inducing M1 phagosome maturation arrest by acute administration of a combination of Wortmannin, Concanamycin A and Chloroquine.
4. Developing a model to qualitatively and quantitatively assess phagocytic and digestive capacity.

5. Determination of relative migration capacity of M1 macrophages after phagosome arrest treatment.

Chapter 3: Materials and Methods

This chapter deviates from the typical format of a thesis methods chapter. Since method development was a big part of my research topic, it is (in my opinion) important to also present the process followed. Therefore, apart from the optimised method, various technical considerations and the process through which the final protocol was derived, will also be presented. Methods are presented chronologically, to illustrate the sequence of multiple steps which all had to be synchronised to achieve a result.

3.1. Cell Type Selection

Primary isolated human monocytes were chosen above immortalised cells lines for a number of reasons. Firstly, it was decided that, given the multi-stepped complexity of the process and the numerous role players involved when manipulating a physiological, and specifically an immunological, process, the *in vitro* work should resemble the *in vivo* situation as closely as possible. In this way, the transfer from *in vitro* to eventual *in vivo* application should progress more smoothly - practical translation of results for human therapeutics was an important consideration in the design of this study. Secondly, and related to the applicability of data to *in vivo* situations, repeated exposures to low temperatures or DMSO (as is common practise in cell culture maintenance) may result in anomalies in these cells that may affect assessments made. Just one example of such a change is the perturbation in cytochrome P-450 activity after exposure to 0.1% DMSO (Busby et al. 1999). Thirdly, established immune cell lines such as THP-1 cells were originally isolated from unhealthy donors, in this case acute monocytic leukaemia (Tsuchiya et al. 1980), but not all abnormalities of these cells have been recorded, so that it is not possible to ascertain normality of the cell mechanics that we proposed to investigate here. Lastly,

in our experience, although primary macrophages are notoriously adherent, commercial macrophage lines are considerably less adherent in culture. This suggests an alteration in adhesion molecule expression in these cells and given the importance of cell adhesion in cell migration, this is perhaps the most clear-cut reason for our choice to opt for using primary cells.

3.2. Ethical Considerations

Ethical clearance exemption for isolation of human monocytes from purposely donated blood was obtained from the Subcommittee C Human Research Ethics Committee (HREC) of Stellenbosch University (Reference # X15/05/013).

3.3. Monocyte Isolation

Buffy coats were collected specifically for our study by the Western Province Blood Transfusion Service (WPBTS), using donors between the age of 18 – 25 years. Donors were informed of the study and consent were obtained from all donors, by the WPBTS. Monocytic population isolation was performed within 8 hours of each donation. A double gradient centrifugation protocol was employed, as this protocol is more widely used in blood cell separation and avoids possible confounding and/or undesired effects, such as possible inactivation of CD14 surface complexes (associated with antibody binding), which is commonly associated with positive Magnetic-Activated Cell Sorting (MACS) and Fluorescence-Activated Cell-Sorting (FACS) (Tomlinson et al. 2013).

Briefly, buffy coats – containing all circulating leukocytes together with residual erythrocytes and platelets – were layered onto Histopaque 1.077 g/ml (Sigma-Aldrich, #10771) at a 2:1 ratio and centrifuged at 400 x g for 30 min at 23°C. Peripheral Blood

Mononuclear Cells (PBMCs) were collected with a plastic Pasteur pipette and washed twice in PBS-EDTA (1x Phosphate Buffered Saline containing 0,5 M Ethylenediaminetetraacetic acid) (Sigma-Aldrich, #P4417 + #E9884) at 300 x g for 10 min at 23°C. Purified PBMCs were resuspended in RPMI 1640 without phenol red (Sigma-Aldrich, #R0883), containing 10% FBS (Fetal Bovine Serum) (Sigma-Aldrich, #12003C) and layered onto a 42.56% iso-osmotic 1.131 g/ml percoll (Sigma-Aldrich, #E0414) solution at a 1.25:1 ratio. The iso-osmotic percoll solution consisted of 48.6% advanced RPMI 1640 with phenol red (Life Technologies, #12633-020), 42.56% percoll, 5.4% FBS and 3.44% 10x PBS. Separation of monocytes from PBMCs was achieved at 550 x g for 30 min at 23°C. Monocytes were collected with a plastic Pasteur pipette and washed once in PBS-EDTA at 400 x g for 10 min at 23°C. Monocytes were then resuspended in Complete Monocyte Media (CMM).

3.4. Culture Conditions

Complete Monocyte Media consisted of advanced Roswell Park Memorial Institute medium (RPMI) 1640 with phenol red containing 10% Human Serum from AB patient (Sigma-Aldrich, #H4522), 100 U/mL Penicillin-Streptomycin (PenStrep) (Life Technologies, #15140148) and 2 mM Glutamax (Life Technologies, #35050-061).

Monocytes were seeded at 4×10^6 cells/well (2×10^6 cells/ml) onto Nunc UpCell™ plates (AEC-Amersham, #174901) or 35 mm culture dishes (Bio-Smart Scientific, #20035) and cultured with CMM. Images of cell monolayers were taken at time points 24 hours, 96 hours and 144 hours to assess differentiation. In order to promote differentiation into M1 type macrophages, 50 ng/ml GM-CSF (Granulocyte Macrophage Colony-Stimulating Factor) (Sigma-Aldrich, #SRP3050) was added to each well directly after seeding (Mia et al. 2014). Similar, 50 ng/mL M-CSF (Macrophage Colony-Stimulating

Factor) (Sigma-Aldrich, #SRP3110) was added to each well to promote M2 type macrophage differentiation, when appropriate. Growth factors were added after every media change. Cells were allowed to adhere for 24 hours after which media was aspirated, cell monolayers washed with warm PBS and fresh media introduced. Thereafter media was changed every 72 hours. Cells were cultured for a total of 6 days. Incubator conditions were kept at 37°C with an 80% humidified environment and 5% CO₂.

3.5. Pre-differentiation and Polarisation

Following pre-differentiation with GM-CSF and M-CSF as described earlier, macrophages were polarised to M1 phenotype via pre-treatment with 50 ng/ml LPS (Lipopolysaccharide) (Sigma-Aldrich, #L2762) and 20 ng/ml IFN- γ (Interferon-gamma) (Sigma-Aldrich, #I3265) for a period of 24 hours (Liu & Yang 2013). Similarly, M2 macrophage polarisation was done with 20 ng/ml each of IL-4 (Interleukin 4) (Sigma-Aldrich, #SRP4137), IL-10 (Interleukin 10) (Sigma-Aldrich, #SRP3071) and TGF- β (Transforming Growth Factor beta) (Sigma-Aldrich, #SRP3171) for a period of 24 hours. A M1 and M2 population was cultured to better determine induction of M1 phenotype when expressed against the opposite, M2 phenotype. This is a better representation than an unpolarised population, defined as M0, but likely consisting of a mixed population of M1 and M2 macrophages, expressed in scatter plots as a double signal peak for M1 markers (as shown in **Section 4.1, Figure 4.2**). The pro-inflammatory M1 phenotype was specifically used in this study for its transendothelial migratory capability (Arnold et al. 2007) that fit the delivery requirements of this project. Furthermore, despite controversial reports of GM-CSF treatment promoting M1 phenotypic differentiation (Mia et al. 2014), other reports led to the choosing of this

cytokine for our study purposes. For example, a recent paper claimed increased migration and chemotaxis after treatment with this cytokine (Dabritz et al. 2015), which would further promote cell migratory capacity. Additionally, the phagocytic capacity or engulfment capacity of macrophages has been shown to increase after treatment with this cytokine (Eischen et al. 1991). This is important for our study because the engulfment aspect of phagocytosis needs to be maintained after phagosome maturation arrest. The arrest inducing agent, Wortmannin, has been shown to prevent engulfment of large (>3 μm) particles (Vieira et al. 2001). In this regard, GM-CSF treatment was used to maintain engulfment capacity.

Macrophage differentiation was also recorded over time using a phase contrast DSZ5000X inverted biological microscope (Lasec, South Africa) with ScopeTek software and DCM-510, 5 mega pixel camera. A representative population was imaged 24 hours, 96 hours and 144 hours after isolation at 20x magnification. This was done to evaluate morphological changes during differentiation.

3.6. Culture Detachment

Monocytic cells are notoriously adherent, which poses some technical difficulties when cultures have to be maintained for a number of days. Cells used in the transmigration assay were seeded and harvested from Nunc UpCell™ plates. To save costs, cells designated for analysis using live cell imaging and flow cytometry were seeded, maintained and harvested from 35mm culture dishes using Accutase® (Sigma-Aldrich, #A6964) cell detachment solution. Macrophages were challenged against antibody opsonised polystyrene bead (AbsBeads) after being harvested with either method. The ability of both UpCell™ and Accutase® methods to allow AbsBeads phagocytosis directly after reseeding, was similar, indicating well preserved functionality with both

methods for the purposes of this study. The next paragraphs will provide some more specific detail on these two culture methods.

3.6.1. Nunc UpCell™ Plates

UpCell™ plates are coated with a temperature responsive polymer called poly(N-isopropylacrylamide) (PIPAAM). This dynamic polymer is capable of cycling between hydrophobic and hydrophilic states, depending on ambient temperature. PIPAAM is hydrophilic at 20°C, causing hydration and extension of the polymer. The hydrophilicity of the surface interferes with protein adsorption and subsequently results in cell detachment (Collier et al. 2001). The turning point of PIPAAM between hydrophilicity and hydrophobicity is 32°C; this point is defined as the lower critical solution temperature. At 37°C the hydrophobic polymer is dehydrated, causing contraction of PIPAAM. The hydrophobic surface is capable of stronger binding to the interior of cell surface proteins, compared to hydrophilic surfaces, leading to cell adhesion (Lampin et al. 1997). Accordingly, UpCell™ plates were placed onto warmed (37°C) gel packs when removed from the incubator to change media or introduce growth factors, in order to maintain the hydrophobic state. Cell detachment was achieved by removing UpCell™ plates from the incubator, aspirating media and replacing with advanced RPMI 1640 at a temperature of only 10°C. Plates were then incubated at 10°C. Similar to Collier et al. (2001), we found that primary macrophages optimally detached when incubated for 60 min. Cell viability was maintained after this incubation period. In order to limit exposure time to low temperature, plates were only incubated for 30 min at 10°C after which the cell monolayer was carefully scraped off with a cell scraper. This adaption increased total cell yield, but had no noticeable effect on viability. Thus 60 min incubation was used to limit mechanical stress associated with handling cells.

3.6.2. 35mm Culture Dish with Accutase® Method

A pilot study using 8-chamber slides with glass culture surfaces (which was required to facilitate live cell imaging and reduce reagent turnover) revealed a reluctance of primary monocytes to adhere to glass. Conversely, monocytes potently adhered to polystyrene surfaces of 35mm culture dishes. These dishes were also compatible with confocal live cell imaging. Harvesting primary monocytes with trypsin broke down surface pseudopodia resulting in cell death. Accordingly, macrophages were harvested with Accutase® cell detachment solution. Media was aspirated, cell monolayer washed with 23°C PBS and 1 ml Accutase® injected onto dishes. Cells were incubated at 23°C for 10 min after which dishes were swirled and another 1 ml Accutase® added for further incubation of 10 min at 23°C. Cells were collected and centrifuged at 400 x g for 5 min at 37°C. Accutase® cell detachment solution auto-inhibits at 37°C eliminating the need to neutralise with media.

3.7. Macrophage Phenotype Analysis

After pre-differentiation and macrophage M1/M2 polarisation, macrophage phenotype was quantitatively confirmed by flow cytometry (BD FACSAria Cell Sorter, Becton Dickinson, USA), using BD FACSDiVa v6.1.3 software. Single stain and multiple stain solutions were prepared by mixing appropriate amounts of fluorescent antibody markers with 1 ml PBS. Media was aspirated from culture dishes and replaced with appropriate 1 ml single stain or multiple stain PBS solution. Antibody binding was facilitated at 37°C for 10 min before PBS was removed and cells harvested with Accutase®. Harvested populations were centrifuged at 400 x g for 5 min at 37°C and resuspended in warm PBS. Populations were filtered, relocated to flow cytometry tubes and immediately analysed. Unstained samples were prepared to determine

background fluorescence. Single stain samples (containing only one marker) were used for fluorescent signal optimisation and compensation for potential spill-over between fluorophores. Multiple stain samples were used for data collection and labelled with the following fluorescent antibody markers: Alexa Fluor 647 Rabbit Anti-Human CD274 (PD-L1) (640/665nm) (Cell Signalling, #15005S), BB515 Mouse Anti-Human CD86 (490/515nm) (BD Bioscience, #564544) and V450 Mouse Anti-Human MHCII (HLA-DR) (405/448nm) (BD Bioscience, #561359). The appropriate lasers were used to excite fluorophores and emission was captured using appropriate band pass filters. Data collection was done by recording 3×10^5 events for every donor in triplicate and thresholds were set up by recording 8×10^6 events. After appropriate training in the technical flow cytometry procedures by a staff member of the Central Analytical Facility (CAF) at Stellenbosch University, I was able to perform these analyses independently.

3.8. Modulating Macrophage Phagosome Maturation

Phagosome maturation arrest was induced in order to preserve the “cargo” to be delivered by macrophages within M1 macrophages. Briefly, cells were pre-treated with $10 \mu\text{M}$ Chloroquine (Sigma-Aldrich, #C6628) from 1h before initiation of phagocytosis, followed by 100 nM Wortmannin (Sigma-Aldrich, #W1628) at 30 min prior to phagocytosis and 100 nM Concanamycin A (Sigma-Aldrich, #C9705) immediately before initiation of phagocytosis. Macrophages were incubated in an 80% humidified environment at 37°C with 5% CO_2 throughout this period. Chloroquine is a weak base capable of permeating cell membranes. Exposure to this compound specifically leads to its accumulation in lysosomes, causing alkalinisation thereof and preventing fusion with phagosomes (Yang et al. 2013). This agent also non-specifically increases the

pH of phagosomal as well as other vacuolar cell structures, such as autophagosomes. Similarly, Concanamycin A contributes to a less acidic phagosomal lumen by specific inhibition of V-APase proton pump. Covalent binding to this enzyme prevents proton influx into phagosomes (Huss et al. 2002). The higher alkalinity induced by these agents functionally contribute to phagosome maturation arrest by preventing protein degradation. Conversely, Wortmannin directly contributes to the induction of phagosome maturation arrest by covalently binding to PI3ks (Vieira et al. 2001). Binding inhibits production of PI3P and other phosphatidylinositols chiefly needed for phagosome maturation.

3.9. Visualisation of Ingested “Cargo” Using Fluorescent Beads (AbsBeads)

Blue fluorescent carboxylate modified polystyrene beads (either 4.5 μm or 6 μm in diameter) (Polysciences, #18340-5 + #19102-2) were used as a stem cell model. The 4.5 μm diameter beads were chosen for their similar size to skeletal muscle satellite cells and served as representation during transmigration assays. Furthermore, the 6 μm beads were used to determine the phagocytic capacity of phagosome maturation arrested macrophages compared to digestive macrophages, since Wortmannin treatment was previously reported to limit the size capacity of phagocytosis (Vieira et al. 2001). Since normal digestive phagosomes are unable to break apart polystyrene beads, beads were coated with a digestible IgG protein in order to facilitate visualisation of intraphagosomal digestion. (The carboxylate modification on these microspheres can be activated to allow covalent binding to proteins.) Fluorescent Alexa Fluor 647 Goat Anti-Human IgG (Life Technologies, #A21445) was chosen as protein coating. The antibody coating allowed visualisation and identification of beads

in maturation arrested phagosomes in comparison to those in digestive phagosomes. A loss in red fluorescent signal would be suggestive of digestion – irrespective of the reason for the signal loss, which could be antibody protein degradation, conjugated fluorophore inactivation or breakage of covalent bonds between antibody and bead. Antibodies were coated onto beads using a protocol obtained from Life Technologies (Invitrogen 2001). After adaptation of this protocol, antibody coating was achieved by dissolving 2 mg/ml IgG solution in 50 mM MES (2-(*N*-morpholino)ethanesulfonic acid) buffer (Sigma-Aldrich, #M5287) and adding 5 ml of 4.5 μm or 6 μm bead suspension to the solution. The solution was incubated at 23°C for 30 min to allow for antibody coating. EDAC (1-ethyl-3-(3-dimethylaminopropyl)- carbodiimide) (Sigma-Aldrich, #E2247) was added to a final concentration of 0.4 mg/ml and thoroughly vortexed. The pH was adjusted to 6.5 ± 0.2 using dilute NaOH and placed on an orbital shaker to incubate overnight at 23°C. The addition of EDAC and increase in pH serves to prevent bead agglomeration during overnight incubation. Glycine (Sigma-Aldrich, #G7126) was added to a final concentration of 100 mM and solution was incubated at 23°C for 1h. Beads were pelleted by centrifuging at 4000 x g for 20 min at 23°C and washed three times with 50 mM PBS at the same centrifugal velocity. Beads were resuspended for storage in 50 mM PBS containing 2 mM sodium azide at $2.89 \times 10^7/\text{ml}$ stock. According to the supplier, these antibody coated beads, hereafter referred to as AbsBeads, retained the IgG coating for up to 17 months when stored at 4°C.

Noteworthy, false positives can be yielded from passive adsorption (not absorption) of positively charged particles to the external surface of the cell membrane (Thiele et al. 2001). However, this is not applicable to our study as the negatively charged carboxylate modified beads used, do not tend to do this. Flow cytometric analysis also

served to distinguish between free bead populations and beads ingested into macrophages (**Appendix C**), averting this problem.

3.10. Phagocytosis

Macrophage recognition and engulfment of foreign material is achieved *in vivo* through secondary stimulation by other cell types such as CD4⁺ T-cells and NK cells (Liu et al. 2013). In the absence of these supportive cells *in vitro*, engulfment is possible through Fcγ receptor engagement with IgG opsonised material, as shown in numerous studies (Vieira et al. 2001; Hazeki et al. 2012; Segawa et al. 2014). However, this is only achieved if IgG opsonin is of same-species origin or if the FcγR possesses cross-species reactivity to foreign IgG. Specifically, a lack of human neonatal Fc receptor (FcRn) cross-reactivity to sheep, rat, mouse and bovine IgG has been reported (Ober et al. 2001). This antibody scavenging FcRn did however possess rabbit and guinea pig cross reactivity. These findings can be extrapolated to other FcR subtypes such as FcγR. Therefore, the cross reactivity of macrophage FcγR to goat IgG was addressed in the present study. The Alexa Fluor 647 Goat Anti-Human IgG used to coat and opsonise AbsBeads was not recognised by primary M1 macrophages, expanding on previous FcRn-cross-reactivity data. Thus, the AbsBeads required additional IgG opsonisation to induce engulfment by human macrophages, and therefore, AbsBeads were incubated in serum obtained from a healthy (O+) donor. Experimentally-induced perpetually activate unbound carboxylate modifications on AbsBeads allowed nonspecific binding of serum proteins, resulting in macrophage recognition and engulfment.

AbsBeads solution was incubated with serum at a 1:1 ratio for 24h. AbsBeads were then introduced into M1 macrophage population at 1.156×10^6 AbsBeads/well, marking

the initiation of phagocytosis. Phagocytosis and particularly phagosome maturation arrest was assessed over a 2h period.

3.10.1. Live Cell Imaging of Phagocytosis

Visual representation of phagocytosis was recorded with a Carl Zeiss LSM780 confocal microscope with ELYRA S.1 Superresolution platform (Carl Zeiss, Germany) using ZEN 2011 imaging software. This allowed qualitative analysis of digestive capacity as well as cell viability, motility and pseudopod extension during recognition and engulfment. Monocytes were appropriately cultured into a M1 macrophage population after which phagosome maturation arrest was induced in treatment groups and AbsBeads introduced into arrest-treatment as well as control groups. Time lapse images were taken for 2 hours from initiation of phagocytosis. Cells were imaged in a humidified environment at 37°C in the presence of 5% CO₂. CellMask™ Orange Plasma Membrane Stain (554/567nm) (Life Technologies, #C10045) was used to label macrophages. CellMask™ non-specifically binds phospholipid bilayers with its hydrophobic anchoring tail and fluorescently labelled hydrophilic head. Fluorescent labelling of conventional membrane markers such as CD14 or CD45 was avoided as antibody binding to these membrane proteins could influence phagocytosis resulting in a statistical false negative. The pH sensitive pHrodo® Green *E. coli* BioParticles® (509/533nm) (Life Technologies, #P35366) were introduced onto cells to distinguish acidic phagosomes. This marker is fluorescent in acidic pH (<6.0) while non-fluorescent in physiological pH. Acidic phagosomes are present in unaffected control samples where phagocytosis is unaltered, while phagosome maturation arrested macrophages exhibit more alkaline pH (>6.0) values. pHrodo® was introduced at a final concentration of 1 mg/ml immediately before the initiation of phagocytosis. AbsBeads were introduced into control as well as treated groups at 1.156×10^6

cells/well. Indigestible blue fluorescent beads distinguished cells devoid of cargo due to digestion thereof from cells devoid of cargo due to not participating in phagocytosis. Similarly, digestible red IgG distinguished cells capable of cargo degradation from phagosome maturation arrested macrophages. Appropriate tracks were set up with optimal individual laser intensities. A random field of view was chosen as representative for the population and imaged at 20x magnification with minimal cycle time between images.

3.10.2. Flow Cytometric Quantification of Phagocytosis

Macrophage engulfment and digestive capacity was quantified with BD FACSAria Cell Sorter flow cytometer using BD FACSDiVa v6.1.3 software. Monocytes were appropriately cultured into M1 population after which phagosome maturation arrest was induced in treated groups. Similar to live cell imaging, AbsBeads and pHrodo® were introduced into media and phagocytosis allowed to commence for 2 hours. No CellMask™ was used to label cells. Media was then aspirated and cells harvested with Accutase®. Harvested populations were centrifuged at 400 x g for 5 min at 37°C and resuspended in warm PBS. Populations were filtered, relocated to flow cytometry tubes and immediately analysed. Unstained samples consisting only of macrophages were prepared to determine background fluorescence. One single stain sample consisted of only AbsBeads with no cells while the second was only pHrodo® treated macrophages. These samples were used in fluorescent signal optimisation and compensation for possible spill-over between fluorophores. Multiple stain samples were used for data collection and consisted of AbsBeads at 1.156×10^6 cells/well and pHrodo® at 1 mg/ml final concentration. The appropriate lasers were used to excite fluorophores and emission was captured using appropriate band pass filters. Data collection was done by recording 3×10^5 events (in this case both cells and beads will

be counted as events) for every donor in triplicate and thresholds were set up by recording 8×10^6 events.

3.11. Transmigration System

The transendothelial migratory capacity of cargo-carrying macrophages was assessed in a co-culture model using BD Falcon Cell Culture Inserts and Companion Plates. The transmigration complex consisted of inserts with membranes at the bottom which were placed into accompanying wells of 24-well plates. Migration through these inserts toward a chemotactic agent was indicative of *in vivo* diapedetic capacity. Inserts had a transparent polyethylene terephthalate (PET) membrane with pore sizes of either 3 μm or 8 μm (BD Bioscience, #353096 + #353067). Inserts were coated with Human Umbilical Vein Endothelial Cells (HUVEC) to better simulate the *in vivo* environment for migration. Reasons for this are; under *in vivo* conditions chemokines bind proteoglycans exposed on endothelial cells, which directs the movement of migrating leukocytes, and effective migration entails movement of macrophages through an endothelial cell layer (Imhof & Aurrand-Lions 2004). Proteoglycan binding maintains access to the leukocyte chemokine receptor binding site on the chemokine (Proudfoot et al. 2000). This allows presentation of the proteoglycan bound chemokine to leukocytes on the luminal side of endothelium. Leukocyte recognition via its G-protein-coupled receptor induces a prompt integrin-activation signal that culminates in migration from circulation into tissue (Imhof & Aurrand-Lions 2004).

Additionally, we simulated different cellular environments under which to test migration efficiency. Firstly, endothelial exposure to LPS and IFN- γ are characteristic of inflamed tissue. This being the tissue type M1 macrophages infiltrate, it is of importance to ascertain the effect thereof on cargo carrying phagosome maturation arrested

macrophages. Secondly, GM-CSF was also added along with the chemokine to appropriate groups. GM-CSF is argued to promote macrophage differentiation more strongly toward a M1 phenotype than M2 (Jaguin et al. 2013). In part, the reason therefore is its production in inflamed tissue areas where monocytes predominantly differentiate to M1, compared to the presence of M-CSF in circulation before migration has occurred (Mia et al. 2014). Additionally, GM-CSF was reported to promote migration and chemotaxis in macrophages (Dabritz et al. 2015) as well as recruitment of undifferentiated monocytes to tissue areas, due to local production of GM-CSF by resident macrophages (Shi et al. 2006). Taken together, these reports could have a profound effect on migration of macrophages into tissue areas expressing this cytokine.

3.11.1. Fibronectin Coating

Human Umbilical Vein Endothelial Cells (HUVECs, gifted from University of Cape Town) are unable to adhere to culture plate surfaces without the appropriate coating. For this reason, HUVECs were cultured on fibronectin-coated surfaces. Briefly, prior to introducing HUVECs, tissue culture flasks as well as transmigration insert-well complexes were coated with 1 $\mu\text{g}/\text{cm}^2$ fibronectin (Sigma-Aldrich, #F0895). The appropriate amount, according to growth area, of 1 mg/ml fibronectin stock was mixed with enough 1x PBS to cover the entire growth area. Flasks or plates were incubated at 37°C for 1 hour to allow coating before the fibronectin-PBS solution was removed and containers left to dry in a laminar flow hood under UV light overnight. Culture containers were placed in resealable sterile bags to preserve sterility. These coated surfaces maintained fibronectin expression and adherence capacity when stored for up to 2 months at room temperature.

3.11.2. HUVEC Cell Culture

HUVEC cells of passage 3 (P3) were thawed from liquid nitrogen-stored cryo vials and injected directly onto fibronectin coated T25 flasks, without centrifugation. DMSO used in freezing was diluted by the addition of 4 ml Complete HUVEC Media (CHM). CHM was made up with Endothelial Cell Growth Medium (EBM) containing 2% FBS, 0.4% Bovine Brain Extract (BBE), 0.1% human Epidermal Growth Factor (hEGF), 0.1% Ascorbic Acid, 0.1% GA (30 µg/ml Gentamicin and 15 µg/ml Amphotericin) and 0.1% Hydrocortisone. EBM was obtained from Lonza (#CC-3121) and the additional compounds were bought as supplementary unit from Lonza (#CC-4133). Media was replaced 24 hours after seeding and there after every 48 hours until 90% confluency. Media was aspirated and HUVEC cells harvested by washing with warm PBS and introducing 0.25% Trypsin (Celtic Diagnostics, #L0931-500). Cell monolayers were incubated at 37°C for 5 min in shaking incubator to allow for cell detachment. Trypsin was neutralised with EBM and cell suspension centrifuged at 1500 RPM for 3 min at 23°C. Supernatant was removed and cell pellet resuspended in appropriate media for seeding in appropriate flask or inserts.

For the transmigration assay, HUVECs were seeded onto fibronectin-coated transmigration inserts at 1×10^5 cells/insert (2×10^4 cells/ml) with 200 µl CHM in the insert as well as 700 µl CHM in the well, to prevent fluid loss through the insert membrane. These HUVECs were cultured for 3 days prior to the start of the transmigration assay to allow formation of a continuous cell monolayer. For migration protocols simulating potential pro-inflammatory physiological conditions, HUVEC cells were also pre-treated with either 50 ng/ml LPS or 20 ng/ml IFN-γ for 24 hours before the start of transmigration assay.

3.11.3. Transmigration Assay

Macrophages were prepared and after a total of 2 hours (UpCell™ harvesting is another 1 hour) AbsBeads-exposed macrophages were collected, centrifuged at 400 x g for 5 min at 23°C and resuspended in Transmigration Media devoid of Chemokine (TM-C) – the latter was prepared with EBM containing 2% FBS, 0.4% BBE and 0.1% Ascorbic acid. Macrophages were introduced onto inserts at 3×10^5 cells/insert (6×10^4 cells/ml) and TM-C media filled up to 200 µl in total for each insert. For this part of the experiment, macrophages were resuspended in EBM media (and not RPMI) in order to prevent adverse effects on the HUVEC monolayer. Hydrocortisone was removed from this step because it is immunosuppressive due to its glucocorticoid nature and could therefore cause a false negative during migration analysis. The hEGF facilitates HUVEC cell proliferation, and because endothelial cells are not proliferative during migration *in vivo* it could influence signalling pathways and hinder chemokine presentation to macrophages, thus it was also omitted from experimentation. Furthermore, since the transmigration step was only 2:30 hours in duration, there was no need for addition of antibiotics such as GA.

Transmigration Media with Chemokine (TM+C) was injected into the bottom well of the insert-well complex at 700 µl final volume for every well. TM+C consisted of 100 ng/ml Monocyte Chemoattractant Protein 1 (MCP-1) (Sigma-Aldrich, #SRP3109) together with the same compounds and concentrations as TM-C. Where appropriate, TM+C also contained 50 ng/ml GM-CSF. LPS and IFN-γ was not added to TM+C. These compounds were used to treat HUVECs and was added to CHM in the upper insert, 24h prior to experimentation, at 50 ng/ml and 20 ng/ml, respectively. MCP-1 was chosen as chemokine for its specificity for monocytes/macrophages, as well as because previous research done in our group has shown it to be effective in a co-

culture setup (Africa & Smith 2015). The MCP-1 protein is relatively large, with a molar mass of 8600 g/mol (8.6kDa), making it susceptible to protein denaturation when made up in solution in the absence of a stabilising agent. Bovine serum albumin (BSA) can be used to stabilize MCP-1 in solution. However, this was not deemed suitable for our purposes, as stabilisation could affect its tertiary structure and interfere with endothelial cell or macrophage recognition and binding to the chemokine (Imhof & Aurrand-Lions 2004).

The transmigration complex was placed in a 80% humidified environment at 37°C with 5% CO₂ and cells were left to migrate for 2:30 hours. At the end of this period, cells were fixed by addition of pre-warmed 4% paraformaldehyde directly into each well and insert, at a volume equal to that of the media in each well. (Fixative was added directly to culturing media to maintain the initial number of cells that could otherwise be washed away if media was removed before fixating). After 10 minutes, the fixative was removed and replaced with 1x PBS. Data acquisition was done using a phase contrast DSZ5000X inverted biological microscope (Lasec, South Africa) using ScopeTek software and DCM-510, 5 mega pixel camera. The entire macrophage population on the bottom of all outer wells were counted at 10x magnification using a cell counter and in the presence of trypan blue (Sigma-Aldrich, #T8154) at a final concentration of 0.014%. Trypan blue was not added to illuminate viable cells (as intact cell membranes are also permeable to trypan blue after fixing), but to increase phase contrast and facilitate counting.

To further simulate *in vivo* conditions, HUVECs were pretreated with IFN- γ and LPS for 24 hours. Treatment of macrophages with IFN- γ has been shown to reduce migratory capacity in response to MCP-1 stimulation via inhibited actin remodelling (Hu et al. 2008). However, this study was done under static *in vitro* conditions and the

cytokine-effect on macrophages was determined, not endothelial cells. IFN- γ induced displacement of the tight junction protein, junctional adhesion molecule (JAM)-A, to the luminal surface of endothelial cells has a negative effect on macrophage migration under static conditions, but no significant effect under simulative blood flow conditions (Imhof & Aurrand-Lions 2004). Furthermore, IFN- γ was reported to induce secretion of macrophage migration inhibitory factor (MIF) in tubular epithelial cells (Rice et al. 2003). The MIF cytokine upregulates macrophage migration, despite its convoluting name, by promoting expression of adhesion molecules such as intercellular adhesion molecule (ICAM)-1 and vascular cell adhesion molecule (VCAM)-1 on vascular endothelium (Cheng et al. 2010). MIF also acts in a paracrine and autocrine fashion to initiate MCP-1 secretion from these endothelial cells, resulting in greater migration into tissue (Kasama et al. 2010). Thus, the effect of IFN- γ on static transmigration following pretreatment of HUVECs with this endogenous pro-inflammatory cytokine was examined. On the other hand, LPS release from gram negative bacteria is associated with inflammation and induced adhesion molecule expression on endothelial cells (Abbas et al. 2014). Although the study at hand focused on macrophage infiltration into damaged tissue areas to facilitate regeneration, phagosome maturation arrested macrophages could infiltrate both these IFN- γ and LPS associated inflammatory sites in response to adhesion molecule expression.

A pilot transmigration study, identical to the one described above, was done using adherent monocytes (i.e. not macrophages) polarized with 50 ng/ml LPS and 20 ng/ml IFN- γ directly after isolation for 24 hours prior to assessment. This was carried out to investigate the possibility of shortening the preparation time of primary macrophages by using monocytes - aiming toward a possible translational application for the treatment for more acute conditions where preparation time is limited. Monocytes were

capable of sufficient AbsBeads uptake after 1h challenge. However, no cell migration was found at experimental end point in any group, including control groups devoid of AbsBeads (data not shown). Thus, in the results section, we will report only the results obtained in macrophages.

3.12. Statistical Analysis

All statistical analysis was done using Graph Pad Prism 5. All data are presented as means \pm SEM. Student's t-test and one-way analysis of variants (ANOVA) were conducted where appropriate. A p-value of <0.05 was considered statistically significant.

Chapter 4: Results

All experiments were conducted at least in duplicate and repeated a minimum of three times. For all experiments with an intervention component, suitable controls were included with every run.

4.1. Monocyte Differentiation and Polarization

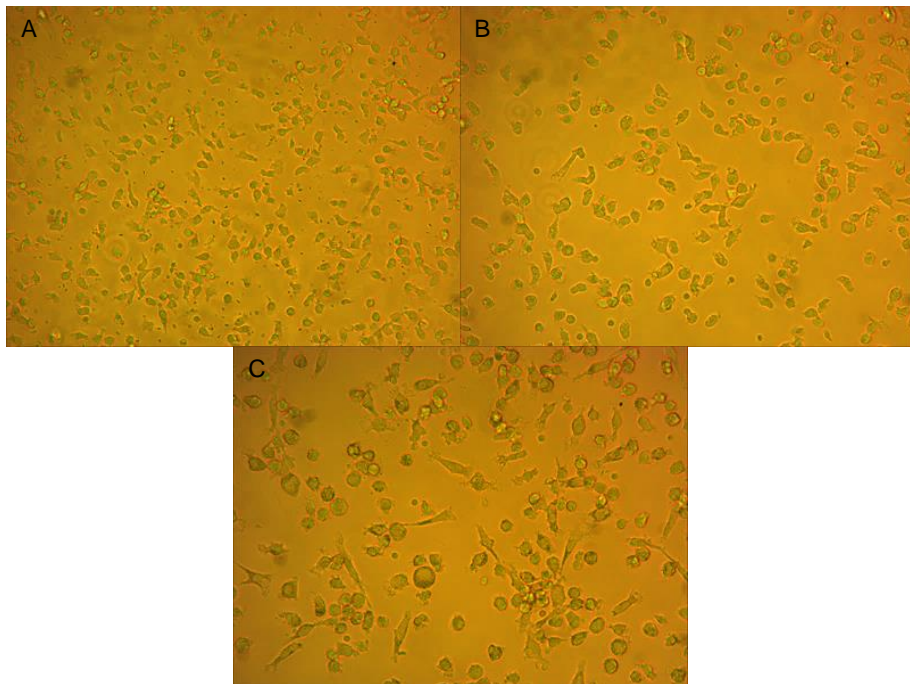


Figure 4.1: Monocyte differentiation into macrophages. Monocytes were cultured under standard conditions in 35mm culture dishes and imaged with a phase contrast microscope at 20x magnification for all images. (A) imaged 24h, (B) 96h and (C) 144h after isolation.

Images were taken of the isolated monocytic cells in culture at different time points from initiation of the GM-CSF-driven pre-differentiation to evaluate general morphological changes during differentiation of monocytes into macrophages. Representative images (**Figure 4.1**) of cells cultured on polystyrene surfaces show a

striking increase in cell size over time. A gradual increase in cell size, across a 72-hour period, can be seen by comparing frame B (96 hours after isolation) to frame A (24 hours), followed by a seemingly more drastic change, as seen in frame C (144 hours). Across this last 48-hour period, cells exhibited greater increases in size and notably developed morphological changes characterized by surface pseudopodia and cell flattening, when compared to the initial 72-hour period.

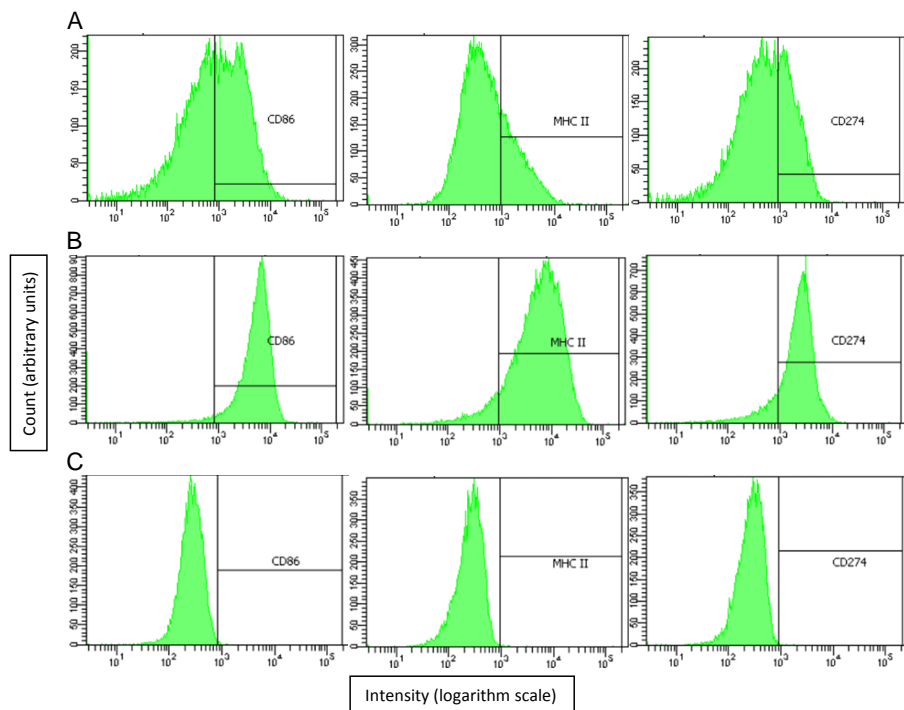


Figure 4.2: Flow cytometry analysis of macrophage differentiation. Cells were assessed after 144-hour (6-day) culture period with fluorescent antibodies against CD86, MHCII and CD274. Panel (A) indicates a M0 population while (B) indicates M1 and (C) M2. Vertical lines indicate fluorescence thresholds, with cell populations to the left staining negative, and those to the right positive for the particular fluorescent label.

To quantitatively support findings shown in **figure 4.1**, flow cytometry was done to determine the efficacy of the M1 polarisation, by phenotyping of differentiated cells using M1 membrane markers.

The M1 polarisation protocol (GM-CSF, LPS and IFN- γ treatment) clearly resulted in an M1 phenotype, with high expression of M1 markers CD86, MHCII and CD274 (**Figure 4.2** panel B), when compared to the much lower M1 membrane protein expression in cells polarised using the M2 (M-CSF, IL-10, IL-4 and TGF- β treatment) protocol (panel C). Panel C in fact illustrates no expression of M1 markers, since only background fluorescence (below threshold) was detected. The undifferentiated M0 population expressed a lower and combined fluorescent signal, indicated by double signal peaks on threshold values (panel A).

4.2. Phagocytosis Model Validation

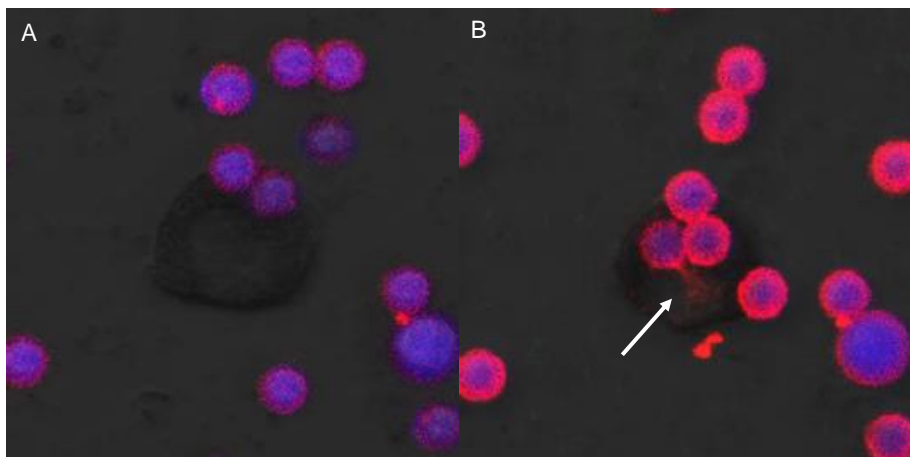


Figure 4.3: Antibody dispersion off of ingested AbsBeads. Enlarged confocal microscope images of a control cell showing red antibody dispersion off of AbsBeads into the cell. Frames taken at 10 min (A) and 60 min (B) after introduction of AbsBeads. Arrow indicates dispersion of antibody. Time lapse images taken at 20x magnification.

Representative images show a cell not treated for phagosome maturation arrest at high magnification (**Figure 4.3**). Frame A shows the cell in the process of engulfment at 10 min. The same cell is shown in frame B at 60 min with red antibody signal expression inside the cell. This illustrates that at this time point, the antibody coating was removed from AbsBeads and was dispersed throughout the phagosome (indicated by arrow), before its complete degradation and accompanying loss of red signal (not shown here). This visually validates our model and confirms that an antibody coating around these beads can be used as a model for phagosomal digestion studies. Note that pHrodo® was not used in **figure 4.3** for the sake of clarity, as doing so would have obscured the intracellular signal which indicates the antibody digestion from the bead.

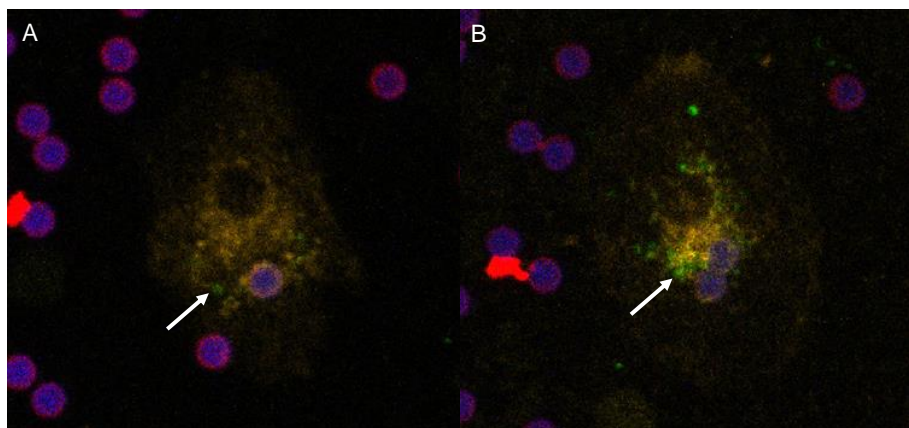


Figure 4.4: Acidification of cellular compartments. Time lapse images of a live control cell showing AbsBeads ingestion coinciding with acidification. Frames captured at 10 min (A) and 60 min (B) after AbsBeads challenge. Arrows indicate individual acidic compartments within the cell. Images taken at 20x magnification.

Having validated the use of AbsBeads to indicate phagosomal digestion, the next validation step was to illustrate that digestion coincides with phagosome acidification. Similar to **figure 4.3**, ingestion of AbsBeads by a representative control cell occurred

10 min after challenge (**Figure 4.4** frame A). At this time some lysosome or phagosome acidification can already be seen (indicated by white arrows). Frame B shows the same cell at 60 min after challenge with green signal expression around two AbsBeads as well as dispersed throughout the cell. This represents unaffected phagosome maturation and acidification during phagocytosis. Additionally, individual green acidic compartments can be distinguished at magnifications as low as 20x, supporting the visual power of pHrodo® as a marker of acidification.

This phagocytic model is completely novel with regard to the quantitative as well as qualitative assessment thereof, and established materials have never before been used in conjunction or for the study of phagocytosis in the context of similar projects.

4.3. Intervention: Phagosome Maturation Arrest

Having sufficiently validated and characterised the model in terms of time course of events and efficacy of markers, the phagosome maturation arrest protocol was implemented. Phagosome maturation arrest is required to preserve the cargo taken up by macrophages, in this case AbsBeads.

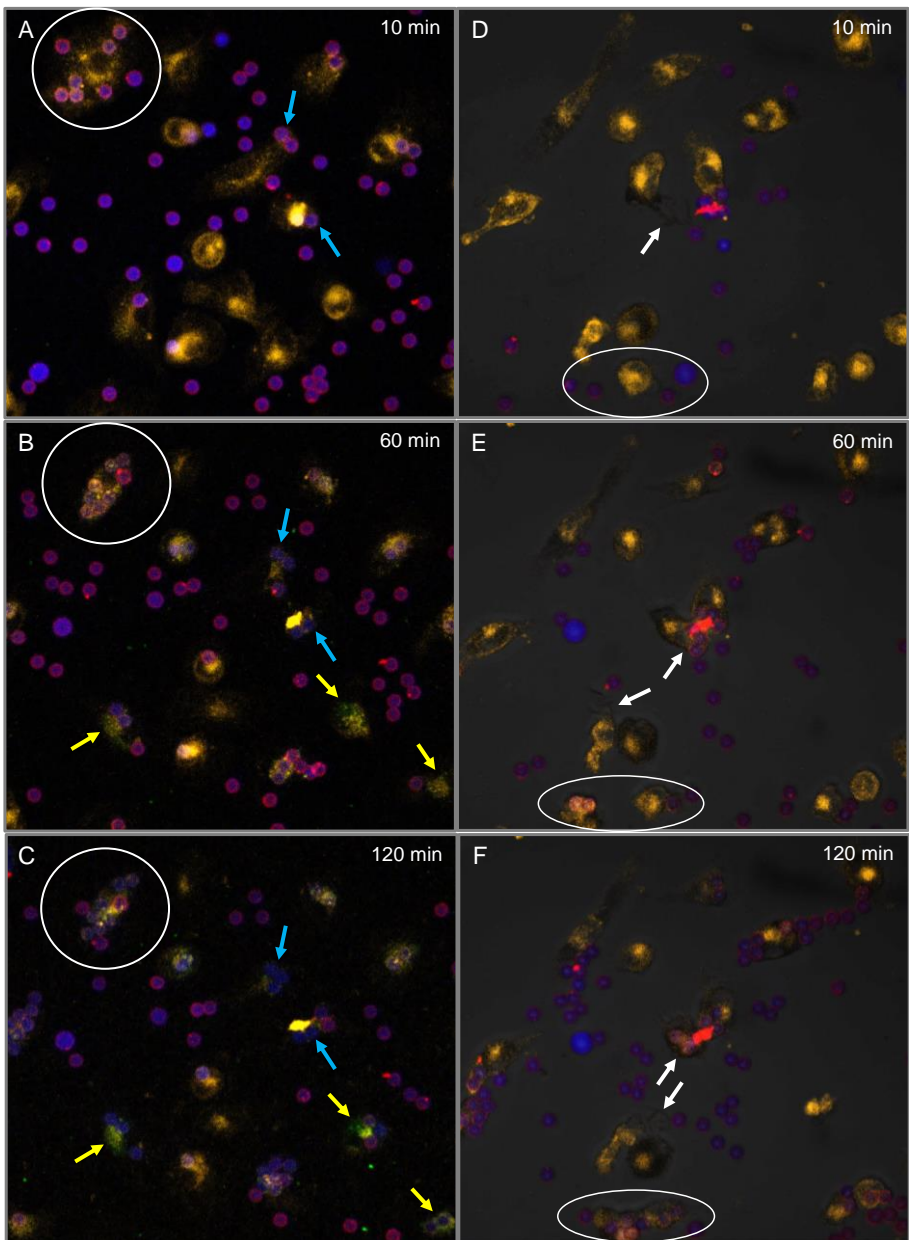


Figure 4.5: Time lapse images of live macrophages. Control cells (panel: A, B, C) and phagosome maturation arrested cells (panel: D, E, F). Frames taken at 10 min, 60 min and 120 min after AbsBeads challenge. Representative cells are indicative of phagocytic capacity (white circles). Loss in red antibody signal is indicated by blue arrows. Green digestive cells with acidic phagosomes showing a loss in red antibody signal are indicated by yellow arrows. Pseudopod extension, cell motility and red antibody preservation are indicated with white arrows. Lighter background shade (D, E, F) is due to phase contrast signal, used to visualise pseudopodia. Images taken at 20x magnification.

Time lapse images of a representative macrophage populations are shown in **figure 4.5**. The right hand side panel (phagosome maturation arrested cells: D, E, F) shows maintained red antibody signal throughout the 2-hour imaging period, with the absence of green acidic signal (indicated by white arrows). Compared to control cells on the left hand side panel (A, B, C) showing green acidification (indicated by yellow arrows) as well as loss in red antibody signal (blue arrows) over the same time period. This illustrates successful induction of phagosome maturation arrest and maintenance thereof for up to 2 hours. White arrows (Frames D, E, F) indicate cells that initiated phagocytosis as early as 10 min after AbsBeads challenge (Frame D) and actively moved toward a bead to achieve ingestion at 60 min (Frame E). Noteworthy, preserved cell motility and pseudopod extension is seen throughout the treated panel, also indicated by white arrows. (Pseudopodia extension likely serves to sample the surrounding environment and it is possible that the cell indicated with a white arrow at the bottom of frame E and F, attempted to ingest the nearby bead.)

4.3.1. Digestive Capacity

Representative quantitative flow cytometry scatter plots are presented in **Figure 4.6**. Scatter plots illustrate macrophage degradative capacity expressed as red antibody fluorescent signal over number of AbsBeads per cell. Control samples show a loss in red signal after the 2-hour phagocytosis endpoint, indicated with a red circle. This “degradation tail” represents cells capable of removing the red antibody coating around beads and subsequently digesting the IgG itself or inactivating the IgG fluorescent label. These outcomes were jointly classified as representatives of digestion. In these representative plots for example, an untreated control population was analysed and yielded 5.88% macrophages, capable of sufficient protein degradation to achieve signal loss below the threshold. Conversely, 55.93% of this

population maintained antibody coating in the absence of arresting agents. This discrepancy is likely due to a relatively short experimental period. The nature of ingested material directly affects digestive tempo, thus, utilization of an extended phagocytic period would yield greater degradation. Nevertheless, this 55.93% yield is overshadowed by 79.22% of a phagosome maturation arrested population expressing sufficient signal after the same period. More importantly, only 0.66% of treated cells contained inviable cargo, compared to a 5.88% control yield. This phenomenon was evident in all samples tested, as supported by statistical analysis showing significant cargo degradation in $1.23 \pm 0.26\%$ of cells after treatment, compared to $7.52 \pm 0.98\%$ of untreated cells ($p < 0.0001$) (**Figure 4.7**).

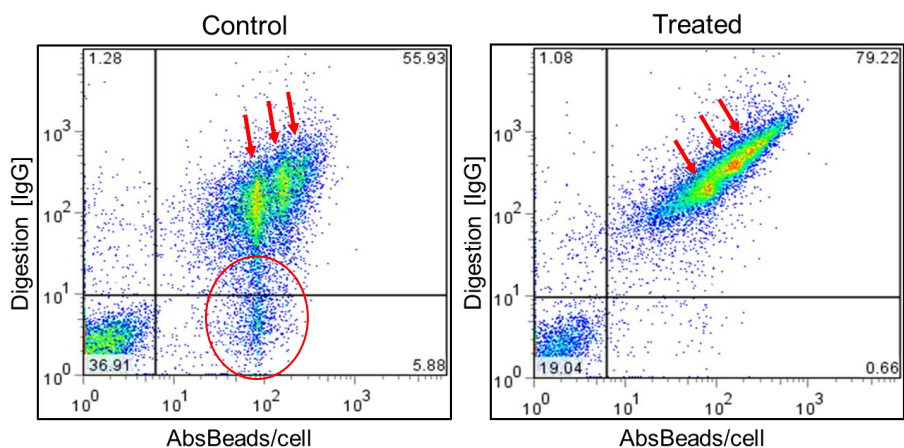


Figure 4.6: Representative flow cytometry scatter plot of macrophage digestion with intensity clusters. Antibody signal intensity (y-axis) expressed over number of AbsBeads per cell (x-axis). 3×10^5 events collected.

Scatter plots (**Figure 4.6**) also present a linear relationship between the number of beads per cell and the antibody expressed on each bead. This is represented by the red intensity regions indicated with arrows and is shown more clearly in the “treated” scatterplot. These are clusters of cells expressing similar fluorescent signal for both

beads and antibodies. Additionally, the most prominent region of degradation, indicated by a degradation tail, is found in clusters expressing a lower density of beads. Thus, it can be derived that the degree of digestion is correlated to number of beads in the cell i.e. the nature of the material is dependent on time needed to degrade it.

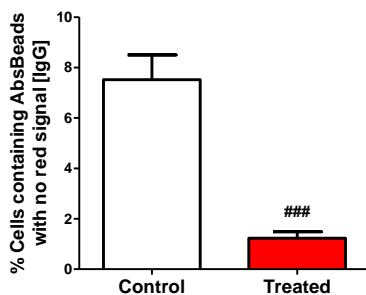


Figure 4.7: Statistical analysis of macrophage digestive capacity. Measured by loss in red antibody signal intensity of cells containing AbsBeads. Cells were analysed with flow cytometry. Values expressed as percentages from scatter plots and presented as mean \pm SEM (n=3). ### = $p < 0.0001$ vs control.

4.3.2. Engulfment Capacity

Macrophage engulfment capacity, defined as the number of cells containing any number of beads after 2 hours, was determined. A representative bead positive population, shown in **figure 4.6** scatter plots, yielded 61.81% (55.93% + 5.88%) under control conditions, whereas 79.88% (79.22% + 0.66%) of phagosome maturation arrested cells contained beads. This is supported when inversely determining engulfment i.e. assessing the number of cells unable to ingest material, represented by populations negative to both beads and antibody, from control and treatment conditions (**Figure 4.6**). Representative phagocytically uninvolved macrophages constituted 36.91% and 19.04% with and without phagosome maturation arrest, respectively (**Figure 4.6**). Statistical analysis of all populations (**Figure 4.8**) indicated maintained engulfment capacity. The non-significant difference is represented as

68.67 ± 3.51% of treated cells containing beads while 61.19±4.68% of cells were capable of engulfment in control groups (p=0.207). Considering these findings, it seems phagosome maturation arrest had no effect on engulfment capacity. This is also seen in **figure 4.5** where the number of AbsBeads ingested is not notably affected under control or treatment conditions, respectively (indicated by white circles).

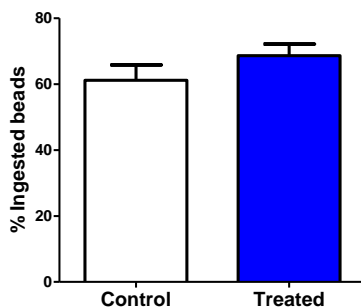


Figure 4.8: Statistical analysis of macrophage engulfment capacity. Measured as the percentage of cells containing any number of ingested AbsBeads. Cells were analysed with flow cytometry. Values expressed as percentages from scatter plots and presented as mean ± SEM (n=3). p=0.207 vs control.

4.3.3. Acidification

Macrophage degradative capacity and phagosome maturation is dependent on phagosome acidification (Fairn & Grinstein 2012). For this reason, fluorescent antibody signal was plotted over pHrodo® fluorescence intensity (**Figure 4.9**). Representative cells under control conditions achieved phagocytosis to near completion as indicated by a collective acidity signal of 94.39% (54.47% + 39.92%) above threshold. Taking into account that this figure represents the same cell population assessed in **figure 4.6**, one can extrapolate that almost all cells were phagosomally mature and in the process of digestion, however, were not allowed sufficient time to completely degrade antibody. Conversely, the phagocytic process

was interrupted in phagosome maturation arrested cells. These cells maintained a more alkaline (pH >6) intracellular environment, presented by 95.42% (76.50% + 18.92%) of cells with insufficient signal intensity. Only a small cell population of 4.59% (3.84% + 0.75%) achieved phagosomal acidification after treatment, compared to 94.39% under control conditions. Phagosome inability to acidify was also statistically significant with $29.17 \pm 8.40\%$ acidic cells after treatment, compared to $92.09 \pm 1.09\%$ under control conditions ($p < 0.0001$) (**Figure 4.10**). This acidification is also visually presented in **figure 4.4** indicated by white arrows, as well as in **figure 4.5** indicated by yellow arrows.

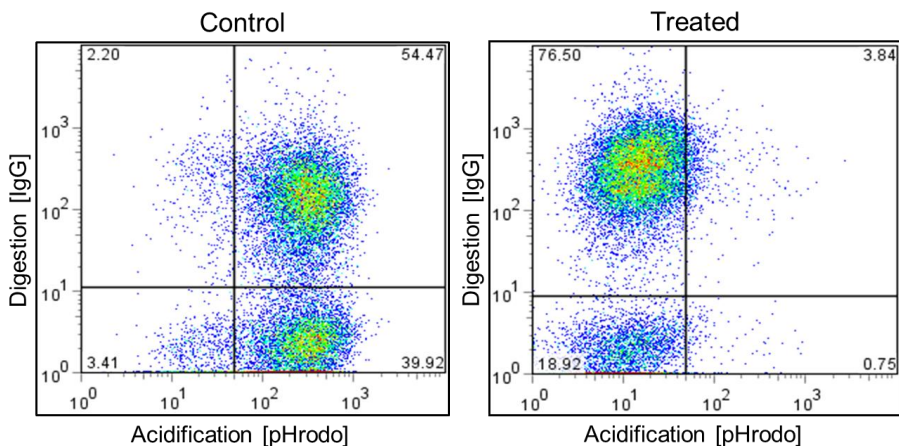


Figure 4.9: Representative flow cytometry scatter plots of macrophage acidification with intensity clusters. Antibody signal intensity (y-axis) expressed over acidic pHrodo® signal intensity (x-axis). 3×10^5 events collected.

The control population of 39.92% (**Figure 4.9**) represent acidic cells expressing no antibody signal. This population can be defined in two ways. Firstly, this population could have ingested AbsBeads or only residual antibody and degradation thereof was completed before cells were assessed, however, insufficient time was available to regain homeostatic pH at >6.0 before the 2-hour time point. Secondly, the ingestion of

pHrodo® BioParticles® into these cells could have induced acidification in an attempt to degrade this marker, leading to cells devoid of antibody but still acidic. Additionally, autophagy could also play a role in representing a false degradative phagosome or acidic autophagosome. Due to the above reasons these plots were used for statistical assessment of acidification only and not degradation directly.

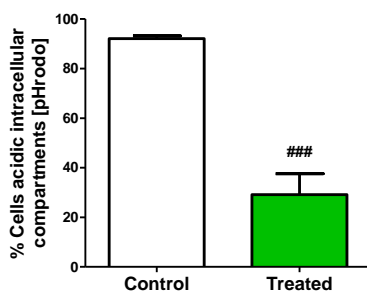


Figure 4.10: Statistical analysis of macrophage acidification. Measured by green fluorescence signal intensity. Cells were analysed with flow cytometry. Values expressed as percentages from scatter plots and presented as mean \pm SEM ($n=3$). ^{###} = $p < 0.0001$ vs control.

4.4. Macrophage Migration

Arrested macrophages exposed to a MCP-1 chemokine gradient significantly migrated through HUVEC coated membranes with 8 μm pores (72.86 ± 16.0 cells per well) compared to arrested control samples (22.43 ± 3.60 cells per well), not exposed to MCP-1 ($p < 0.01$) (**Figure 4.11**). This verifies a significant induction of migration in response to chemokine stimulation as opposed to a passive migration, driven by gravity. Additionally, phagosome maturation arrested macrophages maintained ability to transverse endothelial barriers in response to MCP-1. Macrophages containing 4.5 μm AbsBeads maintained migration capacity, as indicated by 70.14 ± 12.6 migrated cells per well when compared to cells without AbsBeads (72.86 ± 16.0 cells per well) However, migration of these AbsBeads containing macrophages was still significantly

more when compared to control (22.43 ± 3.60 cells per well, $p < 0.005$). Of note, migrated cells were frequently inviable and presented as perforated cell membranes containing AbsBeads. The likely cause of this reduced viability, is uncontrolled AbsBeads engulfment causing membrane shattering during attempted migration through pores with insufficient size.

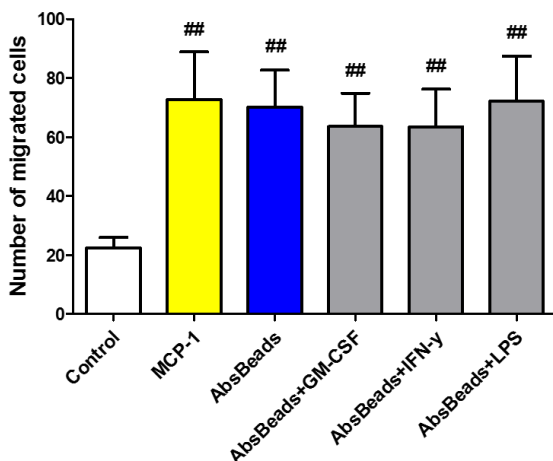


Figure 4.11: Statistical analysis of migratory capacity of phagosome maturation arrested macrophages. Macrophages were incubated with Control; 100 ng/ml monocyte chemoattractant protein-1 (MCP-1); 1.156×10^6 AbsBeads/ml and MCP-1 (AbsBeads); 50 ng/ml GM-CSF, AbsBeads and MCP-1 (AbsBeads + GM-CSF); 20 ng/ml IFN- γ 24 hours before assessment, AbsBeads and MCP-1 (AbsBeads + IFN- γ); 50 ng/ml LPS 24 hours before assessment, AbsBeads and MCP-1 (AbsBeads + LPS). Migration allowed for 2:30 hours. Cells were analysed with phase contrast microscopy. Values expressed as absolute cell count and presented as mean \pm SEM (n=7). ## = $p < 0.01$ vs control.

The influence of potentially confounding *in vivo* factors was also determined (**Figure 4.11**). The GM-CSF cytokine was added to MCP-1 containing media. Although not significant, there seemed to be a trend for reduction in migration, with 63.57 ± 11.3 migrated cells in this group. However, migration was still significantly increased when compared to control ($p < 0.005$). Noteworthy, the addition of cytokine did not diminish MCP-1 stimulated migration ($p = 0.704$) compared to AbsBeads group. However, the

slight reduction in migration is contradictory to previous reports that presented an exposure to GM-CSF upregulated migration and chemotaxis (Dabritz et al. 2015).

No significant outcome after treatment with either LPS (72.14 ± 15.3) or IFN- γ (63.43 ± 12.8) was found, compared to AbsBeads group. However, the somewhat lower trend in migrated cell population following IFN- γ pretreatment could be argued as a result of prior macrophage polarisation together with IFN- γ induced displacement of JAM-A, as our assay was also done under static conditions (previously discussed in section 3.11.3.).

Chapter 5: Discussion

The aims of this study were met with the development of a modified, non-destructive macrophage population capable of engulfment and transmembrane movement. This was achieved by re-evaluation of previous findings in the literature regarding phagosome maturation arrest and application of this knowledge in a novel context. By combining subdisciplines in physiology, these customarily detrimental effects in the context of immune cell function, were used in a manner and setting which may bring about therapeutic outcome. More specifically, the known positive effects of macrophage infiltration on tissue healing – or more specifically muscle healing and regeneration (Arnold et al. 2007) – was manipulated to achieve a vehicle for the delivery of therapeutic modalities such as stem cells or even pharmaceuticals.

Since the development of an *in vivo* delivery system is by nature a complex, multi-stepped process, the entire process was outside of the scope of a single MSc thesis. Therefore, this thesis focused on the manipulation of macrophages to render them incapable of digestion of engulfed “cargo”, while maintaining their capacity for engulfment and transendothelial migration. We report on the successes achieved in this more limited context.

5.1. Macrophage Polarisation

Monocytes were cultured and exposed to GM-CSF for 144 hours as well as LPS and IFN- γ for 24 hours, in order to polarise them into a M1 macrophage phenotype (Mia et al. 2014). This phenotype was necessary for the purpose of our study, as this is the only phenotype previously shown to migrate endothelial barriers after differentiation (Arnold et al. 2007; Chazaud et al. 2009). The M1 phenotype is also capable of particle engulfment and digestion as this is the main phenotype to which inflammatory

monocytes are differentiated (Imhof & Aurrand-Lions 2004; Freeman & Grinstein 2014). This being said, the main function of circulating undifferentiated monocytes are tissue infiltration during inflammation. In an attempt to circumvent extended culture periods, we assessed the migratory capacity of phagosome maturation arrested monocytes containing AbsBeads. Unfortunately, no migration was seen (section 4.4). Our data thus confirms that only differentiated macrophages, and not peripheral monocytes, would be suitable carrier cells.

In terms of the pre-differentiation step, there are two major results to interpret: the size increase of cells, and changes in their expression of macrophage markers. Successful differentiation into macrophages was evident from the images shown in **Figure 4.1**, which illustrates a striking increase in cell size over the 6-day culture period. A time dependent increase in proximity between cells, allowing cytokine or paracrine production to effectively influence differentiation (Silverthorn 2010; Freeman & Grinstein 2014), was considered as an inductive effect to cell enlargement. However, cell proximity was not noticeably increased and the number of cells did, in fact decrease, in relation to enlargement. Therefore, cell enlargement can be attributed to experimentally introduced GM-CSF that acts both as a cytokine and growth factor to increase cell adherence (represented in **figure 4.1** as cell flattening) and also cell enlargement (Dabritz et al. 2015). This can be applied to cell enlargement seen in frame A to B (24 hours and 96 hours after isolation, respectively), however, does not sufficiently explain the considerable cell enlargement, over a relatively shorter time period (48 hours of elapsed time), seen when comparing frames C and B. The experimental concentration of GM-CSF remained constant throughout. However, differentiated macrophages could have sufficiently matured to locally produce

additional GM-CSF by this time point (Shi et al. 2006), which could explain this abrupt cell enlargement (Abbas et al. 2014).

Interestingly, the reduction in cell number observed (**Figure 4.1**) could be as a result of repeated media changes and PBS washes, but seeing as monocyte/macrophages are particularly adherent *in vitro* (Collier et al. 2001), this is unlikely. A more feasible explanation could simply be the relatively short lifespan of monocytes in circulation (10-20 hours) (Guyton & Hall 2011). Monocyte *in vivo* extravasation is needed to induce differentiation into resident tissue macrophages. This process ensures a prolonged lifespan by providing a protective and nutrient- and chemokine-rich extra-circulatory environment which augments cell survival. In contrast, under *in vitro* conditions, monocytes were unable to infiltrate tissue and was forced to differentiate under relatively unprotected and chemokine-poor conditions. The absence of tissue infiltration, exposed cells to possible apoptotic and/or autophagic inducers that would normally be attenuated in tissue niches. Thus, macrophages were kept in a circulatory environment as opposed to tissue and likely underwent some degree of apoptotic cell death throughout this time. However, this should be seen as an artefact of the *in vitro* nature of cell culture models, rather than a confounding factor in this study.

In terms of evidence for macrophage polarisation, the flow cytometry signal intensity graphs show monocyte differentiation as well as successful polarisation to achieve macrophage M1 phenotype in the majority of cells (**Figure 4.2**). This marker profile is in accordance with published studies on this topic (Mia et al. 2014; Ka et al. 2014) and confirms that our protocol successfully polarised primary peripheral monocytes into M1 macrophages, which should have high capacity for transendothelial migration (Arnold et al. 2007; Chazaud et al. 2009). Interestingly, changes in MHCII expression are used for identification of both M1 and M2 populations in the literature. Since M1

polarisation is associated with elevated MHCII expression (Mia et al. 2014) and exposure to IL-10 (used during our M2 polarisation protocol) is known to down-regulate MHCII expression (Abbas et al. 2014), MHCII is (in our opinion) a particularly useful marker with which to assess macrophage phenotype polarisation in our context.

5.2. Manipulating Phagosome Maturation

Previous research has been centred around microbial and parasitic immune evasion with ensuing reports linking phagosome maturation arrest as part of pathogenesis, throughout. A plethora of interventions is employed to achieve immuno-protection, including interference with PI3ks, Rab5, Rab7, EEA1, V-ATPase, endosomal and lysosomal fusion events and recruitment of digestive proteases (Rai et al. 2015; Clemens et al. 2000; Seto et al. 2011; Vergne et al. 2003; Puri et al. 2013; Ghigo et al. 2002). Manipulation of these detrimental aspects has never before been attempted in the context of regeneration or drug delivery. As no previous research has focussed on intentional induction of phagosome maturation arrest, notwithstanding previous studies into autophagy modulation, no literature exists with which to compare current data. Similarly, the viability of mammalian proteins after phagosome maturation or arrest thereof has never before been determined and previous work in this context has focused on viability and immunogenicity of microorganisms, which is not relevant to the current study design, although it may provide some hints for interpretation of current data in terms of the efficacy with which digestion was inhibited.

In the current study, Concanamycin A and Chloroquine treatment was employed to block phagosome acidification. The rationale therefore is underpinned by observations gathered from two microorganisms capable of blocking phagosome acidification and

inducing phagosome maturation arrest in that manner: *Mycobacterium tuberculosis* and the *Leishmania* superfamily.

Concanamycin A is a selective V-ATPase inhibitor that directly affects phagosomal acidification by preventing formation of a proton gradient (Huss et al. 2002). It simulates a situation similar to *Leishmania* that prevents recruitment of the V-ATPase. Chloroquine, on the other hand, is a weak base able to alkalinise phagosomes that leads to a block in lysosome fusion due to this raised phagosomal pH (Akpovwa 2016). This in turn then simulates the block in endosome/lysosome fusion seen under conditions of TACO retention. In our study, blocked phagosome acidification was represented by a reduction or absence of green pHrodo® signal in treated cell populations (**Figures 4.5, 4.9, 4.10**).

We also utilized the PI3k inhibitory effect of Wortmannin to prevent formation of PI3P on maturing phagosomes (Vieira et al. 2001; Hawkins & Stephens 2015). Wortmannin is a steroidal fungal metabolite that non-specifically inhibits subtype I, II and III PI3ks by covalent binding to lysine residue in the catalytic unit of this enzyme (Wymann et al. 1996; Liu et al. 2005). Supported by previous studies (Nakanishi et al. 1995; Yano et al. 1993; Jackson et al. 2004), Wortmannin has shown prolonged effective inhibition of PI3ks, resulting in phagosome maturation arrest.

An interesting point for discussion, given the ultimate goal for *in vivo* application, is the fact that the 20 position carbon (C20) of Wortmannin is highly reactive with nucleophiles in solution, resulting in an extremely short half-life of 0.99 min (59.4 seconds) in culture media (Yuan et al. 2006). Therefore, a Wortmannin paradox was proposed and investigated by Yuan and colleagues (Yuan et al. 2007) to determine the relative effectiveness of this metabolite *in vivo* and *in vitro* against its highly reactive

nature. Briefly, investigation found that Wortmannin resides within cell culture solution under various C20 amino acid derivatives that undergo dynamic transitioning between different nucleophile donors to form other derivatives, while also reverting to unmodified Wortmannin. These derivatives vary in their capability to inhibit PI3ks. Noteworthy, of the nucleophiles tested, the C20-lysine derivative was the weakest PI3k inhibitor and also the most stable, forming a physiologically irreversible binding that yields negligible Wortmannin reformation. We extrapolated from this that Wortmannin cycles between C20 derivatives until exposure to lysine, found free within cell culture or contained in the PI3k catalytic unit. The resultant irreversible covalent binding induces prolonged inhibition, however, due to steric hindrances in the catalytic unit, Wortmannin is vulnerable to intramolecular attack by its C6 position hydroxyl group (responsible for the reversibility of C20 derivatives to reform Wortmannin and other compounds after binding to different nucleophiles (Yuan et al. 2007)). Subsequently, the bond can be broken and PI3k regains fractional activity until repeated binding with C20 derivatives. Together, this poses an explanation for why macrophages in this study readily engulfed 6 μm as well as 4.5 μm AbsBeads, contradictory to previous reports of Wortmannin-induced haltering of phagocytosis (at the same concentration), in a size dependant manner and an inability to engulf particles larger than 3 μm (Cox et al. 1999; Vieira et al. 2001). A possible additional reason for the discrepancy in reports could also be altered adhesion molecules of the immortalised cells (RAW264.7) used by Vieira and colleagues. This alteration could have negatively influenced phagocytosis and prevented large particle engulfment, which was not observed during our study with use of primary cells.

5.3. Maintenance of Engulfment Capacity and Migration

The capacity for engulfment of AbsBeads was maintained in macrophages after treatment to induce phagosome maturation arrest. This engulfment capacity of primary differentiated macrophages has never before been assessed after experimental induction of phagosome maturation arrest. Previous studies touching on this aspect, focus on absolute engulfment as maintained or blocked, rather than determination and quantification of the extent to which engulfment was mediated. For this reason, no data exists to which our findings can be compared – in the artificial bead ingestion context as well as microbiology context. The most applicable research done in this context, was that of Vieira et al. (2001) who treated RAW264.7 with Wortmannin and reported an inability to engulf larger particles (this topic was already discussed above). Similarly, Cox et al. (1999) reported an abortive form of “frustrated phagocytosis” where macrophages attempted to engulf the culture plate they were grown on (section 2.2.2.). Furthermore, the almost limitless capacity for engulfment is supported by findings of membrane enlargement via stretching and “ruffling” out of grooves (Hallett & Dewitt 2007) as well as *de novo* membrane production (Huynh et al. 2007), which enables engulfment of particles similar in size to the macrophages themselves. Thus, the number of ingested particles is unlikely to be a limiting factor in migration capacity. In order to support this interpretation, further studies can more directly determine whether the number of ingested particles affects migration. Aside from these few reports, no other studies have quantified the capacity for phagocytosis and none exist on migration of cells containing extensive phagosomal content. Nevertheless, current data indicates that phagosome maturation arrest does not affect engulfment capacity or migration capacity in primary cells. Importantly, our results obtained in primary cells, stresses the importance of study design to minimise confounding factors (in this case

e.g. changes in adhesion molecule expression in primary vs. immortalised cells), to allow for most accurate data yield and data interpretation.

5.4. Bioactivity and *in vivo* Translation

Turning attention to considerations related to *in vivo* application, it is important to consider feasible time frames within which our model could function, as this would dictate conditions that could benefit from this particular model. Despite the known, very short physiological half-life for Wortmannin (59.4 seconds) (Yuan et al. 2006), it is known to elicit prolonged perturbation (Jackson et al. 2004), as discussed earlier. Notwithstanding research into this “Wortmannin paradox”, no time dependant studies have determined bioactivity of this compound. Similarly, Concanamycin A has been used in numerous studies to determine the role of V-ATPase and its associated processes *in vitro*, however, research has not elucidated the period of V-ATPase inhibition by Concanamycin A – irrespective of concentration. Nonetheless, Chloroquine was recently proposed as a possible therapeutic treatment for Ebola due to its pH elevating effect (Akpovwa 2016). As proposed by Akpovwa, one problem regarding the feasibility of Chloroquine as an Ebola treatment is un-perpetuated bioactivity. Thus, the bioactivity of these compounds have not been determined. Currently our knowledge on the modulation for maturation arrest as employed in the current study, only extends to 2 hours, and drug-interaction was not comprehensively assessed. The combination of drugs could potentially augment activity of one or more of the other drugs used, or even create some redundancy. Future studies should investigate drug-interactions and assess more doses of the three compounds in isolation or in combination. Also, the effective time frame limits of our maturation arresting cocktail should be investigated to further optimise the intervention protocol

with the aim of *in vivo* therapeutic application. For example, should a longer period be required for effective treatment than achieved with the current protocol, a possibility is to coat the AbsBeads/cargo with the arrest inducing cocktail to initiate phagosome maturation arrest only after engulfment, so as to prolong effectiveness without increasing dosage of the treatment and by releasing compounds in a delayed-release fashion.

Time constraints of the current working model of this delivery system are a key consideration for therapeutic application. Currently, preparation time from isolation of stem cells and monocytes, culturing and reintroduction into host is ± 7 days. To shorten this period, a pilot transmigration study was done using phagosome maturation arrested monocytes activated and cultured for a total of 24h (Section 4.4). As mentioned earlier, although sufficient uptake of AbsBeads was recorded – providing proof for engulfment capacity – these cells failed to transverse endothelium. Explanations for this outcome could be insufficient cell maturation to allow a M1 phenotype (also not assessed during pilot) that has been shown to transmigrate *in vitro* (Arnold et al. 2007; Chazaud et al. 2009). Additionally, these unmaturing monocytes could be less robust, compared to M1 macrophages, and their exposure to the arrest inducing cocktail could have had adverse effects. Thus, taken all of these data and literature into consideration, this model is probably not suitable for acute application. Rather, it should be applied to chronic pathological conditions where more effective regeneration would improve prognosis, such as in myodystrophy.

Chapter 6: Conclusions and Recommendations for Future Studies

In conclusion, this thesis describes a novel technique with which successful phagosome maturation arrest was achieved in pre-differentiated and polarised M1 macrophages. The intervention cocktail was shown to result in satisfactory preservation of intra-phagosomal cargo after engulfment, without negatively affecting engulfment capacity or macrophage migratory capacity.

As mentioned in the introduction section of the thesis in Chapter 1, this study is the first step in a much bigger endeavour. Thus, many more studies are required before arriving at a feasible therapeutic option for clinical application. Minor optimisation steps have already been touched on in the discussion section. However, in addition, several follow-up studies are envisaged. For example, probably the first step would be to replace AbsBeads with stem cells in order to assess viability of ingested cells via assessment of physiological indicators of viability. Since traditional XTT or propidium iodide staining is not feasible for a cell-in-cell situation, we propose assessment of markers of cell survival, apoptosis and/or autophagy using immunocytochemical staining of permeabilised cells. Pilot studies are already under way to investigate the feasibility of coating these stem cells with a protective co-block polymer, which could contribute to cell survival.

A second study could use a more physiologically relevant *in vitro* model, such as the SynVivo microfluidics system, to simulate capillary networks with which to evaluate macrophage migration capacity under physiologically accurate sheer flow rates.

At this point, the first *in vivo* study can be considered. Importantly, the specificity of migration to only the intended areas for regeneration has to be assessed, in order to prevent cargo delivery and thus undesired tissue growth in unwanted tissue areas.

Current literature in the context of stem cell therapy by infusion into circulation, suggest that this is probably not a problem, since progression of stem cells to more differentiated forms is largely determined by the cellular environment. However, this has to be confirmed as a safety precaution. We propose labelling macrophages or stem cells with a suitable marker and to assess the migratory path and speed of macrophages in live, sedated rodents, using a whole body visualisation system, such as the IVIS (*in vivo* Imaging System) already accessible to us.

In order to optimise macrophage mobility *in vivo*, it is also important to consider physical limits of cells in an *in vivo* environment, i.e. whether there should be a limit to the number of consecutive engulfments and thus number of stem cells contained in any single macrophage. Macrophages containing too many stem cells may physically not be able to migrate through the smaller blood vessels, or have difficulty migrating across endothelium. To address this, fluorescence activated cell sorting (FACS) can be used to optimise the migrating macrophage population in terms of phagosomal contents/number, to ascertain optimal migration capacity. By using similar interventions as used in this study to quantify digestion and engulfment, one can separate single or double bead/cell containing macrophages via setting up a threshold and polarizing cells in real time for sorting according to attraction to voltage gates.

Finally, induced release of macrophage cargo has to be achieved after tissue infiltration. The aim is to design the co-block polymer coating of stem cells so that it could assist with the release of the satellite cell. For example, these polymers can be designed to break-down in response to specific externally applied stimuli, such as infrared light or vibration at specific frequency (given the superficial nature of skeletal muscle, this is a feasible option). In this scenario, the inner layer of the polymer could be decorated with an agent inducing macrophage cell lysis or even apoptosis, to

facilitate release of the stem cell. However, this step is still some time off and the processes by which this may be achieved is less clearly defined at this point.

Although many more steps are required in the development of this delivery system, an autologous delivery system such as this has immense translational applicability, not only in the context of regenerative medicine for stem cell delivery but also delivery of therapeutic compounds. For example, the anthracycline Doxorubicin, is currently being researched and used to treat an array of cancerous tissue growths. Regrettably, current administrative methods are focussed on a 'saturation' approach, as with the greater embodiment of medicine. This approach results in the exposure of non-target or non-cancerous tissue to drugs. In the case of Doxorubicin specifically, cardiotoxicity is a major problem brought about in this manner. Thus, if successful, a delivery system such as the one proposed here, could be adapted also for application here.

References

- Abbas, A.K., Lichtman, A.H. & Pillai, S., 2014. *Basic Immunology: Functions and Disorders of the Immune System* 4th ed., Philadelphia: Elsevier Ltd. Available at: <http://www.clinicalkey.com/dura/browse/bookChapter/3-s2.0-C20100672063>.
- Africa, L.D. & Smith, C., 2015. Sutherlandia frutescens may exacerbate HIV-associated neuroinflammation. *Journal of Negative Results in BioMedicine*, 14(14), pp.1–9. Available at: <http://www.jnrbm.com/content/14/1/14>.
- Akbar, M.A. et al., 2011. The full-of-bacteria gene is required for phagosome maturation during immune defense in Drosophila. *The Journal of Cell Biology*, 192, pp.383–390.
- Akopova, H., 2016. Chloroquine could be used for the treatment of filoviral infections and other viral infections that emerge or emerged from viruses requiring an acidic pH for infectivity. *Cell Biochemistry and Function*, 34, pp.191–196.
- de Almeida, A.C. et al., 2012. IFN-beta, IFN-gamma, and TNF-alpha decrease erythrophagocytosis by human monocytes independent of SIRP-alpha or SHP-1 expression. *Immunopharmacology and Immunotoxicology*, 34, pp.1054–1059. Available at: <http://www.ncbi.nlm.nih.gov/pubmed/22738830>.
- Alvarez, C. & Sztul, E.S., 1999. Brefeldin A (BFA) disrupts the organization of the microtubule and the actin cytoskeletons. *European Journal of Cell Biology*, 78(1), pp.1–14. Available at: [http://dx.doi.org/10.1016/S0171-9335\(99\)80002-8](http://dx.doi.org/10.1016/S0171-9335(99)80002-8).
- Anderson, R. & Wade, A.A., 2012. Innate immune mechanisms confer essential first-line host defence against the unrelenting threat posed by environmental microbial and viral pathogens. *Continuing Medical Education*, 30(8), pp.273–277.
- Arnold, L. et al., 2007. Inflammatory monocytes recruited after skeletal muscle injury switch into antiinflammatory macrophages to support myogenesis. *Journal of Experimental Medicine*, 204(5), pp.1057–1069. Available at: <http://www.ncbi.nlm.nih.gov/pubmed/17485518>
<http://www.ncbi.nlm.nih.gov/pmc/articles/PMC2118577/pdf/jem2041057.pdf>.
- Babu, M.M. et al., 2006. A database of bacterial lipoproteins (DOLOP) with functional assignments to predicted lipoproteins. *Journal of Bacteriology*, 188(8), pp.2761–2773.
- Backer, J.M., 2008. The regulation and function of Class III PI3Ks: novel roles for Vps34. *Biochemical Journal*, 410, pp.1–17.
- Bardoel, B.W. & Van Strijp, J.A.G., 2011. Molecular battle between host and bacterium: Recognition in innate immunity. *Journal of Molecular Recognition*, 24(6), pp.1077–1086.
- Becken, U. et al., 2010. Cell-free fusion of bacteria-containing phagosomes with endocytic compartments. *Proceedings of the National Academy of Sciences*, 107(48), pp.20726–20731. Available at: <http://www.pubmedcentral.nih.gov/articlerender.fcgi?artid=2996438&tool=pmcentrez&rendertype=abstract>.
- Becker, T., Volchuk, A. & Rothman, J.E., 2005. Differential use of endoplasmic reticulum membrane for phagocytosis in J774 macrophages. *Proceedings of the National Academy of Sciences of the United States of America*, 102(11), pp.4022–6. Available at: <http://www.pnas.org/content/102/11/4022.long>.
- Beemiller, P., Hoppe, A.D. & Swanson, J.A., 2006. A phosphatidylinositol-3-kinase-dependent signal transition regulates ARF1 and ARF6 during Fc-gamma receptor-mediated phagocytosis. *Public Library of Science Biology*, 4(6), pp.0987–0999.

- Berón, W. et al., 2001. Recruitment of coat-protein-complex proteins on to phagosomal membranes is regulated by a brefeldin A-sensitive ADP-ribosylation factor. *Biochemical Journal*, 355, pp.20726–20731.
- Blagoveshchenskaya, A.D. et al., 2002. HIV-1 Nef downregulates MHC-I by a PACS-1- and PI3K-regulated ARF6 endocytic pathway. *Cell*, 111(6), pp.853–866.
- Blocker, A. et al., 1996. Microtubule-associated protein-dependent binding of phagosomes to microtubules. *Journal of Biological Chemistry*, 271, pp.3803–3811.
- Blocker, A. et al., 1997. Molecular requirements for bi-directional movement of phagosomes along microtubules. *The Journal Cell Biology*, 137, pp.113–129.
- Botelho, R.J. et al., 2000. Localized biphasic changes in phosphatidylinositol-4,5-bisphosphate at sites of phagocytosis. *The Journal of Cell Biology*, 151, pp.1353–1368.
- Busby, W.J., Ackermann, J. & Crespi, C., 1999. Effect of methanol, ethanol, dimethyl sulfoxide, and acetonitrile on in vitro activities of cDNA-expressed human cytochromes P-450. *Drug Metabolism and Disposition*, 27(2), pp.246–249.
- Cardoso, C.M.P., Jordao, L. & Vieira, O.V., 2010. Rab10 regulates phagosome maturation and its overexpression rescues Mycobacterium-containing phagosomes maturation. *Traffic*, 11, pp.221–235.
- Chazaud, B. et al., 2009. Dual and beneficial roles of macrophages during skeletal muscle regeneration. *Exercise and Sport Sciences Reviews*, 37(1), pp.18–22.
- Cheng, Q. et al., 2010. Macrophage migration inhibitory factor increases leukocyte-endothelial interactions in human endothelial cells via promotion of expression of adhesion molecule. *The Journal of Immunology*, 185(2), pp.1238–1247.
- Chou, T.F. et al., 2011. Reversible inhibitor of p97, DBE_Q, impairs both ubiquitin-dependent and autophagic protein clearance pathways. *Proceedings of the National Academy of Sciences of the United States of America*, 108, pp.4834–4839.
- Clemens, D.L., Lee, B.Y. & Horwitz, M.A., 2000. Deviant expression of Rab5 on phagosomes containing the intracellular pathogens *Mycobacterium tuberculosis* and *Legionella pneumophila* is associated with altered phagosomal fate. *Infection and Immunity*, 68(5), pp.2671–2684.
- Collier, T.O. et al., 2001. Adhesion behavior of monocytes, macrophages, and foreign body giant cells on polyNIPAM temp-respons surfaces. *Journal of Biomedical Materials Research*, 59(1), pp.136–143.
- Collins, R.F. et al., 2002. Syntaxins 13 and 7 function at distinct steps during phagocytosis. *The Journal of Immunology*, 169, pp.3250–3256.
- Coppolino, M.G. et al., 2001. Requirement for Nethylmaleimide-sensitive factor activity at different stages of bacterial invasion and phagocytosis. *The Journal of Biological Chemistry*, 276, pp.4772–4780.
- Cox, D. et al., 2000. A Rab11- containing rapidly recycling compartment in macrophages that promotes phagocytosis. *Proceedings of the National Academy of Sciences of the United States of America*, 97, pp.680–685.
- Cox, D. et al., 1999. A requirement for phosphatidylinositol 3-kinase in pseudopod extension. *Journal of Biological Chemistry*, 274, pp.1240–1247.
- Cullen, P.J. & Korswagen, H.C., 2011. Sorting nexins provide diversity for retromer-dependent trafficking events. *Nature cell biology*, 14, pp.29–37.
- Curtis, L.M. & Gluck, S., 2005. Distribution of Rab GTPases in mouse kidney and comparison with

- vacuolar H⁺-ATPase. *Nephron Physiology*, 100, pp.31–42.
- Dabritz, J. et al., 2015. Reprogramming of Monocytes by GM-CSF Contributes to Regulatory Immune Functions during Intestinal Inflammation. *The Journal of Immunology*, 194(5), pp.2424–2438. Available at: <http://www.jimmunol.org/cgi/doi/10.4049/jimmunol.1401482>.
- Dayanidhi, S. et al., 2015. Reduced satellite cell number in situ in muscular contractures from children with cerebral palsy. *Journal of Orthopaedic Research*, 33(7), pp.1039–1045.
- Desjardins, M., 1995. Biogenesis of phagolysosomes: the “kiss and run” hypothesis. *Trends Cell Biology*, 5, pp.183–186.
- Desjardins, M., 2003. ER-mediated phagocytosis: a new membrane for new functions. *Nature Reviews Immunology*. *Nature Reviews Immunology*, 3, pp.280–291.
- Donaldson, J.G., Finazzi, D. & Klausner, R.D., 1992. Brefeldin A inhibits Golgi membrane–catalysed exchange of guanine nucleotide onto ARF protein. *Nature*, 360, pp.350–352.
- Dumas, A. et al., 2015. The HIV-1 protein Vpr impairs phagosome maturation by controlling microtubule-dependent trafficking. *The Journal of cell biology*, 211(2), pp.359–72. Available at: <http://www.ncbi.nlm.nih.gov/pubmed/26504171>.
- Eischen, A. et al., 1991. Long term cultures of human monocytes in vitro. Impact of GM-CSF on survival and differentiation. *Journal of Immunological Methods*, 143(2), pp.209–221.
- Fairn, G.D. & Grinstein, S., 2012. How nascent phagosomes mature to become phagolysosomes. *Trends in Immunology*, 33(8), pp.397–405. Available at: <http://dx.doi.org/10.1016/j.it.2012.03.003>.
- Falasca, M. & Maffucci, T., 2012. Regulation and cellular functions of class II phosphoinositide 3-kinases. *Biochemical Journal*, 443, pp.587–601.
- Ferrari, G. et al., 1999. A coatprotein on phagosomes involved in the intracellular survival of mycobacteria. *Cell*, 97(435–447).
- Firestone, A.J. et al., 2012. Small-molecule inhibitors of the AAA1 ATPase motor cytoplasmic dynein. *Nature*, 484, pp.125–129.
- Fratti, R.A. et al., 2001. Role of phosphatidylinositol 3-kinase and Rab5 effectors in phagosomal biogenesis and mycobacterial phagosome maturation arrest. *Journal of Cell Biology*, 154(3), pp.631–644.
- Freeman, S.A. & Grinstein, S., 2014. Phagocytosis: Receptors, signal integration, and the cytoskeleton. *Immunological Reviews*, 262(1), pp.193–215.
- Gagnon, E. et al., 2002. Endoplasmic reticulum- mediated phagocytosis is a mechanism of entry into macrophages. *Cell*, 110, pp.119–131.
- Gangwani, M.R. et al., 2013. Human immunodeficiency virus type 1 viral protein R (Vpr) induces CCL5 expression in astrocytes via PI3K and MAPK signaling pathways. *Journal of neuroinflammation*, 10(1), p.136. Available at: <http://www.pubmedcentral.nih.gov/articlerender.fcgi?artid=3831867&tool=pmcentrez&rendertype=abstract>.
- Garin, J. et al., 2001. The phagosome proteome: insight into phagosome functions. *The Journal of Cell Biology*, 152, pp.165–180.
- Gaur, N.A. et al., 2013. Vps factors are required for efficient transcription elongation in budding yeast. *Genetics*, 193, pp.829–851.
- Ghigo, E. et al., 2002. Survival of *Tropheryma whipplei*, the Agent of Whipple’s Disease, Requires

- Phagosome Acidification. *Infection and Immunity*, 70(3), pp.1501–1506.
- Gillooly, D.J. et al., 2000. Localization of phosphatidylinositol 3-phosphate in yeast and mammalian cells. *European Molecular Biology Organization Journal*, 19, pp.4577–4588.
- Gogulamudi, V.R. et al., 2015. Downregulation of host tryptophan-aspartate containing coat (TACO) gene restricts the entry and survival of *Leishmania donovani* in human macrophage model. *Frontiers in Microbiology*, 6, pp.1–10.
- Groothuis, T.A. & Neefjes, J., 2005. The many roads to cross-presentation. *The Journal of Experimental Medicine*, 202, pp.1313–1318.
- Guyton, C. & Hall, E., 2011. *Medical Physiology* 12th ed., Philadelphia: Elsevier Ltd.
- Hackam, D.J. et al., 1998. v-SNARE-dependent secretion is required for phagocytosis. *Proceedings of the National Academy of Sciences of the United States of America*, 95, pp.11691–11696.
- Hallett, M.B. & Dewitt, S., 2007. Ironing out the wrinkles of neutrophil phagocytosis. *Trends in Cell Biology*, 17, pp.209–214.
- Harrison, R.E. et al., 2003. Phagosomes fuse with late endosomes and/or lysosomes by extension of membrane protrusions along microtubules: role of Rab7 and RILP. *Molecular and Cellular Biology*, 23, pp.6494–6506.
- Hatsuzawa, K. et al., 2006. Involvement of syntaxin 18, an endoplasmic reticulum (ER)-localized SNARE protein, in ER-mediated phagocytosis. *Molecular Biology of the Cell*, 17, pp.3964–3977.
- Hawkins, P.T. & Stephens, L.R., 2015. PI3K signalling in inflammation. *Biochimica et Biophysica Acta - Molecular and Cell Biology of Lipids*, 1851(6), pp.882–897.
- Hazeki, K. et al., 2012. Essential roles of PIKfyve and PTEN on phagosomal phosphatidylinositol 3-phosphate dynamics. *FEBS Letters*, 586(22), pp.4010–4015. Available at: <http://dx.doi.org/10.1016/j.febslet.2012.09.043>.
- Hazeki, K. et al., 2006. Opposite effects of wortmannin and 2-(4-morpholinyl)-8-phenyl-1(4H)-benzopyran-4-one hydrochloride on toll-like receptor-mediated nitric oxide production: negative regulation of nuclear factor-kappa B by phosphoinositide 3-kinase. *Molecular Physiology*, 69(5), pp.1717–1724.
- Hetz, C., 2012. The unfolded protein response: controlling cell fate decisions under ER stress and beyond. *Molecular Cell Biology*, 13, pp.89–102.
- Hickey, C.M. & Wickner, W., 2010. HOPS initiates vacuole docking by tethering membranes before trans-SNARE complex assembly. *Molecular Biology of the Cell*, 21, pp.2297–2305.
- Honda, A. et al., 1999. Phosphatidylinositol 4-phosphate 5-kinase a is a downstream effector of the small G protein ARF6 in membrane ruffle formation. *Cell*, 99, pp.521–532.
- Horiuchi, H. et al., 1997. A novel Rab5 GDP/GTP exchange factor complexed to Rabaptin-5 links nucleotide exchange to effector recruitment and function. *Cell*, 90, pp.1149–1159.
- Hu, Y. et al., 2008. IFN-gamma and STAT1 arrest monocyte migration and modulate RAC/CDC42 pathways. *The Journal of Immunology*, 180(12), pp.8057–8065.
- Husebye, H. et al., 2010. The Rab11a GTPase controls Toll-like receptor 4-induced activation of interferon regulatory factor-3 on phagosomes. *Immunity*, 33, pp.583–596.
- Huss, M. et al., 2002. Concanamycin A, the specific inhibitor of V-ATPases, binds to the VO subunit c. *Journal of Biological Chemistry*, 277(43), pp.40544–40548.
- Huss, M. & Wieczorek, H., 2012. Inhibitors of V-ATPases: old and new players. *The Journal of*

Experimental Biology, 212, pp.341–372.

- Huynh, K.K. et al., 2007. Fusion, fission, and secretion during phagocytosis. *Physiology Bethesda*, 22(46), pp.366–372.
- van Ijzendoorn, S.C., 2006. Recycling endosomes. *Journal of cell science*, 119(Pt 9), pp.1679–81. Available at: <http://www.ncbi.nlm.nih.gov/pubmed/16636069>.
- Imhof, B.A. & Aurrand-Lions, M., 2004. Adhesion mechanisms regulating the migration of monocytes. *Nature Reviews Immunology*, 4(6), pp.432–444. Available at: <http://dx.doi.org/10.1038/nri1375>.
- Invitrogen, 2001. Working With FluoSpheres® Fluorescent Microspheres. *Manual*.
- Jackson, S.P., Yap, C.L. & Anderson, K.E., 2004. Phosphoinositide 3-kinases and the regulation of platelet function. *Biochemical Society Transactions*, 32, pp.387–392.
- Jaguin, M. et al., 2013. Polarization profiles of human M-CSF-generated macrophages and comparison of M1-markers in classically activated macrophages from GM-CSF and M-CSF origin. *Cellular Immunology*, 281(1), pp.51–61.
- Jahn, R. & Scheller, R.H., 2006. SNAREs: Engines for membrane fusion. *Nature Reviews Molecular Cell Biology*, 7, pp.631–643.
- Jahraus, A. et al., 1998. In vitro fusion of phagosomes with different endocytic organelles. *Journal of Biological Chemistry*, 273(46), pp.30379–30390.
- Jahraus, A. et al., 1994. Molecular characterization of phagosomes. *Journal of Cell Science*, 107, pp.145–157.
- Jahreiss, L., Menzies, F.M. & Rubinsztein, D.C., 2008. The itinerary of autophagosomes: From peripheral formation to kiss-and-run fusion with lysosomes. *Traffic*, 9(4), pp.574–587.
- Johansson, M. et al., 2007. Activation of endosomal dynein motors by stepwise assembly of Rab7-RILP-p150Glued, ORP1L, and the receptor betaIII spectrin. *The Journal of Cell Biology*, 176, pp.459–471.
- Johansson, M. et al., 2005. The oxysterol-binding protein homologue ORP1L interacts with Rab7 and alters functional properties of late endocytic compartments. *Molecular Biology of the Cell*, 16(12), pp.5480–5492.
- Ka, M.B. et al., 2014. Phenotypic Diversity and Emerging New Tools to Study Macrophage Activation in Bacterial Infectious Diseases. *Frontiers in Immunology*, 5, pp.1–7. Available at: <http://www.pubmedcentral.nih.gov/articlerender.fcgi?artid=4193331&tool=pmcentrez&rendertype=abstract>.
- Kasama, T. et al., 2010. Macrophage Migration Inhibitory Factor: A Multifunctional Cytokine in Rheumatic Diseases. *Arthritis*, 2010, pp.1–10. Available at: <http://www.hindawi.com/journals/arthritis/2010/106202/>.
- Kinchen, J.M. et al., 2008. A pathway for phagosome maturation during engulfment of apoptotic cells. *Nature Cell Biology*, 10, pp.556–566.
- Kreis, T.E., Lowe, M. & Pepperkok, R., 1995. COPs regulating membrane traffic. *Annual Review of Cell and Developmental Biology*, 11, pp.457–466.
- Lampin, M. et al., 1997. Correlation between substratum roughness and wettability, cell adhesion, and cell migration. *Journal of Biomedical Materials Research*, 36(1), pp.99–108.
- Lemmon, S.K. & Traub, L.M., 2000. Sorting in the endosomal system in yeast and animal cells. *Current Opinion in Cell Biology*, 12, pp.457–466.

- Letourneur, F. et al., 1994. Coatamer is essential for retrieval of dilysinetagged proteins to the endoplasmic reticulum. *Cell*, 79, pp.1199–1207.
- Li, X. et al., 2016. A molecular mechanism to regulate lysosome motility for lysosome positioning and tubulation. *Nature Cell Biology*, 18(4), pp.404–417.
- Lin, T. et al., 2015. Spindle-F Is the Central Mediator of I κ B Kinase-Dependent Dendrite Pruning in *Drosophila* Sensory Neurons. *Public Library of Science Genetics*, 11(11), p.e1005642.
- Liu, G. & Yang, H., 2013. Modulation of macrophage activation and programming in immunity. *Journal of Cellular Physiology*, 228(3), pp.502–512.
- Liu, W. et al., 2013. The innate NK cells and macrophages recognize and reject allogeneic non-self in vivo via different mechanisms. *The Journal of Immunology*, 188(6), pp.2703–2711.
- Liu, Y. et al., 2005. Wortmannin, a widely used phosphoinositide 3-kinase inhibitor, also potently inhibits mammalian polo-like kinase. *Chemistry and Biology*, 12(1), pp.99–107.
- Marie, E. et al., 2014. Amphiphilic macromolecules on cell membranes: from protective layers to controlled permeabilization. *The Journal of Membrane Biology*, 247(9), pp.861–881.
- Marshall, J.G. et al., 2001. Restricted accumulation of phosphatidylinositol 3-kinase products in a plasmalemmal subdomain during Fc γ receptor-mediated phagocytosis. *Journal of Cell Biology*, 153(7), pp.1369–1380.
- Mazaki, Y., Nishimura, Y. & Sabe, H., 2012. GBF1 bears a novel phosphatidylinositol-phosphate binding module, BP3K, to link PI3K γ activity with Arf1 activation involved in GPCR-mediated neutrophil chemotaxis and superoxide production. *Molecular Biology of the Cell*, 23, pp.2457–2467.
- Mazzolini, J. et al., 2010. Inhibition of phagocytosis in HIV-1-infected macrophages relies on Nef-dependent alteration of focal delivery of recycling compartments. *Blood*, 115, pp.4226–4236.
- McBride, H.M. et al., 1999. Oligomeric complexes link Rab5 effectors with NSF and drive membrane fusion via interactions between EEA1 and syntaxin 13. *Cell*, 98, pp.377–386.
- Meresse, S., Gorvel, J.P. & Chavrier, P., 1995. The rab7 GTPase resides on a vesicular compartment connected to lysosomes. *Journal of Cell Science*, 108, pp.3349–3358.
- Mia, S. et al., 2014. An optimized protocol for human M2 macrophages using M-CSF and IL-4/IL-10/TGF- β yields a dominant immunosuppressive phenotype. *Scandinavian Journal of Immunology*, 79(5), pp.305–314.
- Miki, H., Miura, K. & Takenawa, T., 1996. N-WASP, a novel actin-depolymerizing protein, regulates the cortical cytoskeletal rearrangement in a PIP2-dependent manner downstream of tyrosine kinases. *The European Molecular Biology Organisation Journal*, 15, pp.5326–5335.
- Mills, C.D. et al., 2015. Sequential Immune Responses: The Weapons of Immunity. *Journal of Innate Immunity*, 7, pp.443–449.
- Misawa, T. et al., 2013. Microtubule-driven spatial arrangement of mitochondria promotes activation of the NLRP3 inflammasome. *Nature immunology*, 14(5), pp.454–60. Available at: <http://www.ncbi.nlm.nih.gov/pubmed/23502856>.
- Moradin, N. & Descoteaux, A., 2012. Leishmania promastigotes: building a safe niche within macrophages. *Frontiers in cellular and infection microbiology*, 2, pp.1–6. Available at: <http://www.pubmedcentral.nih.gov/articlerender.fcgi?artid=3445913&tool=pmcentrez&rendertype=abstract>.
- Mukkada, A.J. et al., 1985. Enhanced metabolism of *Leishmania donovani* amastigotes at acid pH: an adaptation for intracellular growth. *Science*, 229, pp.1099–1101.

- Nakanishi, S., Yano, H. & Matsuda, Y., 1995. Novel functions of phosphatidylinositol 3-kinase in terminally differentiated cells. *Cellular Signalling*, 7, pp.545–557.
- Ng, E.L., Wang, Y. & Tang, B.L., 2007. Rab22B's role in trans-Golgi network membrane dynamics. *Biochemical and Biophysical Research Communications*, 361, pp.751–757.
- Nie, Z., Hirsch, D.S. & Randazzo, P.A., 2003. Arf and its many interactors. *Current Opinion in Cell Biology*, 15, pp.396–404.
- Niedergang, F. et al., 2003. ADP ribosylation factor 6 is activated and controls membrane delivery during phagocytosis in macrophages. *The Journal of Cell Biology*, 161, pp.1143–1150.
- Nielsen, E. et al., 1999. Rab5 regulates motility of early endosomes on microtubules. *Nature Cell Biology*, 1, pp.376–382.
- Nookala, A.R. et al., 2013. HIV-1 tat-mediated induction of CCL5 in astrocytes involves NF- κ B, AP-1, C/EBP α and C/EBP γ transcription factors and JAK, PI3K/Akt and p38 MAPK signaling pathways. *Public Library of Science*, 8(11), pp.1–13.
- O'Leary, S., O'Sullivan, M.P. & Keane, J., 2011. IL-10 blocks phagosome maturation in Mycobacterium tuberculosis-infected human macrophages. *American Journal of Respiratory Cell and Molecular Biology*, 45(1), pp.172–180.
- Ober, R.J. et al., 2001. Differences in promiscuity for antibody-FcRn interactions across species: implications for therapeutic antibodies. *International Immunology*, 13(12), pp.1551–1559.
- Okkenhaug, K., 2013. Signaling by the phosphoinositide 3-kinase family in immune cells. *Annual Review of Immunology*, 31, pp.675–704.
- Parise, G., McKinnell, I. & Rudnicki, M., 2008. Muscle satellite cell and atypical myogenic progenitor response following exercise. *Muscle and Nerve*, 37(5), pp.611–619.
- Paroutis, P., Touret, N. & Grinstein, S., 2004. The pH of the secretory pathway: measurement, determinants, and regulation. *Physiology Bethesda*, 19, pp.207–215.
- Patki, V. et al., 1998. A functional PtdIns(3)P-binding motif. *Nature*, 394, pp.433–434.
- Posor, Y. et al., 2013. Spatiotemporal control of endocytosis by phosphatidylinositol-3,4-bisphosphate. *Nature*, 499, pp.233–237.
- Press, B. et al., 1998. Mutant Rab7 causes the accumulation of cathepsin D and cation-independent mannose 6-phosphate receptor in an early endocytic compartment. *The Journal of Cell Biology*, 140, pp.1075–1089.
- Proudfoot, A., Power, C. & Wells, T., 2000. The strategy of blocking the chemokine system to combat disease. *Immunological Reviews*, 177, pp.246–256.
- Puri, R.V., Reddy, P.V. & Tyagi, A.K., 2013. Secreted Acid Phosphatase (SapM) of Mycobacterium tuberculosis Is Indispensable for Arresting Phagosomal Maturation and Growth of the Pathogen in Guinea Pig Tissues. *Public Library of Science*, 8(7), p.e70514.
- Rai, M.N. et al., 2015. An essential role for phosphatidylinositol 3-kinase in the inhibition of phagosomal maturation, intracellular survival and virulence in *Candida glabrata*. *Cellular Microbiology*, 17(2), pp.269–287.
- Redpath, S., Ghaza, I. P. & Gascoigne, N.R., 2001. Hijacking and exploitation of IL-10 by intracellular pathogens. *Trends in Microbiology*, 9, pp.86–92.
- Rice, E. et al., 2003. Interferon-gamma induces macrophage migration inhibitory factor synthesis and secretion by tubular epithelial cells. *Nephrology (Carlton)*, 8(3), pp.156–161.

- Rousselle, A.V. & Heymann, D., 2002. Osteoclastic acidification pathways during bone resorption. *Bone*, 30, pp.533–540.
- Sainath, R. & Gallo, G., 2015. The dynein inhibitor Ciliobrevin D inhibits the bidirectional transport of organelles along sensory axons and impairs NGF-mediated regulation of growth cones and axon branches. *Developmental Neurobiology*, 75(7), pp.757–777. Available at: <http://onlinelibrary.wiley.com/doi/10.1002/dneu.22246/abstract> \n<http://onlinelibrary.wiley.com/doi/10.1002/dneu.22246/full>.
- Scott, C.C. et al., 2002. Role of 3-phosphoinositides in the maturation of Salmonella-containing vacuoles within host cells. *The Journal of Biological Chemistry*, 277, pp.12770–12776.
- Segawa, T. et al., 2014. Inpp5e increases the Rab5 association and phosphatidylinositol 3-phosphate accumulation at the phagosome through an interaction with Rab20. *Biochemical Journal*, 464(3), pp.365–375. Available at: <http://www.ncbi.nlm.nih.gov/pubmed/25269936> \n<http://www.biochemj.org/bj/464/bj4640365.htm>.
- Sendide, K. et al., 2005. Mycobacterium bovis BCG attenuates surface expression of mature Class II molecules through IL-10–dependent inhibition of cathepsin S. *The Journal of Immunology*, 175, pp.5324–5332.
- Seto, S. et al., 2010. Differential recruitment of CD63 and Rab7-interacting-lysosomal-protein to phagosomes containing Mycobacterium tuberculosis in macrophages. *Microbiology and Immunology*, 54, pp.170–174.
- Seto, S., Tsujimura, K. & Koide, Y., 2011. Rab GTPases Regulating Phagosome Maturation Are Differentially Recruited to Mycobacterial Phagosomes. *Traffic*, 12(4), pp.407–420.
- Shi, M. et al., 2016. MAP1S protein regulates the phagocytosis of bacteria and toll-like receptor (TLR) signaling. *Journal of Biological Chemistry*, 291(3), pp.1243–1250.
- Shi, Y. et al., 2006. Granulocyte-macrophage colony-stimulating factor (GM-CSF) and T-cell responses: what we do and don't know. *Cell Research*, 16(2), pp.126–133. Available at: <http://www.nature.com/doi/10.1038/sj.cr.7310017>.
- Shin, H.W. & Nakayama, K., 2004. Guanine nucleotide-exchange factors for arf GTPases: their diverse functions in membrane traffic. *The Journal of Biochemistry*, 136, pp.761–767.
- Silverthorn, D.U., 2010. *Human Physiology: An Integrated Approach* 5th ed., San Francisco: Pearson.
- Simonsen, A. et al., 1998. EEA1 links PI3K function to Rab5 regulation of endosome fusion. *Nature*, 394(494–498).
- Smith, C. et al., 2008. The Inflammatory Response to Skeletal Muscle Injury. *Sports Medicine*, 38(11), pp.947–969. Available at: <http://link.springer.com/10.2165/00007256-200838110-00005>.
- Snijders, T. et al., 2016. Muscle fibre capillarization is a critical factor in muscle fibre hypertrophy during resistance exercise training in older men. *Journal of Cachexia, Sarcopenia and Muscle*. Available at: <http://doi.wiley.com/10.1002/jcsm.12137>.
- Song, C.H. et al., 2003. Role of mitogen-activated protein kinase pathways in the production of tumor necrosis factor- α , interleukin-10, and monocyte chemoattractant protein-1 by Mycobacterium tuberculosis H37Rv–infected human monocytes. *Journal of Clinical Immunology*, 23, pp.194–201.
- Strahl, T. & Thorner, J., 2007. Synthesis and function of membrane phosphoinositides in budding yeast, *Saccharomyces cerevisiae*. *Biochimica et Biophysica Acta*, 1771, pp.353–404.
- Swanson, J.A. & Hoppe, A.D., 2004. The coordination of signaling during Fc receptor-mediated phagocytosis. *Journal of Leukocyte Biology*, 76(6), pp.1093–1103. Available at: <http://www.jleukbio.org/content/76/6/1093.full> \npapers3://publication/doi/10.1189/jlb.0804439.

- Thi, E.P., Lambertz, U. & Reiner, N.E., 2012. Sleeping with the enemy: how intracellular pathogens cope with a macrophage lifestyle. *Public Library of Science Pathogens*, 8(3), p.e1002551.
- Thiele, L. et al., 2001. Evaluation of particle uptake in human blood monocyte-derived cells in vitro. Does phagocytosis activity of dendritic cells measure up with macrophages? *Journal of Controlled Release*, 76(1), pp.59–71.
- Tomlinson, M.J. et al., 2013. Cell separation: Terminology and practical considerations. *Journal of Tissue Engineering*, 4, pp.1–14. Available at: <http://www.ncbi.nlm.nih.gov/pubmed/23440031> <http://www.pubmedcentral.nih.gov/articlerender.fcgi?artid=PMC3578272>.
- Touret, N. et al., 2005. Quantitative and dynamic assessment of the contribution of the ER to phagosome formation. *Cell*, 123, pp.157–170.
- Trambas, C.M. & Griffiths, G.M., 2003. Delivering the kiss of death. *Nature Immunology*, 4(5), pp.399–403.
- Tseng, C.N. et al., 2014. Brefeldin A reduces anchorage-independent survival, cancer stem cell potential and migration of MDA-MB-231 human breast cancer cells. *Molecules*, 19(11), pp.17464–17477.
- Tsuchiya, S. et al., 1980. Establishment and characterization of a human acute monocytic leukemia cell line (THP-1). *International Journal of Cancer*, 26(2), pp.171–176. Available at: <http://www.ncbi.nlm.nih.gov/pubmed/6970727>.
- Tucker, S.C. & Casadevall, A., 2002. Replication of *Cryptococcus neoformans* in macrophages is accompanied by phagosomal permeabilization and accumulation of vesicles containing polysaccharide in the cytoplasm. *Proceedings of the National Academy of Science of the United States of America*, 99, pp.3165–3170.
- Vergne, I. et al., 2005. Mechanism of phagolysosome biogenesis block by viable *Mycobacterium tuberculosis*. *Proceedings of the National Academy of Sciences of the United States of America*, 102, pp.4033–4038.
- Vergne, I., Chua, J. & Deretic, V., 2003. *Mycobacterium tuberculosis* Phagosome Maturation Arrest: Selective Targeting of PI3P-Dependent Membrane Trafficking. *Traffic*, 4(9), pp.600–606. Available at: <http://onlinelibrary.wiley.com/doi/10.1034/j.1600-0854.2003.00120.x/full> <http://www.ncbi.nlm.nih.gov/pubmed/12500000>.
- Vieira, O. V et al., 2003. Modulation of Rab5 and Rab7 recruitment to phagosomes by phosphatidylinositol 3-kinase. *Molecular and Cellular Biology*, 23(7), pp.2501–2514. Available at: <http://www.pubmedcentral.nih.gov/articlerender.fcgi?artid=150733&tool=pmcentrez&rendertype=abstract>.
- Vieira, O. V. et al., 2001. Distinct roles of class I and class III phosphatidylinositol 3-kinases in phagosome formation and maturation. *Journal of Cell Biology*, 155(1), pp.19–25.
- Vieira, O. V., Botelho, R.J. & Grinstein, S., 2002. Phagosome maturation: aging gracefully. *The Biochemical journal*, 366(Pt 3), pp.689–704. Available at: <http://www.pubmedcentral.nih.gov/articlerender.fcgi?artid=1222826&tool=pmcentrez&rendertype=abstract>.
- Vinet, A.F. et al., 2009. The *Leishmania donovani* Lipophosphoglycan Excludes the Vesicular Proton-ATPase from Phagosomes by Impairing the Recruitment of Synaptotagmin. *Public Library of Science Pathogens*, 5(10), p.e1000628. Available at: <http://dx.plos.org/10.1371/journal.ppat.1000628>.
- Wang, T. & Hong, W., 2002. Interorganellar regulation of lysosome positioning by the Golgi apparatus through Rab34 interaction with Rab-interacting lysosomal protein. *Molecular Biology of the Cell*, 13, pp.4317–4332.

- Weber, S.M., Levitz, S.M. & Harrison, T.S., 2000. Chloroquine and the fungal phagosome. *Current Opinion in Microbiology*, 3, pp.349–353.
- Wymann, M.P. et al., 1996. Wortmannin inactivates phosphoinositide 3-kinase by covalent modification of Lys-802, a residue involved in the phosphate transfer reaction. *Molecular and Cellular Biology*, 16, pp.1722–1733.
- Xie, R. et al., 2011. Microtubule-associated protein 1S (MAP1S) bridges autophagic components with microtubules and mitochondria to affect autophagosomal biogenesis and degradation. *The Journal of Biological Chemistry*, 286, pp.10367–10377.
- Yang, Y. et al., 2013. Application and interpretation of current autophagy inhibitors and activators. *Acta pharmacologica Sinica*, 34(5), pp.625–635. Available at: <http://www.ncbi.nlm.nih.gov/pubmed/23524572>.
- Yano, H. et al., 1993. Inhibition of histamine secretion by wortmannin through the blockade of phosphatidylinositol 3-kinase in RBL-2H3 cells. *The Journal of Biological Chemistry*, 268(34), pp.25846–25856.
- Yano, K. et al., 2016. Dissection of autophagy in tobacco BY-2 cells under sucrose starvation conditions using the vacuolar HC-ATPase inhibitor concanamycin A and the autophagy-related protein Atg8. *Plant Signalling & Behaviour*, 2324, pp.1–12.
- Yates, R.M., Hermetter, A. & Russell, D.G., 2005. The kinetics of phagosome maturation as a function of phagosome/lysosome fusion and acquisition of hydrolytic activity. *Traffic*, 6, pp.412–420.
- Yuan, H. et al., 2007. Covalent Reactions of Wortmannin under Physiological Conditions. *Chemistry and Biology*, 14(3), pp.321–328.
- Yuan, H. et al., 2006. Wortmannin-C20 conjugates generate wortmannin. *Journal of Medical Chemistry*, 49, pp.740–747.
- Zeeh, J.C. et al., 2006. Dual specificity of the interfacial inhibitor brefeldin A for arf proteins and Sec7 domains. *Journal of Biological Chemistry*, 281(17), pp.11805–11814.
- Zhang, Q. et al., 1998. A requirement for ARF6 in Fcγ receptor-mediated phagocytosis in macrophages. *Journal of Biological Chemistry*, 273(32), pp.19977–19981.
- Zhang, Q. et al., 2010. Circulating mitochondrial DAMPs cause inflammatory responses to injury. *Nature*, 464(7285), pp.104–107.
- Zhu, H., Liang, Z. & Li, G., 2009. Rabex-5 is a Rab22 effector and mediates a Rab22- Rab5 signaling cascade in endocytosis. *Molecular Biology of the Cell*, 20, pp.4720–4729.

Appendix A: Literature Review

Harnessing phagocytosis for regenerative medicine: lessons from microbes

Johan Georg Visser, Carine Smith

Department of Physiological Sciences, Stellenbosch University, South Africa

Corresponding author:

Prof Carine Smith

Department of Physiological Sciences

Stellenbosch University

Private Bag X1

Matieland

7602

South Africa

Conflict of interest.

The authors declare no conflict of interest.

Abstract

Macrophages and neutrophils are evolutionarily equipped for host defence, mainly as a result of their high capacity for phagocytosis and diapedesis. The fact that these processes are highly conserved across species - nearly 95% of the animal kingdom is devoid of both B and T cells - testifies to its effectiveness in neutralising invaders. Despite this, these processes are also manipulated and exploited by bacteria and viruses for their own pathogenic propagation. Perturbation of phagocytosis for intracellular pathogen survival is generally achieved through phagosome maturation arrest. This prevents phagosome acidification, recruitment of enzymes or even modulation of phagocyte killing capacity. In order to understand the complexities of phagocytic evasion, one first needs to appreciate the equally complex and redundant process that is phagocytosis. In this review, the molecular aspects of phagocytosis, from initial recognition and pseudopod extension to successful neutralization and degradation of foreign material is concisely discussed in a temporal manner. This is followed by recent information from the literature related to pathogenic evasion, with focus on specific bacteria and viruses such as *Mycobacterium tuberculosis* and HIV, to illustrate how these pathogens manipulate the phagocytic process. After conveying our understanding of these processes, a hypothesis for an unorthodox approach to regenerative medicine is formulated: that of experimental modification of phagocytes to achieve maturation arrest, to render these cells capable of internalising and transporting cargo such as live stem cells or therapeutic drugs, to specific tissues, without damage to this cargo while in transit.

Introduction

Phagocytes, such as macrophages and neutrophils, are responsible for non-specific recognition and destruction of invading pathogens. At least two characteristics of these cells make them ideally suited for this task. Firstly, they are highly mobile cells, with the ability to readily cross membranes, such as endothelium. This affords them the uncommon cellular trait of migration across different body or tissue compartments to reach sites where they are required. Secondly, these cells have the capacity for phagocytosis – an intricate process, starting with pseudopodia extension to engulf particle matter and ending in particle neutralization within a destructive phagolysosome. The fact that these two mechanisms are highly conserved across species¹ testifies to its potency and overall importance for host health. However, it is also known that the process of phagocytosis is not infallible. Several papers have described the ability of evolved microbes, such as *Mycobacterium tuberculosis*², *Leishmania donovani*³ and *Candida glabrata*⁴, to hide from the immune system by remaining inside phagocytes without being digested in the phagolysosome.

We believe that a lesson can be learned from these microbes, and harnessed to the benefit of regenerative medicine practises. In this review, we will present our hypothesis on how this may be achieved. However, we first present an overview of what is currently known about the molecular processes involved in the phagocytic process, aiming to elucidate the molecular mechanisms of phagosome maturation in a temporal and concise manner as to better understand this phenomenon. This will be followed by a discussion of phagosome maturation arrest and the mechanisms used by microbial agents to evade phagosomal neutralization, before we will elaborate on the potential for application of this knowledge in an unorthodox, novel approach to regeneration.

Molecular basis of phagocytosis

Phagocytosis involves considerable membrane and cytoskeletal rearrangements in order to encircle and capture (engulf) potential pathogens or matter foreign to the immune system – forming

phagosomes – and to mature these nascent phagosomes into phagolysosomes⁵. Microbial material is captured inside a nascent phagosome that matures through events relating to the endocytic and autophagic pathway, where fission and fusion events allow for its destructive ability. In the next few sections, these intricate processes will be explained in detail, using macrophages as representative phagocytic immune cell.

Recognition

Matter is recognised as foreign – and thus as potential threat – via binding to specific pattern recognition receptors (PRRs) located both in the cytosol and cell surface of immune cells of both the innate and adaptive branch of the immune system, as well as on epithelial cells such as the vascular endothelium⁶. PRRs differentiate between molecules that are released by dying self-cells and foreign material through respectively binding to damage-associated molecular patterns (DAMPs) and pathogen-associated molecular patterns (PAMPs) (ref. 7). Necrotic self-cells release formylated peptides like N-formylmethionine from damaged mitochondria⁸. These self-originating proteins (classified under DAMPs) can bind to formyl peptide receptors (FPRs) on monocytic cells, initiating chemotaxis and phagocytosis⁹. Interestingly, these formylated peptides are also characteristic of bacterial proteins. In our opinion, this supports the endosymbiotic theory of mitochondrial evolution, which proposes that mitochondria are foreign organelles that were incorporated into eukaryotic cells for energy production. In this manner, cells containing damaged mitochondria, i.e. metabolically compromised cells, are removed via recognition of these DAMPs, irrespective of self or non-self. Recognition of PAMPs is oriented toward many PRR subtypes, such as NOD-like receptors (NLRs) (recognise DAMPs as well), RIG-like receptors (RLR) and Toll-like receptors (TLRs). NLRs are mainly associated with sterile inflammation via NLRP3-inflammasome activation¹⁰. The membrane bound TLRs bind bacterial hallmark molecules both intra- and extracellularly and exhibit some target specificity. The TLR5 subtype typically binds to flagellae, while TLR2 and TLR4 bind components of the bacterial cell wall like peptidoglycan and lipopolysaccharide (LPS), respectively⁷. TLR2 forms a

heterodimer with TLR1 or TLR6 to bind the N-terminal cysteine modification on lipoproteins of bacteria, as illustrated in mycobacterium⁹. This lipoprotein modification is uniquely conserved in over 2000 different bacterial proteins¹¹, which can all be recognised by binding of this heterodimer. Other TLRs like TLR3, TLR7, TLR8 and TLR9 are intracellular receptors and recognize bacterial dsRNA and DNA.

TLR activation induces recruitment of adaptor proteins and activation of transcription factors for production and release of cytokines, adhesion molecules and costimulators⁷. Active TLRs indirectly regulate phagocytosis through MyD88 signalling and activation of the p38 residue to accelerate phagocytosis¹². The newly identified mitogen-associated protein 1S (MAP1S) autophagy-related protein was also very recently reported to be necessary for TLR activation and effective bacterial phagocytosis¹², but more research is required to fully elucidate its role in this context. Many other receptors including lectin, mannose, complement and RLRs also assist with pathogen recognition, but the IgG receptors are more closely associated with phagocytosis, where IgG-binding opsonises bacteria to facilitate phagocytosis of material otherwise 'invisible' to phagocytes. Macrophage Fc γ surface receptors (CD64) recognise the constant γ heavy chain in Fc regions of the IgG, which induces Fc γ R clustering at the site of material contact that leads to actin polymerization and engulfment through pseudopod extension¹³. Formation of pseudopodia and actin polymerization is highly dependent on phosphatidylinositol 3-kinase (PI3k) recruitment for production of various phosphatidylinositides. The ADP ribosylation factor (ARF) proteins play a pivotal role in activating phosphatidylinositol kinase enzymes to regulate membrane modification¹⁴. Specifically, ARF6 has many functions, such as being recruited to the tip of forming pseudopodia where it activates type I phosphatidylinositol 3 kinase (PI3k) substrate production via activation of other phosphatidylinositol kinases¹⁵, and activation of actin polymerization during pseudopod extension¹⁶. This collectively ensures particle capture and membrane fusion to form a phagosome. Fc γ R mediated phagocytosis is the main form of phagocytosis simulated in experimental phagocytosis models, because engulfment does not require stimulation by lymphoid cells, as explained further by Liu¹⁷.

Pseudopodia and encapsulation

Following recognition, phagocytosis is initiated with the extension of pseudopodia. Particle internalisation and phagosome formation is achieved within 5 min after introduction of the foreign agent under culture conditions (Visser and Smith, unpublished data). Macrophages specifically are extremely ambitious in their phagocytic ability and are able to engulf particles which are closely comparable with their own size⁵. Interestingly, a form of cell suicide termed “frustrated phagocytosis” has been reported, where cultured macrophages attempted to engulf opsonised tissue culture plate surfaces, increasing cell surface area by over 20% (ref. 18). This phenomenon presented a useful model with which to investigate the mechanics of pseudopod formation, and the mechanism(s) by which this phenomenal change in cell shape are achieved has been debated to some extent. One theory postulated that the macrophage membrane is corrugated, possibly allowing a flattening out of the membrane during extra-large particle engulfment¹⁹. However, quantitative spectroscopy has shown that during healthy phagocytosis, membrane surface area indeed enlarge to such an extent that surface flattening alone cannot fully account for it²⁰.

This raises the questions of where the extra membrane comes from. Specific membrane reservoirs have not been identified within cells, but general cellular sources exist. For example, in osteoclasts, exocytosis of late endosomes has been shown to deliver membrane components and increase cell surface area during bone reabsorption. Also in the context of macrophage pseudopod formation, a few candidates have been investigated. Initially, Gagnon²¹ proposed that the ER may fuse with the plasma membrane at the base of extending pseudopodia, forming a continuity through which the particle can slide into the ER lumen. This idea was supported by Becker²², who reported that phagocytosis efficiency of large particles (>3 μ m) was reduced after neutralization of the ER soluble N-ethylmaleimide-sensitive factor-attachment protein (SNARE) receptor, ERS24. The theory of Gagnon and colleagues²¹ was however not accepted by all, as others have argued that the role of the ER during phagocytosis still needs some elucidation²³. More recently, using a variety of techniques including

immunological, biochemical, electron microscopy and fluorescence microscopy, Huynh⁵ indeed could not find any evidence of the ER fusing to the plasma membrane during phagocytosis. Also, since phagosomes acidify during maturation via a proton gradient created by the vacuolar-type H⁺-ATPase (V-ATPase) proton pump, and the ER membrane is permeable to protons and devoid of V-ATPase (ref. 24), the theory of simple ER fusion is probably unlikely to fully explain the phenomenon. We speculate that the ER likely fuses with phagosomal membranes – however, it could be in a ‘kiss and run’ or ‘kiss of death’ fashion, as seen during autophagosome fusion with lysosomes²⁵ and cytotoxic T cell-mediated cell death²⁶. This may result in an exchange or delivery of ER localised proteins to phagosomes, without complete membrane exchange through fusion. Furthermore, since ER engagement was observed during large particle uptake (>3µm) and mostly during FcγR mediated phagocytosis²², ER engagement is likely size- and receptor-specific.

A more likely candidate is the enzyme group of phosphatidylinositol 3 kinases (PI3k) that phosphorylate the 3' inositol phospholipid of inositol rings. These kinases are classified into three families based on their substrate used for lipid phosphorylation: types I, II and III. The type I PI3k consists of four isoforms, PI3k α , β , γ and δ , which all use phosphatidylinositol 4,5-bisphosphate (PI(4,5)P₂) as substrate to generate phosphatidylinositol 3,4,5-triphosphate (PI(3,4,5)P₃, or PIP₃) from phosphatidylinositol 4,5-bisphosphate (PI(4,5)P₂) (ref. 27). This PI3k substrate concentration is kept at optimal level by phosphatidylinositol 4-phosphate 5-kinase α (PI4P-5k α) through its phosphorylation of phosphatidylinositol 4-phosphate (PI4P) to PI(4,5)P₂ (ref. 28). The PI3k δ isoform is unique to immune cells as it is normally only expressed on lymphoid and myeloid cell lineages²⁹.

Botelho³⁰ found transiently high PI(4,5)P₂ expression on extending pseudopodia with its disappearance shortly after phagocytic cup closure and nascent phagosome formation. Furthermore, type I PI3ks recruitment and subsequent PIP₃ expression has been shown to occur on extending pseudopodia during engulfment of antibody-opsonised particles³¹. Throughout the literature, PIP₃ is seen as the main propagating agent during pseudopod extension. However, apart from the apparent

steric association of PI(4,5)P₂ to PI3ks – necessary for its phosphorylation to PIP₃ – PI(4,5)P₂ itself seems to have an equally important role in pseudopod formation. Active ARF6 induces PI(4,5)P₂ production through activation of PI4P-5κ during phagocytosis¹⁵. PI(4,5)P₂ then recruit WASP/N-WASP proteins to facilitate actin polymerization in a G-protein coupled manner during phagocytosis³². The role of type I PI3ks was further elucidated by antibody mediated type I PI3ks inhibition, which illustrated that type I PI3ks – together with its substrate (PI(4,5)P₂) and product (PIP₃) – were essential for ingestion of large particles (>3µm in diameter), but not for phagosome maturation³³.

The Type II PI3ks are not well described but current evidence points to the notion that this enzyme family produces either PI(3,4)P₂ or phosphatidylinositol 3-phosphate (PI3P) on endosomal or plasma membranes³⁴ by either of their three isoforms: PI3KC2α, C2β, C2γ. Thus, type II PI3ks, could contribute to production of PI(3,4)P₂ on extending pseudopodia for actin regulation and additional membrane, or it could facilitate phagosome maturation through production of PI3P on phagosomes.

The last PI3k family is the type III PI3ks that consist of only one catalytic subunit, VPS34, in humans: hVPS34. Type III PI3ks phosphorylate phosphatidylinositol (PI) to PI3P on endosomes and autophagosomal structures³⁵. Formation of PI3P is accompanied by the closure of the phagocytic cup and subsequent disappearance of PI(4,5)P₂ (ref. 30), which lead to and are essential for maturation of newly formed phagosomes³³. Thus the function of PI3P is centred more around phagosomal/endosomal maturation than as a source of extra membrane during engulfment. Additionally, PI3P expression could be negatively regulated during maturation by the (FYVE domain containing protein) PI 5'-kinase, PIKfyve, via phosphorylation at the 5-position to produce PI(3,5)P₂ (ref. 36).

From the literature consulted, it seems that the origin of these relatively large amounts of “extra” membrane is most likely the phosphoinositides produced by PI3k enzymes. In support of this, non-specific inhibition of the PI3ks enzyme superfamily (which induced drastically decreased PIP₃, PI(3,4)P₂ and PI3P synthesis during phagocytosis), prevented production of the 20% increased surface area

usually observed in the “frustrated phagocytosis” model mentioned earlier. This suggests that PI3ks activity is one of the chief sources of membrane during pseudopodia extension and phagocytosis. Additionally, a significant amount of membrane could also be supplied by recycling endosomes and sorting nexins (SNX), which collect membrane and other phagocytic components from endosomes and newly formed phagosomes called nascent phagosomes. Interestingly, this recycling machinery is also dependent on PI3P expression for docking onto intracellular structures³⁷, further supporting our notion of PI3ks as important role player in this context. Not all engulfed material is destined for degradation and subsequently need to be recycled by the recycling endosomes and SNX mentioned above. Recycling endosomes, partly identified by the Rab11 superfamily, is responsible for pinching off reusable cargo during the nascent phagosomal stage³⁸. One of three Rab11 isoforms, Rab11a, is expressed on the nascent phagosome itself and facilitates phagosome fusion with early endosomes and Golgi-derived vesicles³⁷. Rab11a also has a crucial role in pro-inflammatory signalling as it delivers TLR4, responsible for detection of lipopolysaccharide such as E.coli LPS, to maturing phagosomes³⁹. The Rab11 superfamily seems necessary for engulfment itself as well, since Cox⁴⁰ reported that prevention of Rab11 GDP/GTP cycling by mutant alleles, inhibited particle internalization. Furthermore, the GTPase, ARF6, also controls trafficking of recycling endosomes to the membrane and inhibition thereof resulted in a block in pseudopod extension⁴¹, suggesting that recycling endosomes serve as an additional reservoir for plasma membrane during pseudopod extension. The greater part of cargo retrieval and sorting is done in the early phagosomal stage because most of the machinery is dependent on PI3P for docking³⁷, supporting the findings of Cox and colleagues^{18,40} mentioned previously. However, some of the SNX can form higher order structures with Vps26, Vps29 and Vps35 – these are called retromers⁴². These retromers function in the presence of PI3P, but also active Rab7, giving them a limited time gap to recycle cargo between early stage and late stage phagosome maturation (between Rab5 to Rab7 transitioning), discussed below. This is in no doubt a finely tuned, complex process that merits further research in order to be fully elucidated.

Nascent phagosomal stage

This stage can be structurally distinguished from the pseudopod extension/engulfment stage by phagocytic cup closure behind the engulfed material – a process highly dependent on type I PI3k (ref. 28).

In contrast to pseudopod formation, the process of phagosome formation and maturation is relatively well described, although some controversies remain. Successfully engulfed material is encapsulated into nascent phagosomes characterized by Rab5 GTPase expression³⁷. Rabex-5, a guanine nucleotide-exchange factor (GEF), is initially recruited to newly formed endosomes by the already present Rab22a (ref. 43) and functions to activate Rab5 (ref. 44). Active Rab5 then recruits endosomal early antigen 1 (EEA1) (ref. 45) and hVPS34 (ref. 46) to the nascent phagosome. hVPS34 generates PI3P on the cytosolic face of nascent phagosomes that serve as docking station for a variety of maturation effectors. The FYVE domain of EEA1 can then dock onto PI3P to ensure later EEA1-mediated tethering and fusion of phagosomes with late endosomes for further maturation⁴⁷. Inhibition of EEA1 reportedly arrest phagosome maturation⁴⁸, but a dominant negative mutant of EEA1 which did not induce maturation arrest has also been reported³³, suggesting that other FYVE domain containing proteins could be involved in PI3P binding that lead to subsequent maturation. Zinc finger FYVE domains, present in proteins like EEA1 and PIKfyve, recognize the hydrophilic head of PI3P on the cytosolic leaflet and may allow binding of these proteins with substantial specificity to PI3P, resulting in this docking⁴⁹. These contradicting findings on the necessity of EEA1 could be explained by its tendency for complex formation with other proteins. EEA1 has been reported to form a macromolecular complex with Rabaptin-5, Rabex-5 and N-ethylmaleimide-sensitive factor (NSF) that interacts with syntaxin 13 (another SNARE) to facilitate membrane fusion⁵⁰. NSF disassembles these SNARE complexes via ATP hydrolysis after membrane fusion, blocking further action⁵¹. This could mean that the maturation inhibition reported by Fratti⁴⁸ was achieved through the inability of antibody-bound EEA1 to form a macromolecular complex (likely due to steric hindrance), while the dominant negative form of EEA1 can, thus resulting in unperturbed phagosome maturation.

Late phagosomal stage

Transition to the late phagosomal stage is marked by GTPase-activating protein (GAP)-mediated Rab5 inactivation/dissociation³⁷ and Rab7 recruitment, together with late endosome fusion and expression of other markers such as mannose-6-phosphate receptor (MPR), lysobisphosphatidic acid⁴⁸ and lysosome-associated membrane proteins (LAMP) (ref. 52). During this stage, PI3P is incorporated and degraded inside the phagosomal lumen via inward budding of the limiting membrane⁵³. Briefly, the PI 3'-phosphatase (PTEN) and PIKfyve eliminate PI3P via hydrolysis to PI and phosphorylation to PI(3,5)P2, respectively³⁶. Elimination of PI3P is likely necessary for the removal of nascent phagosomal effector proteins dependent on PI3P expression, such as EEA1 and other FYVE domain containing proteins. The late phagosomal stage initiates about 10-30 min after nascent phagosome formation, at least under *in vitro* conditions⁴⁸. This is in accordance with the disappearance of PI3P about 10 min after its formation³³.

Rab7 is expressed on both late endosomes/late phagosomes and lysosomes⁵⁴. This expression profile allows Rab7 to regulate membrane trafficking between early endosome/nascent phagosomes and late endosomes as well between late endosome/late phagosomes and lysosomes⁵⁵. The fusion between nascent phagosomes and late endosomes may allow the close proximity of Rab7 and PI3P that facilitates SNX retromer functioning reported by Cullen & Korswagen⁴². In this manner, the SNX retromers possibly recycle cargo between nascent phagosomes and late phagosomes, rather than nascent phagosomes and recycling endosomes, as hinted at earlier. This Rab7 GTPase accelerates maturation to the phagolysosome biogenesis stage with the help of Rab7-interacting-lysosomal-protein (RILP) (ref. 56). The Rab7 associated proteins RILP and oxysterol-binding protein related-protein 1 (ORP1L) together link phagosomes to dynein⁵⁷, which centripetally moves these late phagosomes along microtubules toward lysosomes for fusion⁵⁶. Johansson⁵⁸ reported that ORP1L preferentially binds to active, GTP-Rab7 and that this association seems to sustain the GTP-bound state of Rab7. This prolonged activation could be required for successful dynein linkage. Dynein

mediated fusion with lysosomes seems to be dependent on the HOPS complex as well as Rab7 (ref. 59). HOPS is a tethering protein responsible for keeping phagosomes in close proximity to lysosomes, a function parallel to that of EEA1 (ref. 60). Furthermore, disassembly of the microtubular network with nocodazole ablated centripetal movement of phagosomes, suggesting a dependency of macrophages to dynein for maturation (more detail later).

Phagolysosome biogenesis stage

Phagosome fusion with lysosomes, or phagolysosome biogenesis, is the last stage of maturation and was reported to occur ≈ 1 h after nascent phagosome formation under *in vitro* conditions⁶¹. Fusion is mediated by the SNARE proteins (syntaxin 7, syntaxin 8, Vesicle-associated membrane protein (VAMP) 7 and VAMP8) (ref. 62) and provides the phagolysosome with the needed proteases (e.g. cathepsin D), reactive nitrogen species (RNS) and reactive oxygen species (ROS) which neutralized the ingested particle. Lysosome fusion also increases LAMP expression and effectuates an acidic phagosomal environment⁶³. Although Rab5 and Rab7 are the chief GTPases regulating endosomal and phagosomal maturation, research has discerned significant roles for other Rab proteins too. For example, Rab10 regulates recycling of proteins back to the plasma membrane and is present on nascent phagosomes even before Rab5 (ref. 64). Also, phagolysosomal protein degradation is hugely dependant on proteases like cathepsin D, which is delivered from the Golgi under control of the trans-Golgi network-localised Rabs (22b, 32, 34,38 and 43) (ref. 65) that were shown to have various association and dissociation kinetics with the maturing phagosome². Rab34 has also been implicated in phagolysosome biogenesis through its association with RILP (ref. 66), while the ER-localized Rab20 was shown to co-localize with V-ATPase on the phagosome, suggesting an involvement in phagosome acidification⁶⁷. Seto² more recently reinforced this finding by reporting that dominant negative alleles of Rab20 and Rab39 prevented phagosomal acidification.

Phagocytosis seem to have evolved from an endocytic nutrient gathering process in almost all eukaryotic cells, to a specialized mechanism of self-defence conserved uniquely to professional

phagocytes. A certain degree of redundancy exists in phagocytosis, most likely in order to be “fool proof”. However, as seen in the literature, at least some pathogens are able to arrest phagosome maturation to ensure their own survival. Interestingly, these pathogens do not evade being transported into the phagocytic cell – rather they use the host cell as nutrient supply, so that they not only survive, but thrive.

Pathogenic modulation

Pathogenic phagosome maturation arrest is a hallmark of bacterial and viral host immune evasion. Many intracellular pathogens like *Mycobacterium tuberculosis*, *Candida glabrata*, HIV-1 and *Leishmania donovani* have evolved divergent mechanisms to modulate phagocytic digestion²⁻⁴. Well characterized mechanisms of phagosome maturation arrest include (a) interference with PI3k function and PI3P biogenesis, (b) perpetuation of Rab5 expression, (c) prevention of centripetal movement of nascent phagosomes, (d) blocking of fission and fusion with lysosomes and endosomal organelles, (e) raising pH levels by causing phagosomal acid leakage, (f) lysis of the phagosomal membrane to escape digestion and even (g) active macrophage killing. Of these, only a few have been sufficiently studied in the context of phagocytosis. For the sake of brevity, we limited ourselves here to a very brief overview of the most relevant mechanisms.

Inhibition of phagosome maturation

M. tuberculosis survive intracellularly mainly by dephosphorylating PI3ks and thus preventing EEA1 docking onto the phagosome⁶⁸. Mycobacterial phagosomes (and also those containing *Leishmania*) also retain the tryptophan-aspartate containing coat (TACO) protein, which causes prolonged Rab5 expression. Although some maturation effectors can still bind the phagosome, absence of PI3P and EEA1 largely prevents lysosome fusion, resulting in a more alkaline, hydrolase deficient phagosome⁶⁹. In addition to the PI3P-dependent pathway, *M. tuberculosis* also effects hydrolase deficiency and

retarded acidification via limiting expression of Rab7 and Rab20, as well as limiting delivery of cathepsin D protease^{2,70}.

In contrast, the survival mechanisms of *C. glabrata* are largely dependent on active PI3ks. *C. glabrata* encodes the enzyme PI3k and produces fungal PI3P through phosphorylation of PI (ref. 71), increasing PI3P content of phagosomes during the early stages of maturation where PI3P has no role yet. However, this early increase elicits endogenous negative feedback which halts maturation, as recently illustrated by deletion of two functional subunits of fungal PI3k in infected THP-1 macrophages⁴.

HIV-1 invasion is associated with inhibited phagosome formation as well as phagosome maturation arrest through microtubule perturbations, for which several viral role players have been implicated, e.g. viral negative factor (Nef) (ref. 72) and regulatory viral protein (Vpr) (ref. 73). Although we could not find a study to specifically implicate PI3k here, these mechanisms are likely also PI3k related, since both Nef and Vpr (as well as Tat) achieve several other effects, such as RANTES production and down-regulation of the ARF6 endocytic pathway, via PI3k-dependent routes^{74,75}.

Modulation of killing capacity

Another similarity between *Mycobacteria* and *Leishmania* is that both result in perturbed ROS production, although via different pathways^{76,77} which inhibits macrophage microbicidal effect.

These studies illustrate quite clearly that pathogens are able to manipulate the phagocytic process to ensure their survival, propagation and distribution through the host. In our opinion, it is also this manipulability of the phagocytic process that makes it ideal for use in regenerative medicine.

Harnessing phagocytosis for medicine

The relatively detailed understanding of molecular mechanisms governing phagocytosis, as well as perturbations achieved by pathogenic mechanisms, allows for therapeutic exploitation of this process.

We have formulated a hypothesis on the use of this knowledge in regenerative medicine and possibly other clinical fields as well.

Firstly, macrophages seem able to engulf particles seemingly endless in size (considering the “frustrated phagocytosis” model), suggesting that they have the capacity to engulf the majority of pathogenic microbes and almost all host somatic cells. Secondly, pathogens evolving alongside macrophages have acquired mechanisms to elude host defence - many of which involve perturbation of phagocytosis. Based on these facts, we hypothesise that by inducing phagosome maturation arrest (without pathogen involvement), the highly motile macrophages may be modified to useful shuttles for carrying “cargo” to specific areas within the host. The nature of this cargo could range from drugs to live stem cells, depending on the therapeutic aim. Of all potential options, the idea of a macrophage carrying a live stem cell – for example to increase muscle regenerative capacity in patients suffering from myodystrophy – is most enticing.

Let us consider what this would practically entail. Fundamentally, these macrophages would have to be isolated from patient blood and modified *in vitro* in order for it to maintain an ingested stem cell in a viable state within its phagosomes after autologous reinfusion. We propose induction of phagosome maturation arrest, but in a manner that will not compromise particle ingestion capacity. A variety of methods by which this may be achieved have been unknowingly uncovered by research on phagosome maturation. Below, we evaluate the feasibility of these methods in terms of safety for *in vivo* application.

Macrophage IL-10 enrichment

IL-10 is used by *M. tuberculosis* as a powerful inhibitor of phagosome maturation, as discussed earlier. Since IL-10 is synthesised endogenously, it seems a promising agent to use. However, IL-10-mediated maturation arrest was demonstrated to be dependent on presence of a bacterial component⁷⁸. Ethical complexities aside, this problem may be overcome by identification of the essential bacterial

component, which – if not antigenic or pathogenic – could be administered as co-treatment. A greater issue here is the phenotypic change that IL-10 effects in macrophages, polarizing macrophages toward the alternatively activated (M2) phenotype^{79,80}. Although this anti-inflammatory phenotype is desired in terms of resolution of inflammation and wound healing, M2 macrophages do not readily cross endothelial barriers⁸¹. This would significantly inhibit the actual delivery of the ingested stem cell to the intended target tissue. This complication however highlights another requirement – only M1 macrophages should be used, to ensure sufficient mobility.

Brefeldin A treatment

The fungal antibiotic Brefeldin A (BFA), inhibits a subtype of Golgi associated GEFs (ARF-GEFs) that facilitate the GDP/GTP cycling of ARF family proteins⁸². These ARF-GEFs express a Sec7 domain that BFA recognises and inhibits by direct binding to it⁸³. ARFs play a central role in regulating actin polymerization and activating phosphatidylinositol kinases for phosphatidylinositol production¹⁶, as well as plasma membrane traffic via coat proteins expressed on cellular transport vesicles⁸⁴. ER and Golgi bilaterally traveling transport vesicles are coated with proteins such as calnexin and coat protein complex type I (COPI) and type II (COPII) (ref. 85). COPI is recruited to phagosomes and contributes to recycling of phagosomal components⁸⁶. Active ARF1 is necessary for this COPI recruitment and inhibited COPI expression has been shown by Berón⁸⁶ to partly perturb phagosomal recycling events. Thus, because BFA-sensitive ARF-GEFs control ARF1 activity that in turn allows COPI recruitment, BFA treatment could potentially induce phagosome maturation arrest by preventing sufficient recycling of phagosomal components. However, Beemiller²⁸ found BFA-mediated inhibition of ARF-GEFs did not lead to subsequent inactive ARF1 expression on phagosomes. This suggests that the cells adapted to ARF-GEF inhibition by recruiting GEFs that are insensitive to BFA treatment. In addition, dual specificity of ARF was reported for BFA: ARF1 and ARF5, but not ARF6 – the main ARF implicated in encapsulation – was reported to be sensitive to BFA (ref. 87). The effect of BFA on phagosome maturation thus remains largely unknown.

Dynein inhibition

As mentioned, dynein is vital for centripetal and centrifugal delivery of phagosomes to lysosomes for fusion. The dynactin complex has been shown to facilitate cargo binding to dynein for centripetal movement⁸⁸, while the Rab5 GTPase regulates motility of endosomes⁸⁹, likely through a phosphoinositide and EEA1 dependent manner. It is widely accepted that microtubule disruption (e.g. by nocodazole) negatively influences phagosome centripetal movement and coinciding maturation. However, the microtubule disassembly associated with nocodazole administration could perturb pseudopod extension via inhibited PI3k delivery, thereby inhibiting uptake of stem cells into macrophages, and may block cellular motility and chemotactic reactivity, ablating the very characteristic of macrophages we intent to exploit.

In the same context, Ciliobrevin D is a dynein motor blocker that inhibits the GTPase activity of dynein specifically⁹⁰ without affecting kinesin-1 and 5 ATPase activity⁹¹ or microtubule structure¹⁰, making this compound a more promising inhibitor of centripetal movement only. Recently, Ciliobrevin D was suggested as modulator of lysosome mechanics⁹² and was utilised to elucidate the formation of NLR pyrin domain containing 3 (NLRP3) mediated inflammasome in bone marrow-derived macrophages¹⁰. Its effects on phagosome maturation remain to be further elucidated.

Wortmannin

This fungal steroid metabolite is a known potent, selective and irreversible inhibitor of all three PI3k subtypes via covalent binding, virtually eliminating phagosome fusion with late endosomes and lysosomes⁹³. However, not all effects of Wortmannin are equally desired. For example, PI3K-inhibition by Wortmannin was reported to enhance TLR-mediated inducible nitric-oxide synthase (iNOS) expression, to activate NF- κ B and to up-regulate cytokine mRNA production⁹⁴, suggesting a pro-inflammatory role. In addition, Wortmannin treatment was also shown to prevent large particle (>3 μ m) engulfment through inhibiting PI3P formation¹⁸. Together these data suggest that the use of

Wortmannin for macrophage modification will require a finely optimised protocol, to ensure maximal phagosome maturation arrest, without compromising the encapsulation process or eliciting an inflammatory response.

Concanamycin A

Concanamycin A is a plecomacrolide that specifically inhibits the V-ATPase proton pump. This enzyme is responsible for energizing the membranes of eukaryotic cells, both intracellular and plasma membranes⁹⁵. V-ATPase is expressed on late phagosomes and ensures an acidic phagosomal pH. Concanamycin A covalently binds to the subunit c of the translocating V_0 complex of V-ATPase (ref. 95), thereby preventing proton influx into phagosomes and maintaining an alkaline environment around pH 7.5 (ref. 96) which inhibits progression of autophagy, making Concanamycin A a candidate worthy of exploration in this context.

Chloroquine

Chloroquine is a 4-aminoquinoline that indirectly prevents acidification of intracellular vacuoles⁹⁷. This compound is readily used as an anti-malarial drug and was very recently suggested as a possible Ebola drug, since its alkalinizing action would prevent intracellular viral replication, provided that its concentration can be maintained at effective dose⁹⁷. The fact that chloroquine is a known medication is a benefit, since its safety for human consumption has been established. Similar to concanamycin A, chloroquine has proven efficacy in the context of (auto)phagosome maturation arrest.

From this information, we conclude that positive basic data exist for a number of potential treatments that may be used for macrophage modification, but that more research is required for optimisation of single-compound or cocktail doses.

Additional factors to consider

Although maintenance of stem cell viability inside phagosomes is a major consideration and an important problem to solve, it is not the only one. In order for the stem cells to be ingested by the modified macrophage, they will also have to be opsonised, especially since autologous cells will ideally be used for this technique. Importantly, opsonisation should not interfere with stem cell function after its delivery. We believe that this can be over the best solution here is using advanced technology and a multidisciplinary approach. Recently, great advances have been made in the field of abiotic membrane-active polymers that can coat cell membranes whilst maintaining cell viability⁹⁸. These polymers can be “decorated” with an opsonin to enhance encapsulation; the polymer can be deconstructed by e.g. slight temperature change or vibration, releasing a largely unaffected stem cell.

Another question is whether the number of stem cells ingested should be limited, to ensure that physical size of macrophages does not hamper migration. It is known that macrophages have an exceptional capacity for membrane “extension”, so that several stem cells can theoretically be ingested by an individual macrophage. Indeed, this was the case in preliminary studies in our lab (Visser and Smith, unpublished data). However, we believe that the number of stem cells ingested per macrophage can simply be optimised via altering the time allowed for engulfment. Alternatively, flow cytometry sorting could be employed to sort for cells with an optimal number of ingested stem cells.

Once reinfused, macrophages should naturally migrate to sites requiring regeneration. Of course, in order to achieve maximal benefit, the chemotactic signal could also be manipulated, and the known vast array of existing tracking methods may be employed to track the final destination of the modified macrophages. These processes are however not within the scope of this review, which is focused on modification of the macrophage itself.

The final consideration to include in this review is the release of the stem cell at the appropriate destination site. A plethora of mechanisms exist to induce cell death or exocytosis. One example is Brefeldin A. Although it has doubtful application for phagosome maturation arrest, BFA may prove useful in later stages of cell cargo delivery, by inducing apoptosis in the macrophage⁹⁹. Apoptosis was

reported under chronic treatment conditions (15h – 40h) (ref. 100), which allows sufficient time for the processes of engulfment, reinfusion and *in vivo* transportation to be completed. A favourable consideration in this context is that BFA does not affect engulfment capacity of large (3 μ m) or small (0.8 μ m) particles, despite its ER traffic inhibitory effects²², possibly due to the insensitivity of ARF6 to BFA mentioned earlier. Of course, as with all other phases, other candidate methods – such as targeted exocytosis – should also be considered and optimised. Again we may take lessons from microbes: *Leishmania donovani* promastigotes multiply and differentiate inside maturation arrested phagosomes, before escaping the macrophage to continue their life cycle⁷⁶. This poorly understood phenomenon could potentially be exploited to induce exocytosis of stem cells from macrophages.

Conclusion

In conclusion, modern science has substantially increased our understanding of molecular role players not only in the phagocytic process, but also in regenerative medicine. We firmly believe that by pooling resources across multiple disciplines, the remaining obstacles can be overcome to achieve the therapeutic technique we outlined here. Delivery of laboratory-enhanced or conditioned stem cells, using an autologous physiological vehicle, will be a significant step forward in terms of individualised medicine, and especially in disease states where no current mainstream therapy has proven effective.

Acknowledgements

The authors would like to acknowledge the South African NRF for funding (student bursary to Johan Georg Visser).

Conflict of Interest

The authors declare no conflict of interest.

References

- 1 Mills CD, Ley K, Buchmann K, Canton J. Sequential Immune Responses: The Weapons of Immunity. *J Innate Immun* 2015; **7**: 443–449.
- 2 Seto S, Tsujimura K, Koide Y. Rab GTPases Regulating Phagosome Maturation Are Differentially Recruited to Mycobacterial Phagosomes. *Traffic* 2011; **12**: 407–420.
- 3 Gogulamudi VR, Dubey ML, Kaul D, Atluri VSR, Sehgal R. Downregulation of host tryptophan-aspartate containing coat (TACO) gene restricts the entry and survival of *Leishmania donovani* in human macrophage model. *Front Microbiol* 2015; **6**: 1–10.
- 4 Rai MN, Sharma V, Balusu S, Kaur R. An essential role for phosphatidylinositol 3-kinase in the inhibition of phagosomal maturation, intracellular survival and virulence in *Candida glabrata*. *Cell Microbiol* 2015; **17**: 269–287.
- 5 Huynh KK, Kay JG, Stow JL, Grinstein S. Fusion, fission, and secretion during phagocytosis. *Physiol Bethesda* 2007; **22**: 366–372.
- 6 Anderson R, Wadee A. Innate immune mechanisms confer essential first-line host defence against the unrelenting threat posed by environmental microbial and viral pathogens. *Contin Med Educ*; **30**: 273–277.
- 7 Abbas AK, Lichtman AH, Pillai S. *Basic Immunology: Functions and Disorders of the Immune System*. 4th ed. Elsevier Ltd: Philadelphia, 2014.
- 8 Zhang Q, Raoof M, Chen Y, Sumi Y, Sursal T, Junger W *et al*. Circulating mitochondrial DAMPs cause inflammatory responses to injury. *Nature* 2010; **464**: 104–107.
- 9 Bardoel BW, Van Strijp JAG. Molecular battle between host and bacterium: Recognition in innate immunity. *J Mol Recognit* 2011; **24**: 1077–1086.
- 10 Misawa T, Takahama M, Kozaki T, Lee H, Zou J, Saitoh T *et al*. Microtubule-driven spatial arrangement of mitochondria promotes activation of the NLRP3 inflammasome. *Nat Immunol* 2013; **14**: 454–60.
- 11 Babu MM, Priya ML, Selvan AT, Madera M, Gough J, Aravind L *et al*. A database of bacterial lipoproteins (DOLOP) with functional assignments to predicted lipoproteins. *J Bacteriol* 2006; **188**: 2761–2773.
- 12 Shi M, Zhang Y, Liu L, Zhang T, Han F, Cleveland J *et al*. MAP1S protein regulates the phagocytosis of bacteria and toll-like receptor (TLR) signaling. *J Biol Chem* 2016; **291**: 1243–1250.
- 13 Swanson JA, Hoppe AD. The coordination of signaling during Fc receptor-mediated phagocytosis. *J Leukoc Biol* 2004; **76**: 1093–1103.
- 14 Nie Z, Hirsch DS, Randazzo PA. Arf and its many interactors. *Curr Opin Cell Biol* 2003; **15**: 396–404.
- 15 Honda A, Nogami M, Yokozeki T, Yamazaki M, Nakamura H, Watanabe H *et al*. Phosphatidylinositol 4-phosphate 5-kinase is a downstream effector of the small G protein ARF6 in membrane ruffle formation. *Cell* 1999; **99**: 521–532.
- 16 Zhang Q, Cox D, Tseng CC, Donaldson JG, Greenberg S. A requirement for ARF6 in Fcγ receptor-mediated phagocytosis in macrophages. *J Biol Chem* 1998; **273**: 19977–19981.

- 17 Liu W, Xiao X, Demirci G, Madsen J, Li1 XC. The innate NK cells and macrophages recognize and reject allogeneic non-self in vivo via different mechanisms. *J Immunol* 2013; **188**: 2703–2711.
- 18 Cox D, Tseng CC, Bjekic G, Greenberg S. A requirement for phosphatidylinositol 3-kinase in pseudopod extension. *J Biol Chem* 1999; **274**: 1240–1247.
- 19 Hallett MB, Dewitt S. Ironing out the wrinkles of neutrophil phagocytosis. *Trends Cell Biol* 2007; **17**: 209–214.
- 20 Hackam DJ, Rotstein OD, Sjolin C, Schreiber AD, Trimble WS, Grinstein S. v-SNARE-dependent secretion is required for phagocytosis. *Proc Natl Acad Sci U S A* 1998; **95**: 11691–11696.
- 21 Gagnon E, Duclos S, Rondeau C, Chevet E, Cameron PH, Steele-Mortimer O *et al.* Endoplasmic reticulum-mediated phagocytosis is a mechanism of entry into macrophages. *Cell* 2002; **110**: 119–131.
- 22 Becker T, Volchuk A, Rothman JE. Differential use of endoplasmic reticulum membrane for phagocytosis in J774 macrophages. *Proc Natl Acad Sci U S A* 2005; **102**: 4022–6.
- 23 Groothuis TA, Neefjes J. The many roads to cross-presentation. *J Exp Med* 2005; **202**: 1313–1318.
- 24 Paroutis P, Touret N, Grinstein S. The pH of the secretory pathway: measurement, determinants, and regulation. *Physiol Bethesda* 2004; **19**: 207–215.
- 25 Jahreiss L, Menzies FM, Rubinsztein DC. The itinerary of autophagosomes: From peripheral formation to kiss-and-run fusion with lysosomes. *Traffic* 2008; **9**: 574–587.
- 26 Trambas CM, Griffiths GM. Delivering the kiss of death. *Nat Immunol* 2003; **4**: 399–403.
- 27 Hawkins PT, Stephens LR. PI3K signalling in inflammation. *Biochim Biophys Acta - Mol Cell Biol Lipids* 2015; **1851**: 882–897.
- 28 Beemiller P, Hoppe AD, Swanson JA. A phosphatidylinositol-3-kinase-dependent signal transition regulates ARF1 and ARF6 during Fcγ receptor-mediated phagocytosis. *PLoS Biol* 2006; **4**: 0987–0999.
- 29 Okkenhaug K. Signaling by the phosphoinositide 3-kinase family in immune cells. *Annu Rev Immunol* 2013; **31**: 675–704.
- 30 Botelho RJ, Teruel M, Dierckman R, Anderson R, Wells A, York JD *et al.* Localized biphasic changes in phosphatidylinositol-4,5-bisphosphate at sites of phagocytosis. *J Cell Biol* 2000; **151**: 1353–1368.
- 31 Marshall JG, Booth JW, Stambolic V, Mak T, Balla T, Schreiber AD *et al.* Restricted accumulation of phosphatidylinositol 3-kinase products in a plasmalemmal subdomain during Fcγ receptor-mediated phagocytosis. *J Cell Biol* 2001; **153**: 1369–1380.
- 32 Mazaki Y, Nishimura Y, Sabe H. GBF1 bears a novel phosphatidylinositol-phosphate binding module, BP3K, to link PI3Kγ activity with Arf1 activation involved in GPCR-mediated neutrophil chemotaxis and superoxide production. *Mol Biol Cell* 2012; **23**: 2457–2467.
- 33 Vieira O V., Botelho RJ, Rameh L, Brachmann SM, Matsuo T, Davidson HW *et al.* Distinct roles of class I and class III phosphatidylinositol 3-kinases in phagosome formation and maturation. *J Cell Biol* 2001; **155**: 19–25.

- 34 Posor Y, Eichhorn-Gruenig M, Puchkov D, Schoneberg J, Ullrich A, Lampe A *et al.* Spatiotemporal control of endocytosis by phosphatidylinositol-3,4-bisphosphate. *Nature* 2013; **499**: 233–237.
- 35 Backer JM. The regulation and function of Class III PI3Ks: novel roles for Vps34. *Biochem J* 2008; **410**: 1–17.
- 36 Hazeki K, Nigorikawa K, Takaba Y, Segawa T, Nukuda A, Masuda A *et al.* Essential roles of PIKfyve and PTEN on phagosomal phosphatidylinositol 3-phosphate dynamics. *FEBS Lett* 2012; **586**: 4010–4015.
- 37 Fairn GD, Grinstein S. How nascent phagosomes mature to become phagolysosomes. *Trends Immunol* 2012; **33**: 397–405.
- 38 Lemmon SK, Traub LM. Sorting in the endosomal system in yeast and animal cells. *Curr Opin Cell Biol* 2000; **12**: 457–466.
- 39 Husebye H, Aune MH, Stenvik J, Samstad E, Skjeldal F, Halaas O *et al.* The Rab11a GTPase controls Toll-like receptor 4-induced activation of interferon regulatory factor-3 on phagosomes. *Immunity* 2010; **33**: 583–596.
- 40 Cox D, Lee DJ, Dale BM, Calafat J, Greenberg S. A Rab11- containing rapidly recycling compartment in macrophages that promotes phagocytosis. *Proc Natl Acad Sci U S A* 2000; **97**: 680–685.
- 41 Niedergang, F., Colucci-Guyon E, Dubois T, Raposo G, Chavrier P. ADP ribosylation factor 6 is activated and controls membrane delivery during phagocytosis in macrophages. *J Cell Biol* 2003; **161**: 1143–1150.
- 42 Cullen PJ, Korswagen HC. Sorting nexins provide diversity for retromer-dependent trafficking events. *Nat Cell Biol* 2011; **14**: 29–37.
- 43 Zhu H, Liang Z, Li G. Rabex-5 is a Rab22 effector and mediates a Rab22- Rab5 signaling cascade in endocytosis. *Mol Biol Cell* 2009; **20**: 4720–4729.
- 44 Horiuchi H, Lippe R, McBride HM, Rubino M, Woodman P, Stenmark H *et al.* A novel Rab5 GDP/GTP exchange factor complexed to Rabaptin-5 links nucleotide exchange to effector recruitment and function. *Cell* 1997; **90**: 1149–1159.
- 45 Scott CC, Cuellar-Mata P, Matsuo T, Davidson HW, Grinstein S. Role of 3-phosphoinositides in the maturation of Salmonella-containing vacuoles within host cells. *J Biol Chem* 2002; **277**: 12770–12776.
- 46 Kinchen JM, Doukometzidis K, Almendinger J, Stergiou L, Tosello-Trampont A, Sifri CD *et al.* A pathway for phagosome maturation during engulfment of apoptotic cells. *Nat Cell Biol* 2008; **10**: 556–566.
- 47 Vieira O V, Botelho RJ, Grinstein S. Phagosome maturation: aging gracefully. *Biochem J* 2002; **366**: 689–704.
- 48 Fratti RA, Backer JM, Gruenberg J, Corvera S, Deretic V. Role of phosphatidylinositol 3-kinase and Rab5 effectors in phagosomal biogenesis and mycobacterial phagosome maturation arrest. *J Cell Biol* 2001; **154**: 631–644.
- 49 Patki V, Lawe DC, Corvera S, Virbasius J V., Chawla A. A functional PtdIns(3)P-binding motif.

Nature 1998; **394**.

- 50 McBride HM, Rybin V, Murphy C, Giner A, Teasdale R, Zerial M. Oligomeric complexes link Rab5 effectors with NSF and drive membrane fusion via interactions between EEA1 and syntaxin 13. *Cell* 1999; **98**: 377–386.
- 51 Jahn R, Scheller RH. SNAREs: Engines for membrane fusion. *Nat Rev Mol Cell Biol* 2006; **7**: 631–643.
- 52 Desjardins M. Biogenesis of phagolysosomes: the ‘kiss and run’ hypothesis. *Trends Cell Biol* 1995; **5**: 183–186.
- 53 Gillooly DJ, Morrow IC, Lindsay M, Gould R, Bryant NJ, Gaullier JM *et al*. Localization of phosphatidylinositol 3-phosphate in yeast and mammalian cells. *Eur Mol Biol Organ J* 2000; **19**: 4577–4588.
- 54 Meresse S, Gorvel JP, Chavrier P. The rab7 GTPase resides on a vesicular compartment connected to lysosomes. *J Cell Sci* 1995; **108**: 3349–3358.
- 55 Press B, Feng Y, Hoflack B, Wandinger-Ness A. Mutant Rab7 causes the accumulation of cathepsin D and cation-independent mannose 6-phosphate receptor in an early endocytic compartment. *J Cell Biol* 1998; **140**: 1075–1089.
- 56 Harrison RE, Bucci C, Vieira OV, Schroer TA, Grinstein S. Phagosomes fuse with late endosomes and/or lysosomes by extension of membrane protrusions along microtubules: role of Rab7 and RILP. *Mol Cell Biol* 2003; **23**: 6494–6506.
- 57 Johansson M, Rocha N, Zwart W, Jordens I, Janssen L, Kuij C *et al*. Activation of endosomal dynein motors by stepwise assembly of Rab7-RILP-p150Glued, ORP1L, and the receptor betaIII spectrin. *J Cell Biol* 2007; **176**: 459–471.
- 58 Johansson M, Lehto M, Tanhuanpää K, Cover TL, Olkkonen VM. The oxysterol-binding protein homologue ORP1L interacts with Rab7 and alters functional properties of late endocytic compartments. *Mol Biol Cell* 2005; **16**: 5480–5492.
- 59 Akbar MA, Tracy C, Kahr WH, Krämer H. The full-of-bacteria gene is required for phagosome maturation during immune defense in *Drosophila*. *J Cell Biol* 2011; **192**: 383–390.
- 60 Hickey CM, Wickner W. HOPS initiates vacuole docking by tethering membranes before trans-SNARE complex assembly. *Mol Biol Cell* 2010; **21**: 2297–2305.
- 61 Jahraus A, Tjelle TE, Berg T, Habermann A, Storrle B, Ullrich O *et al*. In vitro fusion of phagosomes with different endocytic organelles. *J Biol Chem* 1998; **273**: 30379–30390.
- 62 Becken U, Jeschke A, Veltman K, Haas A. Cell-free fusion of bacteria-containing phagosomes with endocytic compartments. *Proc Natl Acad Sci* 2010; **107**: 20726–20731.
- 63 Jahraus A, Storrle B, Griffiths G, Desjardins M. Molecular characterization of phagosomes. *J Cell Sci* 1994; **107**: 145–157.
- 64 Cardoso CMP, Jordao L, Vieira OV. Rab10 regulates phagosome maturation and its overexpression rescues *Mycobacterium*-containing phagosomes maturation. *Traffic* 2010; **11**: 221–235.
- 65 Ng EL, Wang Y, Tang BL. Rab22B’s role in trans-Golgi network membrane dynamics. *Biochem Biophys Res Commun* 2007; **361**: 751–757.

- 66 Wang T, Hong W. Interorganellar regulation of lysosome positioning by the Golgi apparatus through Rab34 interaction with Rab-interacting lysosomal protein. *Mol Biol Cell* 2002; **13**: 4317–4332.
- 67 Curtis LM, Gluck S. Distribution of Rab GTPases in mouse kidney and comparison with vacuolar H⁺-ATPase. *Nephron Physiol* 2005; **100**: 31–42.
- 68 Vergne I, Chua J, Lee HH, Lucas M, Belisle J, Deretic V. Mechanism of phagolysosome biogenesis block by viable *Mycobacterium tuberculosis*. *Proc Natl Acad Sci U S A* 2005; **102**: 4033–4038.
- 69 Clemens DL, Lee BY, Horwitz MA. Deviant expression of Rab5 on phagosomes containing the intracellular pathogens *Mycobacterium tuberculosis* and *Legionella pneumophila* is associated with altered phagosomal fate. *Infect Immun* 2000; **68**: 2671–2684.
- 70 Seto S, Matsumoto S, Tsujimura K, Koide Y. Differential recruitment of CD63 and Rab7-interacting-lysosomal-protein to phagosomes containing *Mycobacterium tuberculosis* in macrophages. *Microbiol Immunol* 2010; **54**: 170–174.
- 71 Strahl T, Thorner J. Synthesis and function of membrane phosphoinositides in budding yeast, *Saccharomyces cerevisiae*. *Biochim Biophys Acta* 2007; **1771**: 353–404.
- 72 Mazzolini J, Herit F, Bouchet J, Benmerah A, Benichou S, Niedergang F. Inhibition of phagocytosis in HIV-1-infected macrophages relies on Nef-dependent alteration of focal delivery of recycling compartments. *Blood* 2010; **115**: 4226–4236.
- 73 Dumas A, Lê-Bury G, Marie-Anaïs F, Herit F, Mazzolini J, Guilbert T *et al*. The HIV-1 protein Vpr impairs phagosome maturation by controlling microtubule-dependent trafficking. *J Cell Biol* 2015; **211**: 359–72.
- 74 Nookala AR, Shah A, Noel RJ, Kumar A. HIV-1 tat-mediated induction of CCL5 in astrocytes involves NF- κ B, AP-1, C/EBP α and C/EBP γ transcription factors and JAK, PI3K/Akt and p38 MAPK signaling pathways. *PLoS One* 2013; **8**: 1–13.
- 75 Gangwani MR, Noel RJ, Shah A, Rivera-Amill V, Kumar A. Human immunodeficiency virus type 1 viral protein R (Vpr) induces CCL5 expression in astrocytes via PI3K and MAPK signaling pathways. *J Neuroinflammation* 2013; **10**: 136.
- 76 Moradin N, Descoteaux A. *Leishmania* promastigotes: building a safe niche within macrophages. *Front Cell Infect Microbiol* 2012; **2**: 121.
- 77 Sendide K, Deghmane AE, Pechkovsky D, Av-Gay Y, Talal A, Hmama Z. *Mycobacterium bovis* BCG attenuates surface expression of mature Class II molecules through IL-10–dependent inhibition of cathepsin S. *J Immunol* 2005; **175**: 5324–5332.
- 78 O’Leary S, O’Sullivan MP, Keane J. IL-10 blocks phagosome maturation in *Mycobacterium tuberculosis*-infected human macrophages. *Am J Respir Cell Mol Biol* 2011; **45**: 172–180.
- 79 Mia S, Warnecke A, Zhang XM, Malmström V, Harris RA. An optimized protocol for human M2 macrophages using M-CSF and IL-4/IL-10/TGF- β yields a dominant immunosuppressive phenotype. *Scand J Immunol* 2014; **79**: 305–314.
- 80 Chazaud B, Brigitte M, Yacoub-Youssef H, Arnold L, Gherardi R, Sonnet C *et al*. Dual and beneficial roles of macrophages during skeletal muscle regeneration. *Exerc Sport Sci Rev* 2009; **37**: 18–22.

- 81 Arnold L, Henry A, Poron F, Baba-Amer Y, van Rooijen N, Plonquet A *et al.* Inflammatory monocytes recruited after skeletal muscle injury switch into antiinflammatory macrophages to support myogenesis. *J Exp Med* 2007; **204**: 1057–1069.
- 82 Donaldson JG, Finazzi D, Klausner RD, Brefeldin A inhibits Golgi membrane–catalysed exchange of guanine nucleotide onto ARF protein. *Nature* 1992; **360**: 350–352.
- 83 Shin HW, Nakayama K. Guanine nucleotide-exchange factors for arf GTPases: their diverse functions in membrane traffic. *J Biochem* 2004; **136**: 761–767.
- 84 Kreis TE, Lowe M, Pepperkok R. COPs regulating membrane traffic. *Annu Rev Cell Dev Biol* 1995; **11**: 457–466.
- 85 Letourneur F, Gaynor EC, Hennecke S, Demolliere C, Duden R, Erm SD *et al.* Coatamer is essential for retrieval of dilysinetagged proteins to the endoplasmic reticulum. *Cell* 1994; **79**: 1199–1207.
- 86 Berón W, Mayorga LS, Colombo MI, Stahl PD. Recruitment of coat-protein-complex proteins on to phagosomal membranes is regulated by a brefeldin A-sensitive ADP-ribosylation factor. *Biochem J* 2001; **355**: 20726–20731.
- 87 Zeeh JC, Zeghouf M, Grauffel C, Guibert B, Martin E, Dejaegere A *et al.* Dual specificity of the interfacial inhibitor brefeldin A for arf proteins and Sec7 domains. *J Biol Chem* 2006; **281**: 11805–11814.
- 88 Blocker A, Severin FF, Burkhardt JK, Bingham JB, Yu H, Olivo JC *et al.* Molecular requirements for bi-directional movement of phagosomes along microtubules. *J Cell Biol* 1997; **137**: 113–129.
- 89 Nielsen E, Severin F, Backer JM, Hyman AA, Zerial M. Rab5 regulates motility of early endosomes on microtubules. *Nat Cell Biol* 1999; **1**: 376–382.
- 90 Chou TF, Brown SJ, Minond D, Nordin BE, Li K, Jones AC *et al.* Reversible inhibitor of p97, DBeQ, impairs both ubiquitin-dependent and autophagic protein clearance pathways. *Proc Natl Acad Sci U S A* 2011; **108**: 4834–4839.
- 91 Firestone AJ, Weinger JS, Maldonado M, Barlan K, Langston LD, O'Donnell M *et al.* Small-molecule inhibitors of the AAA1 ATPase motor cytoplasmic dynein. *Nature* 2012; **484**: 125–129.
- 92 Lin T, Pan PY, Lai YT, Chiang KW, Hsieh HL, Wu YP *et al.* Spindle-F Is the Central Mediator of I κ B Kinase-Dependent Dendrite Pruning in Drosophila Sensory Neurons. *Public Libr Sci Genet* 2015; **11**: e1005642.
- 93 Vieira O V, Buccì C, Harrison RE, Trimble WS, Lanzetti L, Gruenberg J *et al.* Modulation of Rab5 and Rab7 recruitment to phagosomes by phosphatidylinositol 3-kinase. *Mol Cell Biol* 2003; **23**: 2501–14.
- 94 Hazeki K, Kinoshita S, Matsumura T, Nigorikawa K, Kubo H. Opposite effects of wortmannin and 2-(4-morpholinyl)-8-phenyl-1(4H)-benzopyran-4-one hydrochloride on toll-like receptor-mediated nitric oxide production: negative regulation of nuclear factor- κ B by phosphoinositide 3-kinase. *Mol Physiol* 2006; **69**: 1717–1724.
- 95 Huss M, Ingenhorst G, König S, Gaßel M, Dröse S, Zeeck A *et al.* Concanamycin A, the specific inhibitor of V-ATPases, binds to the VO subunit c. *J Biol Chem* 2002; **277**: 40544–40548.

- 96 Yates RM, Hermetter A, Russell DG. The kinetics of phagosome maturation as a function of phagosome/lysosome fusion and acquisition of hydrolytic activity. *Traffic* 2005; **6**: 412–420.
- 97 Akpovwa H. Chloroquine could be used for the treatment of filoviral infections and other viral infections that emerge or emerged from viruses requiring an acidic pH for infectivity. *Cell Biochem Funct* 2016; : 191–196.
- 98 Lemaire S, Mingeot-Leclercq MP, Tulkens PM, Van Bambeke F. Study of macrophage functions in murine J774 cells and human activated THP-1 cells exposed to oritavancin, a lipoglycopeptide with high cellular accumulation. *Antimicrob Agents Chemother* 2014; **58**: 2059–2066.
- 99 Tseng CN, Hong YR, Chang HW, Yu TJ, Hung TW, Hou MF *et al*. Brefeldin A reduces anchorage-independent survival, cancer stem cell potential and migration of MDA-MB-231 human breast cancer cells. *Molecules* 2014; **19**: 17464–17477.
- 100 Alvarez C, Sztul ES. Brefeldin A (BFA) disrupts the organization of the microtubule and the actin cytoskeletons. *Eur J Cell Biol* 1999; **78**: 1–14.

Appendix B: S.O.P.s

Ethical Exception

Ethical exemption for isolation of human monocytes from donated blood (buffy coats) was received from the Health Research Ethics Committee (HREC) of Stellenbosch University on 8 July 2015 (Ethics Reference #: X15/05/013).

Obtaining O+ Buffy coats

1. Contact Hayley at the Western Province Blood Transfusion Service:
haylay@wpbts.org.za
2. Request information to obtain ethical clearance, if needed.
3. Contact Kashief at kashief@wpbts.org.za to arrange a pick up time for buffy coats.
4. **Note:** Fresh blood takes about a day to be processed so the buffy coats will only be available for pick up from 4pm.
5. Arrange with Kashief to look up the ages of the patients (this is a favour).
6. Take a blood transport container with two cold ice packs to keep buffy coats cold and prevent cell clumping.
7. Buffy coats need to be processed as soon as possible to ensure a viable population of cells are gathered.
8. **Note:** Cells clump and die if not isolated as soon as possible.

Monocyte Isolation

To facilitate balancing of the centrifuge, it is recommended to process two buffy coats in parallel. However, take care to use separate materials for each donor and not to mix the cells.

1. Carefully disinfect the plastic bags containing the buffy coats and transfer the contents of each donor buffy coat to a 50mL tubes.
2. For each buffy coat fill two 50mL tubes with 16mL Ficoll/Histopaque solution (1.077 g/mL). The Ficoll/Histopaque should be at room temperature for the preparation.
3. Mix 22mL buffy coat blood with 10mL cold RPMI to facilitate layering.
4. Layer this 32mL buffy/RPMI mixture on top of the Ficoll/Histopaque solution for the first density gradient. Be careful to do this slowly and carefully in order to prevent mixing both layers.
5. Centrifuge at 400 x g without brake for 30 min at 23°C.

6. For each gradient collect the white ring of peripheral blood mononuclear cells (PBMCs) which is located between the two phases with a plastic Pasteur pipette and transfer to a 50mL tube.
7. Fill each tube with 1mM PBS-EDTA up to the 45mL mark.
8. Centrifuge at 300 x g for 10 min without brake at 23°C.
9. Aspirate supernatant and wash pellet again with 45mL PBS-EDTA.
10. For each donor pool the pellets in 20mL RPMI-1640 **without** phenol red containing 10% FBS.
11. Prepare the iso-osmotic Percoll solution for the second density gradient: For two donors mix 23.13mL Percoll solution (density: 1.131 g/mL) in a 50mL tube with 1.87mL 10x PBS. Then transfer 23mL of this solution to a new 50mL tube and add 27mL RPMI-1640 **with** phenol red containing 10% FBS to obtain a 42.56% iso-osmotic Percoll solution. The Percoll should be at room temperature for the preparation.
12. For each donor transfer 24.4mL of the prepared Percoll solution to a 50mL tube and layer the PBMC solution prepared in step **10** on top of the Percoll solution. Be careful to do this very slowly and carefully, both layers tend to mix easily. If done correctly the two phases can be distinguished due to their difference in colour.
13. Centrifuge at 550 x g without brake for 30 min at 23°C.
14. For each gradient collect the white ring of monocytes which is located between the two phases with a plastic Pasteur pipette and transfer to a 50mL tube.
15. Fill each tube with PBS-EDTA up to the 45mL mark.
16. Centrifuge at 400 x g for 10 min without brake at 23°C.
17. Aspirate the supernatant and resuspend the pellets in the needed amount of Complete Monocyte media or FBS to seed or freeze cells, respectively.

EDTA Stock Preparation

1. Make up 0.5M stock
2. Stir 186.1 g EDTA (372.24 g/mol) into 800 ml ddH₂O.
3. Add NaOH solution to adjust the pH to 8.0. The EDTA will slowly go into solution as the pH nears 8.0.
4. After EDTA has dissolved, top up the solution to 1L with ddH₂O.
5. Filter the solution with filter paper or through a 0.5µm filter.
6. Dispense into containers as needed and sterilize in an autoclave.

PBS-EDTA (1mM) Preparation

- Mix 1mL prepared EDTA (0.5M, 8.0 pH) with 500mL sterile PBS (0.1M, 1x).

Culture Conditions

Monocytes

- **Note:** Monocytes struggle to adhere to glass. Recommended alternatives are Crystal-grade polystyrene, Gamma sterilized, Non pyrogenic 35mm culture dishes or Nunc UpCell plates.

35mm Culture Dish

1. Suspend monocytes in Complete Monocyte media for counting and seeding.
2. Seed viable cells at 2×10^6 – 3×10^6 cells/ml (4×10^6 – 6×10^6 cells/well).
3. Add Complete Monocyte media to get final volume of 2mL.
4. Immediately treat with appropriate concentration of GM-CSF or M-CSF (discussed under “Pre-differentiation and polarisation of Monocytes into M1 and M2 Macrophages”).
5. Allow monocytes to adhere to culture plate for 24h.
6. Aspirate media and wash with warm 1x PBS.
7. Refresh media with only 1mL Complete Monocyte media and treat with appropriate cytokine.
8. Refresh media every 3rd day and treat with cytokine.
9. Optimal assessment time is 6 days after seeding, do not culture for more than 10 days.

Nunc UpCell Plates

1. **Work on hot ice pack or at least 6 tissue papers.**
2. Place plate on ice pack or tissues and seed monocytes at 2×10^6 – 3×10^6 cells/mL (4×10^6 – 6×10^6 /well).
3. Repeat step 3. + 4. stated above.
4. UpCell plates are hydrophobic (cell adherent) above 32°C and hydrophilic (cell repellent) below 32°C.
5. **Place plate on warm (>32°C) surface when changing media**
6. Repeat steps 5. – 9. stated above.

Complete Monocyte media

- Advanced RPMI-1640
- 10% Human serum from AB patient (Sigma-Aldrich)
- 100 U/ml Penicillin Streptomycin.
- 2 mM Glutamax.

Human serum preparation

1. Use Human serum from AB patient obtained from Sigma-Aldrich.
2. Heat inactivate this serum to inactivate complement and remove fibrin by incubating at 56°C for 30min.
3. Filter serum if not already done by Sigma-Aldrich.
4. Make working aliquots and store at -20°C.

Preparing Human Serum from AB Donor

1. In the event of import restrictions preventing the buying of serum, serum can be harvested from healthy AB donor.
2. Keep in mind only 38.8% of peripheral blood will yield serum if collected with SST (Serum Separation Tubes).
3. Invert tube ± 5 times.
4. Allow blood to clot for 1h or more if sufficient clotting has not occurred.
5. Centrifuge at 1200 x g for 10 mins at 23°C.
6. Remove top layer of serum with P1000 or Pasteur pipette.
7. **Note:** Be careful not to touch the separating gel with pipette tip.
8. Incubate serum at 56°C for 30min to inactivate complement and remove fibrin.
9. Filter serum.
10. Store at 4°C or make working aliquots to store at -20°C.

HUVECs

1. Have one T25 culture flask coated with 1 $\mu\text{g}/\text{cm}^2$ fibronectin ready for use (explained under "Transmigration System").
2. Thaw cryo vial, remove content and inject into T25.
3. **Note:** Do not centrifuge HUVECs before seeding into flask.
4. Fill T25 up to 3mL with **warm** Complete EBM media and place in incubator.
5. Refresh media and wash with **warm** 1x PBS after 24h.
6. Hereafter cells are washed with warm PBS and media replaced every 48h.
7. Culture cells until 90% confluent.
8. Split cells (explained under "Culture Detachment").
9. Divide cells evenly into 3x T75 coated with 1 $\mu\text{g}/\text{cm}^2$ fibronectin.
10. **Note:** HUVECs rapidly proliferate after 5 days, keep in mind to minimize passages.
11. Fill up T75 to 8 mL in total with Complete EBM media.
12. Change media and wash after 24h.
13. Culture until 90% confluent and freeze down or use in experiments.

Complete EBM media

- Use EBM BulletKit from Lonza to make up HUVEC media.
- Do not mix all compounds into EBM (Endothelium Basal Media) when receiving the BulletKit as this may reduce shelf life and functioning of media.
- Aliquot all compounds into Eppendorfs.
- Store all compounds at -20°C, store EBM at 4°C.
- Complete EBM media
 - EBM
 - 2% FBS
 - 0.4% BBE (Bovine Brain Extract)
 - 0.1% hEGF (human Epidermal Growth Factor)
 - 0.1% GA (Gentamicin/Amphotericin)
 - 0.1% Ascorbic acid
 - 0.1% Hydrocortisone
- Media has to be warm before injecting onto HUVECs.

- **Note:** Hydrocortisone solution is volatile. To prevent incorrect concentrations, it is recommended to aliquot out a known amount into 200 μ L Eppendorfs that corresponds to a known amount of media. In this way the loss of volume would not affect hydrocortisone concentration in Complete EBM media.

Freezing Conditions

Monocytes

NOTE: This is not recommended for primary monocytes

- Counting viable monocytes with Countess.
 - Resuspend cells in 1mL human serum.
 - Make a 0.1% solution of Trypan Blue by diluting with PBS.
 - Mix 10 μ L Trypan Blue and 10 μ L serum cell suspension.
 - Inject 10 μ L of this mixture into each chamber of a Countess counting slide.
 - Ensure Countess is calibrated for cell population.
 - Insert slide into Countess to allow counting of each chamber.
 - Note:** The number of cells is given as cells/mL, i.e., the initial resuspension volume will affect this concentration.
 - Work out the mean from the two chambers.
- Work on ice.
- Inject 200 μ L human serum into each cryo vial and allow to cool on ice.
- Add needed amount of serum cell suspension into each cryo vial to yield 5-8x10⁶ cells/mL.
- Add needed amount of serum to a final volume of 900 μ L.
- Make 10% DMSO solution by adding 100 μ L DMSO to a final volume of 1mL.
- Place tubes in Mr Frosty with isopropanol and store at -80°C for 24hr.
- Remove from Mr. Frosty and store tubes in LN2.

Thawing Monocytes

- Thaw cryo vial and inject content into appropriate flask or dish.
- To remove DMSO from solution and count cells:
 - Mix content of cryo vial with 10mL warm PBS-EDTA. This will prevent cells from clumping together.
 - Centrifuge 400 x g for 5min at 23°C.
 - Aspirate supernatant and resuspend pellet in 1mL Complete Monocyte media.
 - Count viable monocytes. Primary monocytes lose 50% viability after freezing.

HUVECs

- Suspend cells in EBM and count.
- Freeze HUVECs in 80% EBM, 10% FBS and 10% DMSO.
- Inject 200 μ L EBM into each vial followed by 100 μ L FBS.
- Add needed amount of cell suspension to yield 5x10⁵ cells/mL/vial.
- Fill up vial to 900 μ L with EBM.
- Add 100 μ L DMSO to a final volume of 1mL.
- Place in Mr. Frosty with isopropanol and freeze at -80°C for 24h.
- Remove from Mr. Frosty and store in LN2.

Pre-differentiation and Polarisation of Monocytes into M1 and M2 Macrophages

1. M1 Classically activated:
 - a. Culture with 50 ng/mL GM-CSF throughout.
2. M2 Alternatively activated:
 - a. Culture with 50 ng/mL M-CSF throughout.
3. Inject GM-CSF or M-CSF directly into dish every time media is changed.
4. M1 Classically activated:
 - a. Polarize with 50 ng/mL LPS and 20 ng/mL IFN- γ injected directly into dish 24h before assessment.
5. M2 Alternatively activated:
 - a. Polarize with 20 ng/mL IL-10, IL-4 and TGF- β injected directly into dish 24h before assessment.
6. 6 days of culture with polarisation on the 5th day is optimal and recommended.

GM-CSF Stock Preparation

1. Centrifuge vial to ensure lyophilized powder is collected at the bottom of vial.
2. Reconstitute 20 μ g contents of vial with 200 μ L sterile ddH₂O to a concentration of 0.1 mg/mL.
3. Dilute this 200 μ L in 800 μ L 1x PBS to make a stock of 0.02 mg/mL.
4. Make working aliquots of 2 μ g/mL by further diluting 100 μ L stock in 900 μ L 1x PBS.
5. Store aliquots at -20°C.
6. Avoid repeated freeze-thaw cycles.

M-CSF Stock Preparation

1. Centrifuge vial to ensure lyophilized powder is collected at the bottom of vial.
2. Reconstitute 10 μ g contents of vial with 100 μ L sterile ddH₂O to a concentration of 0.1 mg/mL.
3. Dilute this 100 μ L in 900 μ L 1x PBS to make a stock of 0.01 mg/mL.
4. Make working aliquots of 2 μ g/mL by further diluting 200 μ L stock in 800 μ L PBS.
5. Store aliquots at -20°C.
6. Avoid repeated freeze-thaw cycles.

LPS stock preparation

1. Reconstitute 5mg content of vial with 1mL sterile Hank's Balanced Salt Solution (HBSS).
2. Make sure to completely dissolve powder, **do not** vortex solution.
3. Add 1.5mL sterile HBSS to make a stock of 2 mg/mL.
4. **Note:** Do not make up stock solutions or working aliquots under 1 mg/mL. LPS is known to stick to the sides of containers. Concentrations of >1 mg/mL present negligible sticking. Recommended to use silanized tubes to prevent endotoxin sticking.
5. Make up 2 μ g/mL working aliquots directly before use by diluting 1 μ L stock in 999 μ L sterile HBSS.
6. If necessary, working aliquots can be stored at 4°C for 24h.

IFN- γ stock preparation

1. Centrifuge vial to ensure lyophilized powder is collected at the bottom of vial.

2. Reconstitute 100µg content of vial with 200µL sterile ddH₂O to a concentration of 0.5 mg/mL.
3. Dilute this 200µL in 9.8mL ddH₂O to make a stock of 10 µg/mL.
4. Make working aliquots of 1 µg/mL by diluting 100µL stock in 900µL ddH₂O.
5. Store aliquots at -20°C.
6. Avoid repeated freeze-thaw cycles.
7. **Note:** It is recommended to dilute the 0.5 mg/mL solution with RPMI containing 10% FBS or 5% human serum albumin. However, dilution with sterile ddH₂O served the purposes of this study.

Culture Detachment

Macrophages

35mm Culture Dish

1. Optimally harvest macrophages after 6 days of culturing.
2. **Note:** Harvest cells with Accutase® cell detachment solution. Harsh passaging agents such as Trypsin breaks apart cell pseudopodia, leading to cell death.
3. Remove culture media and wash with 1x PBS at 23°C.
4. Inject 1 ml Accutase® onto dish and incubate at 23°C for 10-15min.
5. Swirl dish and add another 1mL Accutase®.
6. Incubate another 10-15min at 23°C.
7. Suck up Accutase® and spray back onto dish to facilitate detachment.
8. For optimal yield gently scrape surface with cell scraper.
9. Tilt dish and collect as many cells as possible.
10. Cells may be spun down at 400 x g for 5 min at 37°C and reseeded or assessed.
11. **Note:** Accutase® auto-inhibits at 37°C, eliminating the need to neutralise with media.

UpCell Plates

1. Optimally harvest macrophages after 6 days of culturing.
2. Place UpCell plate on **cold** ice pack.
3. Aspirate media and replace with **cold** 1x PBS or RPMI.
4. Optimal detachment of human macrophages:
Leave UpCell plate on 10°C ice pack for 1h. During this time suck up PBS or RPMI and spray back onto culture surface to aid detachment.
5. For optimal yield gently scrape surface with cell scraper.
6. Tilt plate and collect as many cells as possible.
7. Cells may be spun down and reseeded or assessed.

HUVECs

1. T25:
 - a. Aspirate media and wash with 3mL 1x PBS.
 - b. Treat with 5mL warm Trypsin.
2. T75:
 - a. Aspirate media and wash with 8mL 1x PBS.
 - b. Treat with 7mL Trypsin.
3. Place flask in 37°C shaking incubator for 5 min.
4. Ensure cells have lifted and neutralize with 5mL (T25) or 7mL (T75) EBM.
5. Centrifuge cells at 1500 RPM for 3 min at 23°C.
6. Resuspend cells in Complete EBM media.

M1/M2 Phenotyping

Flow Cytometry

1. Analysis is done on BD FACSAria Cell Sorter.
2. Differentiate cell populations separately into M1 and M2 phenotypes for 6 days by culturing in 35mm dishes.
3. Prepare single stain and multiple stain solutions by mixing appropriate amount of antibody marker with 1 ml PBS (below).
4. Aspirate media and treat cells with 1 ml single stain or multiple stain PBS solution (below).
5. Incubate dishes at 37°C for 10 min to facilitate antibody binding.
6. Aspirate PBS and harvest cells with Accutase® cell detachment solution.
7. Centrifuge 400 x g for 5 min at 37°C and resuspend pellet in warm PBS.
8. Filter cells with filter paper and relocate to Flow Cytometry tube for immediate analysis.
9. Use unstained samples to determine background fluorescence.
10. Optimise fluorescent signal by adjusting voltage when analysing single stain samples.
11. Compensate for possible fluorophore spill-over using single stain samples.
12. Set up thresholds by recording 8×10^6 events per sample.
13. Analyse samples by recording 3×10^5 events per group in triplicate.

Fluorescent Antibody Markers and Setup

1. Prepare unstained sample by only harvesting cells.
2. Prepare single stain samples for every antibody by labelling with only one marker.
 - M1 single stain samples
 - CD274 (PD-L1)
 - CD86
 - MHCII (HLA-DR)
 - M2 single stain samples
 - CD163
 - IL-10

- CD206
- 3. Prepare multiple stain samples to be analysed by mixing all markers together.
 - CD274 (PD-L1) conjugated with PE-Cy7 (496nm/785nm).
 - 5µL per test.
 - Excitable with solid state Sapphire 488nm blue laser.
 - Detectable with 780/60nm band pass filter.
 - CD86 conjugated with APC (650nm/660nm).
 - 20µL per test.
 - Excitable with HeNe 633nm red laser.
 - Detectable with 660/20nm band pass filter.
 - MHCII (HLA-DR) conjugated with APC-Cy7 (650nm/785nm).
 - 5µL per test.
 - Excitable with HeNe 633nm red laser.
 - Detectable with 780/60nm band pass filter.

Phagosome Maturation Arrest

- **Chloroquine:** Pretreat 1h before onset of phagocytosis with 10µM
- **Wortmannin:** Pretreat 30min before onset of phagocytosis with 100nM
- **Concanamycin A:** At onset of phagocytosis, directly after addition of AbsBeads, treat with 100nM

Chloroquine Stock Preparation

1. Make up directly before use.
2. Dissolve 0.05 g in 1mL sterile ddH₂O.
3. Vortex until solution is clear and colourless.
4. Dilute 10µL in 990µL sterile ddH₂O to get a working concentration of 0.96255mM.
5. Store stock at 4°C.
6. **Note:** Solution cannot be stored for longer than 7 days.

Wortmannin Stock Preparation

1. Reconstitute 1mg content of vial with 2mL sterile DMSO to a concentration of 1.167mM.
2. Remove 1mL from vial and store at 4°C, do not permit to freeze.
3. Dilute the remaining 1mL in 24mL sterile DMSO to make a stock concentration of 46.68µM.
4. Make working aliquots of 4.668µM by diluting 100µL stock in 900µL DMSO.
5. Store solutions at 4°C, do not permit to freeze.

Concanamycin A Stock Preparation

1. Reconstitute 25µg content of vial with 4mL sterile DMSO to a stock concentration of 7.216µM.
2. Make working aliquots directly from stock.
3. Store at -20°C.
4. Avoid repeated freeze-thaw cycles.

AbsBeads preparation

1. Prepare 100mL of 50mM PBS, pH 7.4, containing 0.9% NaCl.
2. Prepare 100mL of 50mM MES (2-(*N*-morpholino)ethanesulfonic acid) buffer, pH 6.0.
3. Dissolve 4mg of Alexa Fluor 647 secondary IgG at 2 mg/ml in MES buffer in a glass centrifuge tube.
4. Add 1.375mL of 2.5% aqueous suspension of carboxylate-modified microsphere. Incubate at room temperature for 30 min.
5. Add 16mg of EDAC (1-ethyl-3-(3-dimethylaminopropyl)- carbodiimide). Mix by vortexing.
6. Adjust pH to 6.5 ± 0.2 with dilute NaOH. Incubate the reaction mixture on a rocker or orbital shaker overnight at 23°C.
7. Add 0.0181g glycine to give a concentration of 100mM to quench the reaction. Incubate 1h at 23°C.
8. Centrifuge 4000 x g for 20min to separate the protein-labeled beads from unreacted IgG.
9. Resuspend the pellet in 2mL of 50mM PBS. Centrifuge as described in step 8.
10. Repeat step 9 twice more (a total of 3 washes).
11. Resuspend the IgG conjugated beads in 10mL of 50mM PBS.
12. Add 1.3mg sodium azide to make a 2mM concentration.
13. Store AbsBeads at 4°C.
14. **Note:** Do not permit to freeze.

MES Buffer Preparation

- Dissolve 0.98g MES powder in 100mL sterile ddH₂O to make a 50mM solution. Store solution at 4°C for up to 6 months.

Phagocytosis Assay

1. Introduce 1.156×10^6 AbsBeads into macrophage culture by injecting 80 μ L AbsBeads/O+ solution into each 35mm dish or well of UpCell plate (below).
2. Addition of AbsBeads is characterised as the onset of phagocytosis.
3. Allow phagocytosis to commence for 2h.
4. **Note:** Phagocytosis is reduced to 1h during transmigration assay.

O+ Serum preparation

1. Collect peripheral blood in SST tube from healthy O+ donor.
2. Keep in mind 38.8% of peripheral blood will yield serum.
3. Invert tube ± 5 times.
4. Allow blood to clot for 1h or more if sufficient clotting has not occurred.
5. Centrifuge 1200 x g for 10mins at 23°C.
6. Remove top layer of serum with P1000 or Pasteur pipette.
7. **Note:** Be careful not to touch the separating gel with pipette tip.
8. Warm up serum to 56°C and incubate for 30min to inactivate complement and remove fibrin.
9. Store at 4°C or make working aliquots to store at -20°C.

AbsBeads incubation

1. Mix 40 μ L of 2.89×10^7 AbsBeads/mL stock with 40 μ L O+ donor serum.
2. Incubate AbsBeads in O+ serum at 4°C for 24h.

Live Cell Imaging

1. Analysis is done on Carl Zeiss LSM780 confocal microscope with Super-resolution platforms.
2. Treat cells with appropriate fluorophore markers for imaging (below).
3. Cells are imaged directly after onset of phagocytosis.
4. Ensure the incubator unit is on and CO₂ tank open before initiating imaging.
5. Place 35mm culture dish containing CellMask™, pHrodo® and AbsBeads/O+ solution on the appropriate microscope stage.
6. Inject ddH₂O into incubation stage to ensure a humidified environment.

7. Carefully place lid onto stage to ensure incubation in a humidified, 37°C with 5% CO₂ environment.
8. Select needed lasers to excite various markers by setting up appropriate tracks.
9. Separately optimise individual laser intensities for each marker.
10. Compensate for possible fluorophore spill-over.
11. Set up time lapse imaging with smallest possible cycle time between images.
12. Image random field of view at 20x magnification for 2h.
13. **Note:** Microscope focus is lost during prolonged time lapse imaging and refocusing is required if automatic focus is not available.

Fluorescent Markers

- **AbsBeads:** This is the onset of phagocytosis. Treat at 1.156x10⁵ AbsBeads per 35mm dish.
- **pHrodo®:** Just before phagocytosis treat at 1 mg/mL.
- **CellMask™:** 10 min before phagocytosis (treatment groups) treat at 1x solution (below).

Setup

1. Carboxylate modified blue fluorescent beads have excitation/emission maxima of 306nm/407nm.
 - a. Excitable with diode 405nm CW/PS (pulsed) for LSM7.
2. Alexa Fluor 647 red fluorescent secondary IgG have excitation/emission maxima of 650nm/668nm.
 - a. Excitable with 633nm laser.
3. pHrodo® BioParticles® green pH indicator have excitation/emission maxima of 509nm/533nm.
 - a. Excitable with Argon multiline laser 25mW at 488nm.
4. CellMask™ orange plasma membrane stain have excitation/emission maxima of 554nm/567nm.
 - a. Excitable with 561nm laser.

Preparing Fluorescent Markers

pHrodo®

1. Thaw one vial of the pHrodo® BioParticles® fluorescent particles.
2. Pipette 200µL sterile PBS into the vial containing 2mg lyophilized pHrodo® and briefly vortex the solution to completely resuspend the particles at a 10 mg/mL stock solution.
3. Transfer the suspension into an Eppendorf and sonicate for 5 minutes, until all the fluorescent particles are homogeneously dispersed.
4. Store at -20°C.

CellMask™

Treated groups

1. Make up directly before use.
2. Thaw one vial containing 1000x stock solution.
3. Mix 1µL with 9µL warm 1x PBS to yield a 100x solution.
4. Inject the 10µL solution into 1mL media to make a final 1x working concentration.
5. **Note:** Swirl dish thoroughly in order to mix CellMask™.
6. Incubate at 37°C with 5% CO₂ before initiating phagocytosis.

Control groups

1. Repeat step 1 + 2 as stated above.
2. Mix 1 μ L stock solution with 999 μ L warm 1x PBS to yield a 1x solution.
3. Remove media from wells and wash with warm PBS.
4. Treat with 1x CellMask™/PBS working solution and incubate at 37°C for 10 mins.
5. Aspirate CellMask™/PBS solution and wash 3x with warm PBS.
6. Replace with complete monocyte media and assess under microscope.

Flow Cytometry Quantification

Digestion, pH and AbsBeads Ingestion

1. Analysis is done on BD FACSAria Cell Sorter.
2. Treat cells with pHrodo® and AbsBeads/O+ as appropriate ("Fluorescent Markers" above).
3. **Note:** Do not treat cells with CellMask™.
4. Allow phagocytosis to commence for 2h.
5. Aspirate media and wash with warm PBS.
6. Fixate cells with by injecting 0.5 mL warm 4% Paraformaldehyde and 0.5 mL warm RPMI into each well or dish (1:1 ratio).
7. Incubate at 37°C for 10 mins.
8. Aspirate Paraformaldehyde/RPMI solution and replace with 1mL PBS.
9. Gently scrape cells off with cell scraper and inject into 2mL Eppendorf for each culture dish.
10. Filter cells with filter paper and relocate to Flow Cytometry tubes.
11. Compensate for possible fluorophore spill-over.
12. Set up thresholds for control and treated groups by recording 16x10⁶ events per group.
13. Analyse samples by recording 3x10⁵ events per group in triplicate.

Setup

1. Carboxylate modified blue fluorescent beads have excitation/emission maxima of 306nm/407nm.
 - a. Excitable with 405nm violet laser.
 - b. Detectable with 450/40nm band pass filter.
2. Alexa Fluor 647 red fluorescent secondary IgG have excitation/emission maxima of 650nm/668nm.
 - a. Excitable with HeNe 633nm red laser.
 - b. Detectable with 660/20nm band pass filter.
3. pHrodo® BioParticles® green pH indicator have excitation/emission maxima of 509nm/533nm.
 - a. Excitable with solid state Sapphire 488nm blue laser.
 - b. Detectable with 530/30nm band pass filter.

Transmigration Assay

Preparation

7 Days Prior to Experiment

1. Start culturing HUVECs in fibronectin coated T75.
2. Coat transmigration inserts and wells with fibronectin (below).

6 Days Prior to Experiment

1. Isolate primary macrophages from peripheral blood or buffy coats.

3 Days Prior to Experiment

1. Seed HUVECs onto transmigration inserts at 1×10^5 cells/insert.
2. Culture in complete EBM media with 0.7mL in bottom well and 0.2mL in insert for every well/insert complex used.

1 Day Prior to Experiment

1. Polarise macrophages to M1 with LPS and IFN- γ .
2. Activate LPS and IFN- γ HUVEC groups with, respectively, 50 ng/mL and 20 ng/mL 24h before experiment.

Experiment

1. Make up fresh Chloroquine stock and working solutions.
2. Make up Transmigration EBM media (only containing FBS, BBE and Ascorbic Acid).
 - a. MCP-1 **containing** Transmigration EBM media
 - i. 0.7mL EBM containing 2% FBS, 0.4% BBE, 0.1% Ascorbic acid and 100 ng/mL MCP-1 for each well used. This media is injected into the well underneath the insert.
 - b. MCP-1 **deficient** Transmigration EBM media
 - i. 0.2mL EBM containing 2% FBS, 0.4% BBE and 0.1% Ascorbic acid for each insert used. This media suspends the AbsBeads-containing macrophages and is injected onto the insets that are placed onto wells.
 - c. **GM-CSF and MCP-1** containing Transmigration EBM media
 - i. 0.7mL EBM containing 2% FBS, 0.4% BBE, 0.1% Ascorbic acid, 100 ng/mL MCP-1 and 50 ng/mL GM-CSF for each GM-CSF well used. This media is injected into the well underneath the insert.
3. Treat macrophages with 10 μ M Chloroquine.
4. Start timer at 1h. After treatment with Chloroquine, phagosome maturation arrest is set in motion. Phagocytosis starts when timer reaches 0min.
5. Timer at 30min. Treat macrophages with 100nM Wortmannin.
6. **Note:** Do not use 46.7 μ M stock, the additional DMSO in the 4.67 μ M working solution facilitate entry of Wortmannin into cells.
7. Timer at 0min. Treat macrophages with 100nM Concanamycin A.
8. Directly after step 7. introduce AbsBeads onto macrophage population.
9. Swirl dish and place in incubator for 1h to allow phagocytosis of AbsBeads.

10. After 1h split macrophages with UpCell plates or Accutase® passaging solution.
11. Resuspend macrophages in MCP-1 deficient Transmigration EBM media.
12. Count macrophages with 0.4% Trypan Blue.
13. Remove complete EBM media from transmigration well/insert complexes and wash with PBS.
14. Inject 0.7mL MCP-1 **containing** Transmigration EBM media into appropriate wells used.
15. Inject 0.7mL MCP-1 **deficient** Transmigration EBM media into appropriate wells used.
16. Inject 0.7mL **GM-CSF and MCP-1** containing Transmigration EBM media into appropriate wells used.
17. Place inserts into wells containing Transmigration EBM media.
18. Seed macrophages containing AbsBeads as well as those deficient of AbsBeads onto appropriate inserts at 3×10^5 cells/insert.
19. Fill up media in insert to 200 μ L with MCP-1 **deficient** Transmigration EBM media.
20. Incubate in 80% humidified, 37°C with 5% CO₂ environment for 2:30h.
21. Fixate cells by matching the amount of media with 4% paraformaldehyde in each well or insert.
22. **Note:** Do not remove media before fixing, this prevents loss of non-adhered cells.
23. Place in 37°C incubator with 5% CO₂ for 10min and aspirate fixative.
24. Inject 0.7mL 1x PBS into each well and 0.2mL 1x PBS into each insert
25. Store at 4°C.

Quantifying Migrated Cells

1. Quantification is done by hand due to small number of migrating cells.
2. Remove inserts from wells.
3. Inject 25 μ L 0.4% Trypan Blue into each well containing 0.7mL PBS, this assists in counting.
4. Count cells with cell counter under 20x magnification.
5. Start counting at the top and move side to side in order to cover the entire well.

MCP-1 Stock Preparation

1. Centrifuge vial to ensure lyophilised powder is collected at the bottom of vial.
2. Reconstitute 20 μ g content of vial with 200 μ L sterile ddH₂O to a concentration of 0.1 mg/mL.
3. **Note:** Do not vortex.
4. Dilute this 200 μ L in 800 μ L 1x PBS to make a stock solution of 0.02 mg/mL.
5. **Note:** Dilution in 1x PBS containing 0.1% BSA is not advised. The BSA stabilizes the MCP-1, however also prevents sufficient receptor binding to induce macrophage transmigration.
6. Use MCP-1 at 100 ng/mL.

Fibronectin coating

1. Culture surfaces are coated with fibronectin in order to allow HUVEC adhesion.
2. Recommended coating density of 1 μ g/cm².
3. 0.1% (1 mg/ml) fibronectin stock solution.
4. To coat 1 μ g/cm² growth area:

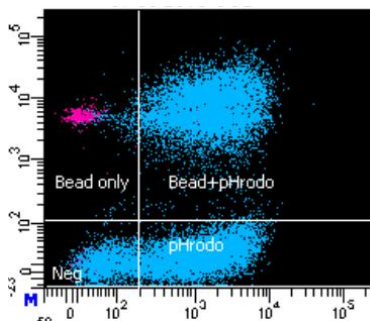
- a. Mix 1 μl fibronectin stock for every cm^2 of growth area with enough 1x PBS to cover the area.
5. Growth areas with accompanying volumes:
 - a. T25 = 25 cm^2 (2.5 ml)
 - b. T75 = 75 cm^2 (6 ml)
6. Incubate flasks at 37°C in 80% humidified incubator for 1h (applicable to all surfaces areas).
7. Aspirate fibronectin/PBS solution.
8. Remove caps from flasks and place in laminar flow hood under UV light to dry for 2 - 24h.
9. Store flasks in original resealable packaging to keep sterile.

Transmigration Inserts Coating with Fibronectin

1. Inserts as well as their accompanying wells are coated with fibronectin.
2. The minimum volume in a well of a 24 multiwell transmigration plate is 0.7mL and the approximate growth area is 1.9 cm^2 .
3. The minimum volume in an insert of a 24 multiwell transmigration plate is 0.2mL and the approximate growth area is 0.33 cm^2 (rounded up to 0.5 cm^2).
4. Thus, the total growth area to be coated is 2.4 cm^2 /insert.
5. Mix 2.4 μL fibronectin stock with 0.9mL 1x PBS for every well/insert complex coated.
6. Inject 0.7mL fibronectin/PBS solution into each well and place insert into well.
7. Inject 0.2mL fibronectin/PBS solution into insert.
8. Incubate and dry as stated above.
9. **Note:** Do not remove 24 multiwell plate lid when drying in laminar flow hood.
10. Place plates in original resealable packaging to keep sterile.

Appendix C: Supplementary Results

Flow Cytometric Distension of AbsBeads and Cells



Differentiation between Beads and Cells containing beads, using flow cytometry. In the scatter plot above, bead (blue, but pink in image) fluorescent intensity (y-axis) and pHrodo® (green, but blue here) fluorescent intensity (x-axis) is illustrated.